Copyright Warning & Restrictions

The copyright law of the United States (Title 17, United States Code) governs the making of photocopies or other reproductions of copyrighted material.

Under certain conditions specified in the law, libraries and archives are authorized to furnish a photocopy or other reproduction. One of these specified conditions is that the photocopy or reproduction is not to be "used for any purpose other than private study, scholarship, or research." If a, user makes a request for, or later uses, a photocopy or reproduction for purposes in excess of "fair use" that user may be liable for copyright infringement,

This institution reserves the right to refuse to accept a copying order if, in its judgment, fulfillment of the order would involve violation of copyright law.

Please Note: The author retains the copyright while the New Jersey Institute of Technology reserves the right to distribute this thesis or dissertation

Printing note: If you do not wish to print this page, then select "Pages from: first page # to: last page #" on the print dialog screen

ABSTRACT

A MULTIMODAL APPROACH TO INVESTIGATE BRAIN REORGANIZATION AFTER SPINAL CORD INJURY USING FUNCTIONAL MAGNETIC RESONANCE IMAGING AND FUNCTIONAL NEAR-INFRARED SPECTROSCOPY

by
Keerthana Deepti Karunakaran

Traumatic Spinal Cord Injury (SCI) results in structural and functional neurological changes at both the brain and the level of the spinal cord. Anatomical studies indicate decreased grey matter volume in sensorimotor and non-sensorimotor regions of the cortex following SCI; whereas, neurophysiological findings mostly report altered functional activity in the sensorimotor nodes of the cortex, subcortex, and cerebellum. Therefore, it is currently unknown whether tissue atrophy observed in non-motor related areas has any concomitant functional consequences. Furthermore, the neural underpinnings of adaptive neuroplasticity after SCI is not well-defined in the current literature. Hence, this dissertation is a pioneer study investigating the structural and functional changes in the whole brain after SCI, with particular focus on subcortical regions, using a multimodal approach employing magnetic resonance imaging (MRI), resting-state functional MRI (fMRI) and functional near-infrared spectroscopy (fNIRS), that may take best advantage of each of these three tools. MRI scans from 23 healthy controls (HC) and 36 individuals with complete SCI within two years of injury were used to demonstrate that both injury level and duration since injury are important factors contributing to recovery. Specifically, cervical level injury when compared to thoracolumbar level injury exhibits a greater loss of cortical grey matter volume in the orbitofrontal cortex, insula, and anterior cingulate cortex. Next, using the fMRI scans of the same participants during a resting-state scan, the

intrinsic functional connectivity of the mediodorsal, pulvinar and ventrolateral nuclei of the thalamus to the regions of salient network and the fronto-parietal network is observed to be dynamic and altered in the SCI group. Lastly, a continuous-wave fNIRS is used to reliably measure brain function in individuals with SCI during both dynamic and static tasks while accounting for cerebrovascular reactivity. Five min of resting-state data and 26 min of motor data including finger tapping, finger tapping imagery and ankle tapping were acquired to identify the spatial activation pattern unique to each of the movement type. A breath-hold paradigm is also used to quantify cerebrovascular reactivity as a means to calibrate task activity from neurovascular constraints. Sixteen HC were scanned at two separate visits to determine the sensitivity and test-retest reliability of fNIRS data from the sensorimotor cortex. Following validation, the same procedure was repeated in 13 individuals with paraplegia resulting from SCI and 13 HC to quantify alterations in the cortical activity of the motor cortex and cerebrovascular reactivity between the two groups. Results indicate that SCI group exhibit altered cerebrovascular reactivity with greater delay in response and greater pre-stimulus undershoot. As hypothesized, the hemodynamic response to ankle movement resulted in only a small change in oxyhemoglobin concentration in the sensorimotor cortex of SCI group when compared to HC. The application of fNIRS to assess cortical reorganization following SCI is unique and expands our understanding of the neurophysiology after SCI. It paves the groundwork for extending the implementation of fNIRS to rehabilitation research and other clinical populations with vascular dysfunction. This dissertation is one of the first studies to comprehensively examine both the structural and functional alterations of the brain in humans with complete SCI and opens promising avenues for SCI research using fNIRS modality.

A MULTIMODAL APPROACH TO INVESTIGATE BRAIN REORGANIZATION AFTER SPINAL CORD INJURY USING FUNCTIONAL MAGNETIC RESONANCE IMAGING AND FUNCTIONAL NEAR-INFRARED SPECTROSCOPY

by
Keerthana Deepti Karunakaran

A Dissertation
Submitted to the Faculty of
New Jersey Institute of Technology
and Rutgers University Biomedical and Health Sciences – Newark
in Partial Fulfillment of the Requirements for the Degree of
Doctor of Philosophy in Biomedical Engineering

Department of Biomedical Engineering

May 2019

.

APPROVAL PAGE

A MULTIMODAL APPROACH TO INVESTIGATE BRAIN REORGANIZATION AFTER SPINAL CORD INJURY USING FUNCTIONAL MAGNETIC RESONANCE IMAGING AND FUNCTIONAL NEAR-INFRARED SPECTROSCOPY

Keerthana Deepti Karunakaran

Dr. Bharat B. Biswal, Dissertation Co-Advisor — Date
Distinguished Professor of Biomedical Engineering, NJIT

Dr. Tara L. Alvarez, Dissertation Co-Advisor — Date
Professor of Biomedical Engineering, NJIT

Dr. Nancy Chiaravalloti, Committee Member — Date
Director of Neuropsychology and Neuroscience Lab, Kessler Foundation

---

Dr. Xiaobo Li, Committee Member — Date
Associate Professor of Biomedical Engineering, NJIT

Dr. Xin Di, Committee Member — Date
Research Assistant Professor of Biomedical Engineering, NJIT

Dr. Yiyan Liu, Committee Member — Date
Professor of Radiology, Rutgers New Jersey Medical School

BIOGRAPHICAL SKETCH

Author: Keerthana Deepti Karunakaran

Degree: Doctor of Philosophy

Date: May 2019

Undergraduate and Graduate Education:

- Doctor of Philosophy in Biomedical Engineering,
  New Jersey Institute of Technology, Newark, NJ, 2019

- Bachelor of Engineering in Electronics and Instrumentation Engineering,
  St. Joseph's College of Engineering, Anna University, Chennai, India, 2008

Major: Biomedical Engineering

Presentations and Publications:

Karunakaran, K.D., He, J., Zhao, J., Cui, J.L., Zang, Y.F., Zhang, Z. & Biswal, B.B. Differences in Cortical Gray Matter Atrophy of Paraplegia and Tetraplegia after Complete Spinal Cord Injury. *J Neurotrauma* (2018)

Karunakaran, K. D., Yuan R., He, J., Zhao, J., Cui, J. L., Zang, Y. F., Zhang, Z., Alvarez, T.L., & Biswal, B. B. Resting-State Functional Connectivity of the Thalamus in Complete Spinal Cord Injury. (Under review)

Karunakaran, K.D., Wolfer, M., & Biswal, B.B. In: Diwadkar V, Eickhoff SB (Ed.). Review of Resting-State Functional Connectivity Methods and Application in Clinical Population. New York, USA: Springer, (2019) (in press)

Karunakaran, K.D**.**, Alvarez T.L. & Biswal, B.B. Detection of Brain Motor Activity and Calibration using Breath Hold: A Functional Near Infrared Spectroscopy Study," (Manuscript in preparation)

Karunakaran, K.D., Ji, K., Chiaravalloti N.D. & Biswal, B.B. Test-Retest Reliability of Hemodynamic Response to Breath Hold using Functional Near Infrared Spectroscopy. (Manuscript in preparation)

Karunakaran, K.D., Chiaravalloti N.D. & Biswal, B.B. Altered Cortical Activation in Spinal Cord Injury using Functional Near-Infrared Spectroscopy. (Manuscript in preparation)

Algarin, C., Karunakaran, K.D., Reyes, S., Morales, C., Lozoff, B., Peirano, P. & Biswal, B. Differences on Brain Connectivity in Adulthood Are Present in Subjects with Iron Deficiency Anemia in Infancy. *Front Aging Neurosci* **9**, 54 (2017).

Egbert, A.R., Biswal, B., Karunakaran, K., Gohel, S., Pluta, A., Wolak, T., Szymanska, B., Firlag-Burkacka, E., Sobanska, M., Gawron, N., Bienkowski, P., Sienkiewicz-Jarosz, H., Scinska-Bienkowska, A., Bornstein, R., Rao, S. & Lojek, E. Age and Hiv Effects on Resting State of the Brain in Relationship to Neurocognitive Functioning. *Behav Brain Res* 344, 20-27 (2018).

Egbert, A.R., Biswal, B., Karunakaran, K.D., Pluta, A., Wolak, T., Rao, S., Bornstein, R., Szymanska, B., Horban, A., Firlag-Burkacka, E., Sobanska, M., Gawron, N., Bienkowski, P., Sienkiewicz-Jarosz, H., Scinska-Bienkowska, A. & Lojek, E. Hiv Infection across Aging: Synergistic Effects on Intrinsic Functional Connectivity of the Brain. *Prog Neuropsychopharmacol Biol Psychiatry* 88, 19-30 (2019).

Karunakaran, K.D. Single-Subject Analysis: AFNI/ICA. Invited Speaker in the Pre-conference Workshop, Fifth Biennial Resting-state Brain Connectivity Conference, University of Vienna, Austria 2016.

Abstracts:

Karunakaran, K.D. & Biswal B.B. Cortical Activation during Breath Hold using Functional Near-Infrared Spectroscopy. 45th Northeast Bioengineering Conference DOI: 10.13140/RG.2.2.19143.34722 (2019).

Karunakaran, K.D., Yuan R., He J., Zhao J., Cui J.L., Zang Y.F., Zhang Z. & Biswal B.B. Resting state functional connectivity of the thalamus in complete spinal cord injury. Society for Neuroscience, San Diego (2018).

Alvarez T.L., Scheiman M., Santos E.M., Morales C., Karunakaran K.D., Jaswal R., Yaramothu C., Antonio-Bertagnolli J.V., Biswal B.B. & Li X. Functional Cortical Differences between Convergence Insufficiency Patients and Binocularly Normal Controls. American Academy of Optometry, San Antonio (2018).

Karunakaran K.D., Gohel S., Azeez A.K., Alvarez T.L. & Biswal B.B. Calibrating task evoked hemodynamic response of functional near infrared spectroscopy using resting state fluctuations. Society for Neuroscience, Washington D.C. (2017).

Karunakaran, K.D., He J., Zhao J., Cui J.L., Zang Y.F., Zhang Z. & Biswal B.B. Resting State Functional Connectivity of Supplementary Motor Area in Spinal Cord Injury.

43rd Northeast Bioengineering Conference. DOI: 10.13140/RG.2.2.31873.51044 (2017).

Karunakaran, K. D., Gohel, S., Azeez, A.K., & Biswal, B.B. "Calibrating Task Evoked Hemodynamic Response of Functional Near Infrared Spectroscopy (fNIRS) Using Resting State Fluctuations.", Fifth Biennial Conference on Resting State and Brain Connectivity, Vienna, Austria: University of Vienna (2016).

Karunakaran, K. D. & Biswal, B.B. "Altered Regional Homogeneity in Spinal Cord Injury using Resting state FMRI." GSA Research Day, Newark, New Jersey: New Jersey Institute of Technology (2015).

To my dear mother and father, Kasthuri and Karunakaran for being my pillars of strength during this rollercoaster of a journey with their unconditional love.

To my sister, Kiran, for never letting me give up on my dreams and for the everyday encouragement and motivation.

To my grandparents for loving me proudly no matter my success or failure.

To my friends, old and new, for their continuous support and confidence.

To my beloved fiancé, Balaaji for being my best friend and sticking by my side through the ups and downs.

ACKNOWLEDGMENT

I want to express my deepest gratitude to my dissertation advisor, Dr. Bharat B Biswal for being a remarkable mentor and an inspiring researcher. Your knowledge and experience have immensely shaped my ability as a researcher and will guide me for the rest of my life. Through you, I have had the opportunity to contribute and be part of important research from around the world.

I am thankful for my co-advisor, Dr. Tara L. Alvarez, for her continued faith and guidance from the start to the end of this Ph.D. I also extend my sincere thanks to Dr. Yiyan Liu, Dr. Xiaobo Li, Dr. Xin Di, and Dr. Nancy Chiaravalloti for their time and invaluable feedback to improve the quality of this dissertation. Especially, appreciate the support from Dr. Nancy Chiaravalloti and her group for their help in participant recruitment that made this dissertation possible. I want to also thank all the physicians, scientists, psychologists, undergraduates and BME staff who helped me and joined me in this venture to understand the human brain.

I want to acknowledge the support from the New Jersey Commission for Spinal Cord Research for the pre-doctoral fellowship (CSCR15FEL002) conferred upon me. The award not only allowed the successful execution of my dissertation but inspired me to work hard towards the vision of the project.

Last, but not least, I am genuinely grateful to my father and my sister, for meticulously reading and reviewing this dissertation. I consider myself lucky to have met and worked with some wonderful people during my Ph.D. tenure. My heartfelt thanks to my friends, Thushini and Maryam for cheering me all these years and my colleagues and good friends, Rui, Suril, Xin, Marie and Azeezat for our shared passion of the brain.

TABLE OF CONTENTS

TABLE OF CONTENTS
(Continued)

Chapter **Page**

TABLE OF CONTENTS
(Continued)

Chapter **Page**

TABLE OF CONTENTS
(Continued)

Chapter **Page**

TABLE OF CONTENTS
(Continued)

Chapter **Page**

LIST OF TABLES

LIST OF FIGURES

LIST OF FIGURES
(Continued)

LIST OF FIGURES
(Continued)

Figure **Page**

LIST OF ABBREVIATIONS

ACC	Anterior Cingulate Cortex
AFNI	Analysis of Functional Neuroimages
ANOVA	Analysis of Variance
ANCOVA	Analysis of Covariance
ASIA	American Spinal Injury Association
AT	Ankle Tapping
AUC	Area Under the Curve
BA	Brodmann Area
BOLD	Blood Oxygen Level Dependent
CAT	Computational Anatomy Toolbox
CERB	Cerebellum
CO_2	Carbon Dioxide
DARTEL	Diffeomorphic Anatomical Registration Through Exponential Lie Algebra
FC	Functional Connectivity
FDR	False Discovery Rate
fMRI	Functional Magnetic Resonance Imaging
fNIRS	Functional Near-Infrared Spectroscopy
FOV	Field of View
FT	Finger Tapping
FTI	Finger Tapping Imagery
FTI + AO	Finger Tapping Imagery with Action Observation

LIST OF ABBREVIATIONS
(Continued)

FSL	FMRIB's Software Library
FUS	Fusiform Gyrus
GMV	Grey Matter Volume
Hb	Hemoglobin
HbO	Oxy-hemoglobin
HbR	Deoxy-hemoglobin
HbT	Total hemoglobin
HC	Healthy Controls
ICC	Intraclass Correlation Coefficient
IFG	Inferior Frontal Gyrus
INS	Insula
LI	Lateralization Index
M1	Primary Motor Cortex
MATLAB	Matrix Laboratory
MELODIC	Multivariate Exploratory Linear Optimized Decomposition into Independent Components
MD	Mediodorsal
MFG	Middle Frontal Gyrus
MNI	Montreal Neurological Institute
MOG	Mid Orbital Gyrus
MPRAGE	Magnetization-Prepared Rapid Gradient Echo Sequence
MRI	Magnetic Resonance Imaging

LIST OF ABBREVIATIONS
(Continued)

MTG	Middle Temporal Gyrus
PARA	Paraplegia
PCC	Posterior Cingulate Cortex
PCG	Precentral Gyrus
PFC	Prefrontal Cortex
PAF	Pure Autonomic Failure
PUL	Pulvinar
ROI	Regions of Interest
RSFC	Resting-State Functional Connectivity
RS-fMRI	Resting-State Functional Magnetic Resonance Imaging
S1	Primary Somatosensory Cortex
SCI	Spinal Cord Injury
SFG	Superior Frontal Gyrus
SMA	Supplementary Motor Area
SMN	Sensorimotor Network
SMG	Supramarginal Gyrus
SPM	Statistical Parametric Mapping
STG	Superior Temporal Gyrus
TE	Echo Time
TETRA	Tetraplegia
THAL	Thalamus

LIST OF ABBREVIATIONS
(Continued)

TIV	Total Intracranial Volume
TTG	Transverse Temporal Gyrus
TR	Repetition Time
VL	Ventrolateral

CHAPTER 1

OBJECTIVE

Traumatic Spinal Cord Injury (SCI), often caused by compression or contusion of the spinal cord, is characterized by neurological changes at both spinal and supra-spinal level of the central nervous system. Hence, even a minor injury has long-term impact on the patient's sensory-motor and autonomic functionality leading to paralysis of lower (paraplegia) or both lower and upper limbs (tetraplegia) with severe cases affecting respiratory, urinary and gastrointestinal functioning as well[1]. As of 2018, there are 17,700 new cases of SCI every year in the United States[2]. Rehabilitative and pharmacological approaches are found to be effective in regaining, to varying extent, motor, sensory and autonomic functions[3]. In spite of treatment, 60-80% of the patients develop maladaptive outcomes such as nociceptive/neuropathic pain and phantom limb syndrome [4-8]. This disparity among treatment outcomes can be explained only partly by the heterogeneity in factors such as age, type of injury, time after injury, duration of therapy, etc., while the treatment outcomes seem to be predominantly regulated by underlying neuroplasticity (recovery mechanism)[9].

Neuroplasticity is a normal characteristic of the brain during learning and memory encoding which, in the event of an injury is accelerated, triggering a rapid neural reshaping at both the level of local synapses and neuronal networks[10]. Previous research in SCI shows that lack of sensorimotor drive induces cortical gray matter atrophy accompanied by functional expansion of the affected sensorimotor area [11-13]. Such cortical alterations may directly or indirectly be influenced by lower motor centers [12,14,15]. Neurophysiological

findings of SCI patients mostly report an overall decrease in functional activity of cortical sensorimotor nodes with only a few cases of increased thalamic and cerebellar activity [16-18]. As structural findings of SCI patients show decreased grey matter and white matter volume in both sensorimotor and non-sensorimotor related regions after SCI [19-21], it is unknown whether tissue atrophy observed in non-motor related areas has concomitant functional consequences. Further, it is important to note that not all cortical/subcortical reorganization after SCI leads to functional recovery as they may also lead to misfiring causing spasticity, phantom sensations and neuropathic pain[9]. For example, thalamus dysfunction has long been associated with SCI pain but is often overlooked due to lack of non-invasive techniques that can reliably study changes in these regions following SCI [22,23].Therefore, understanding and identifying biomarkers of maladaptive plasticity will require a systematic investigation of structural and functional reorganization in cortical and sub-cortical areas of both sensorimotor and non-sensorimotor function.

Hence, we propose a multimodal approach using Magnetic Resonance Imaging (MRI), resting-state Functional Magnetic Resonance Imaging (fMRI) and Functional Near-Infrared Spectroscopy (fNIRS) to investigate changes in the structural integrity, intrinsic functional activity and task-evoked activity after SCI.

MRI provides the opportunity to non-invasively and reliably study structural neuroplastic changes in the human brain. fMRI signal measured in response to different motor tasks can indirectly elucidate the local changes in neural activity associated to the motor task between patients and motor-intact individuals. Resting-state fMRI is a popular variant of fMRI widely used to study whole brain intrinsic activity in the absence of an exogenous stimulus[24-27]. Large-amplitude spontaneous low-frequency (~0.01-0.1 Hz)

fluctuations in the fMRI signal can be temporally correlated across brain regions to obtain a measure of functional integration across cortical and subcortical areas [28]. However, task-fMRI is based on the assumption of consistent neurovascular coupling between different regions[29]. Individuals with SCI especially at or above the T5 level experience impairment in the properties of cerebral blood flow viz dynamic cerebral autoregulation, cerebrovascular reactivity and neurovascular coupling[30] signifying that motor task-evoked activation measured using fMRI may not represent true neuronal effects without consideration of its vascular etiology. fNIRS, unlike task-based fMRI, can directly measure the oxy and deoxyhemoglobin concentration in response to diverse type of movements[31]. By quantifying the net increase in hemoglobin concentration in response to a simple vasoactive stimulus termed as cerebrovascular reactivity[32], we could independently assess the effect of vascular differences on task-evoked functional alterations after SCI. In addition to improving our understanding of supraspinal pathophysiology after SCI, the feasibility of fNIRS in detecting motor-related reorganization would also help future studies to test naturistic movements involved in physical therapy to understand and improve therapeutic techniques. To this end, we propose the following specific aims and sub aims,

1 Investigate the differences in the brain tissue volume between SCI and healthy controls (HC) and the effect of duration of injury on brain tissue volume in SCI using MRI. (Chapter 3)

   1.a To examine the differences in grey matter volume and white matter volume of the brain between paraplegic SCI, tetraplegic SCI and HC

   Hypothesis: Deafferentation will lead to widespread decrease in grey matter volume and white matter volume in SCI and the extent of grey matter loss will be proportional to the extent of injury.

1.b Investigate the effect of duration of injury on the grey matter and white matter volume after SCI.

Hypothesis: Longer durations of deafferentation will lead to greater loss of grey matter volume and white matter volume in the brain after SCI.

2 Investigate differential functional connectivity patterns of cortical and subcortical structures in SCI in comparison to HC using fMRI. (Chapter 4)

2.a Determine the differences in resting state functional connectivity (RSFC) of whole brain between SCI group and HC.

Hypothesis 1: SCI will result in greater resting state parameters in sensorimotor and secondary sensorimotor regions involved in sensory-based attention as a compensatory response to loss of sensory afferents.

Hypothesis 2: SCI will result in altered functional connectivity in regions of altered grey matter volume.

2.b Determine, using RSFC, alterations in the spatial and temporal extent of thalamus in SCI when compared to HC.

Hypothesis: As most of the thalamic nuclei relay sensory information associated to motor commands, SCI will result in altered functional connectivity of multiple thalamic sub-nuclei associated to various sensory and motor processing.

3 Validate the use of fNIRS to differentiate the brain activity associated to different motor tasks in SCI when compared to HC. (Chapter 5)

3.a Compute the test-retest reliability of a) resting-state, b) motor-task and c) breath hold data in HC recorded during two time points.

Hypothesis 1: Hemodynamic response measured using fNIRS during the different types of tasks are reliable and reproducible.

3.b Evaluate alterations in the RSFC of the sensorimotor network in SCI group in comparison to HC.

Hypothesis: SCI will result in decreased intrinsic functional connectivity of bilateral primary motor cortex when compared to HC.

3.c Determine the cerebrovascular reactivity in response to breath holding task in SCI and HC.

Hypothesis: Net increase in total hemoglobin concentration in response to a breath hold induced hypercapnia task will be reduced in SCI patients in comparison to HC.

3.d Determine differences in task-evoked hemodynamic response of different motor tasks while accounting for differences in the cerebrovascular reactivity after SCI.

Hypothesis 1: Hemodynamic response to the different motor tasks are task-specific and are quantifiable using fNIRS.

Hypothesis 2: Impaired supraspinal control of sympathetic nervous system after SCI will result in altered neurovascular coupling in SCI patients hence calibration using breath hold activation will account for the vascular effects on task induced hemodynamic response.

CHAPTER 2

NEUROPHYSIOLOGY OF SPINAL CORD INJURY

2.1 Background

Traumatic SCI is usually the result of a contusion or compression of one or more vertebrae caused by a sudden blow to the spine due to falls, automobile accident, violence etc. As the spinal cord is the transmission line that carries neuronal signals, SCI disrupts nerve conduction including somatic and autonomic signals from the brain to the rest of the body (Figure 2.1a). Depending on the severity of the damage, the injury could result in partial to complete loss of motor, sensory and autonomic function. The American Spinal Injury Association (ASIA) has detailed the International Standards for Neurological Classification of Spinal Cord Injury to classify the neurological extent of injury based on the completeness of injury (complete or incomplete), level of injury (paraplegia or tetraplegia) and type of deficit (dermatome/sensory and/or myotome/motor)[33].

In a complete spinal cord injury, the spinal cord is severely injured to the extent that no signals are transmitted beyond the point of injury, resulting in complete loss of motor and sensory functions in the regions below the injury. In partial or incomplete SCI, some of the nerve endings are still intact hence retaining some level of motor and/or sensory functions below the point of injury [34]. The body regions with motor and/or sensory function loss is dependent on the level of the injury/lesion on the spinal cord. Based on the level of the injury/lesion on the spinal cord, SCI can be classified as paraplegia or tetraplegia. Paraplegia is the result of an injury or lesion to the thoracic or lumbar regions

(i.e., T1 or below) of the spinal cord, resulting in complete or partial paralysis of the lower limbs.

Tetraplegia is caused by an injury to the cervical segments (i.e., C7 and above) of spinal cord, resulting in complete or incomplete/partial paralysis of all four limbs with varying levels of autonomic impairment[35]. Based on the anatomical location of lesion within the cord the injury may also be classified as anterior cord, brown-sequard's, cauda equina, central cord or posterior cord syndrome.

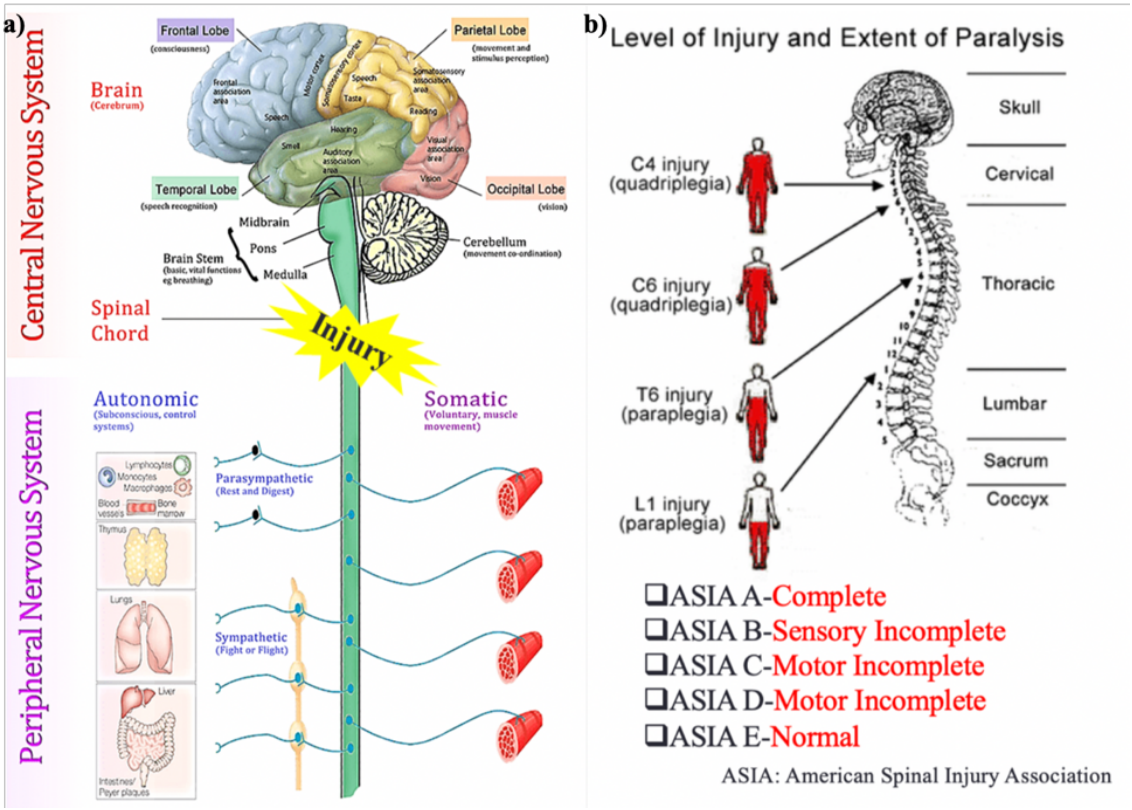

Figure 2.1 a) Autonomic and somatic effects of Spinal Cord Injury, b) Level of injury and the extent of paralysis after Spinal Cord Injury.

(Source: https://pin.it/umvcy4jc265ldl)

Injury or lesion to thoracic cord segments T1 –T5 affects mid-back and abdominal muscles resulting in the inability of the injured to use their trunk or legs. Injury or lesion to thoracic nerves T6 –T12 affects the abdominal muscles to below abdominal muscles leading to weak or no voluntary control of lower extremities but normal upper body movement with some ability to control and balance the trunk. Injuries to lumbar and sacral regions also cause some loss of function to lower extremities especially legs and hips as shown in Figure 2.1b. Consequently, individuals with thoracolumbar injury with no sensory or motor functions in their sacral segments are referred to as individuals with complete paraplegia. While individuals with cervical cord level injury and no sensory or motor functions in sacral segments with or without autonomic dysfunction are referred to as individuals with complete tetraplegia[33]. The most prevalent form of SCI is the incomplete tetraplegia, followed by incomplete paraplegia, although, both complete and incomplete types impose a challenge for treatment[2].

There are currently 288,000 people living in the United States with SCI with approximately 17,700 new cases added every year. The average age of individuals with SCI is 43 years and the average life expectancy for someone at 40 years of age is between 9-35 years depending on the level and extent of the injury[2]. With improved life expectancy and mounting number of people living with SCI, there is an urgent need to address the various functional limitations and altered quality of life in these individuals. SCI primarily affects the mobility of individuals, most of whom are young and middle-aged people in the most productive phase of their life. Thus, adversely affecting their ability to perform activities of daily living and their quality of life, in many cases requiring caregivers to perform activities of daily living. In addition, they also present with secondary

complications (such as cardiovascular, genitourinary and respiratory problems etc.) requiring frequent hospital revisits. The incidence of sensory abnormalities such as neuropathic pain, phantom limb syndrome and spasticity are also high, unpredictable and resistant to pharmacological treatment[36,37]. In addition to the personal costs, the societal cost is substantial with approximately $14 billion expenditure on their care and management each year.

Immediately after SCI there is a high risk of developing spinal shock which is the loss or depression of spinal reflexes below the level of injury[38]. Development of spinal shock has been associated with poor neurorecovery than those without. Further the pathological changes at the site of injury include hemorrhagic necrosis in the grey matter and white matter leading to edema and ischemia[38]. Hence the immediate treatment strategy of the physician is to prevent further damage to the spinal cord, prevent spinal shock and preserve neural tissue for neurorecovery. Subsequent treatment involves conventional physical therapy to induce functional recovery, although, complete neurological recovery is elusive with only a small fraction (~1%) attaining complete recovery at the time of hospital discharge.

Researchers are continually studying the mechanisms of secondary damage to the spinal cord including restriction of blood flow, excitotoxicity, inflammation, free radical release, and apoptosis to save axons and reduce disabilities[1]. Again however, the number of individuals achieving complete neurological recovery is miniscule compared to the 60-80% of patients developing maladaptive conditions such as neuropathic pain[6,39]. The huge variance among patients in terms of age, type of injury, severity of injury, time after injury, duration of therapy, mechanism of recovery etc. makes it difficult to determine a definite

recovery path. Therefore, identifying the mechanisms leading to desirable and undesirable outcomes is of clinical importance that is yet to be fully understood.

2.2 Neuroplasticity after SCI

The neurorecovery process of the central nervous system (at the spinal cord as well as the brain) entails a phenomenon known as neuroplasticity. Neuroplasticity is a normal characteristic of the nervous system necessary for learning, and memory encoding that in the event of an injury becomes accelerated to protect and induce a rapid neural reshaping at the level of local synapses as well as at the level of neuronal networks[10]. The course of this reshaping (reorganization or remapping) in the spinal cord and brain is thought to be decided by the set of cellular events that occur during the acute phase (1-3 months post-injury). And may continue in the spinal cord, brainstem and brain for months to years after the injury and do not always result in functional recovery[9]. Molecular and neurochemical changes at the site of injury include neuronal and glial cell death by necrosis and hemorrhage[40]. In addition to the cellular damage, immune response to the injury releases cytokines, growth factors and neurotrophins that influence the outcome of nerve damage at the site of injury and in supraspinal centers of the body[40]. Hence, neuroplasticity after SCI involves an intricate relationship between neurochemical, physical and functional changes at the level of the spinal cord, that reflect/drive neuroplastic changes in the brainstem, subcortex and cortex.

It is known through animal and human studies that the lack of sensory drive induces a protective functional reorganization in the primary motor (M1) and somatosensory (S1) cortex of the brain associated with lost peripheral function[9,13,15,18,41-44]. Reorganization or

rewiring may occur due to long term deafferentation leading to dendritic sprouting or deafferentation causing disinhibition of suppressed inputs or even due to long term potentiation of weaker synapses[41]. Such cortical changes are thought to originate from both dormant synapses and emergence of lateral connections at the level of brainstem and thalamus[15,41]; however, it is unknown whether subcortical changes influence other cortical and subcortical regions (outside of the sensorimotor core) to adapt, compensate or respond to the cortical region that lost sensory afferent innervations[15].

CHAPTER 3

ANATOMICAL BRAIN DIFFERENCES AFTER SPINAL CORD INJURY (AIM 1)

3.1 Introduction

3.1.1 Background

The pathophysiology of SCI is not caused by lesions in the brain, although animal and human studies have shown that structural alterations in S1 and M1 contribute significantly to behavioral recovery in both SCI and stroke[45-47]. Our ability to gain a detailed understanding of the mechanisms that mediate such cellular to large-scale changes in the human central nervous system has been limited by the lack of noninvasive tools. Neuroimaging provides the perfect opportunity to reliably and non-invasively study the neuroplastic changes of the brain in humans. Current neuroimaging techniques enable examine the structure, function and biochemical activity of the nervous system either directly or indirectly[48]. Techniques such as magnetic resonance imaging (MRI) or computed tomography are primarily used to capture high-resolution structural characteristics of the brain to measure the morphological differences associated to injury, neurological conditions and healthy aging process. MRI is predominantly favored over other imaging modalities for diagnosis and prognosis due to the high spatial resolution and non-invasive non-ionizing nature of the technique[49].

3.1.2 Magnetic Resonance Imaging

MRI was first developed in late 1970's after the discovery of the nuclear magnetic resonance phenomenon[50]. Based on the nuclear magnetic resonance property, a

radiofrequency emitted at the resonance frequency can excite the hydrogen molecules in the biological tissue triggering it to switch energy states and emit electromagnetic signal in the process. The electromagnetic signal is then acquired in the frequency space and transformed using inverse Fourier transform to generate 3-D images. Since its development, MRI has become the gold standard for studying neurological changes in tissue structure due to its excellent resolution and detail in differentiating the different tissue types. MRI allows the visualization and segmentation of the spinal cord, soft tissues, disc, brain tissue and fluid better than other imaging modalities. Kulkarni and colleagues were the first to apply MRI in people with SCI to identify patterns and features such as hemorrhage and edema in the spinal cord that could help prognosticate the injury[51]. Subsequently, MRI of the brain stem and brain in the sub-acute or chronic period has become an excellent tool to gain insight into the evolution of changes in supraspinal tissue morphology especially in individuals with pathological conditions such as SCI, traumatic brain injury, Alzheimer's etc[52-55].

3.1.3 Application of Magnetic Resonance Imaging in SCI

An early study by Wrigley and others showed reduced cortical grey matter volume (GMV) in M1, medial prefrontal cortex, anterior cingulate cortex, temporal cortex, hypothalamus and insular cortex in individuals with complete paraplegic SCI subjects using MRI. [56] Similar effects on sensorimotor cortex have been demonstrated in tetraplegic SCI using voxel based morphometry (VBM) and cortical thickness technique.[19] Particularly, decrease in grey matter density or GMV has been observed in denervated leg area of M1 and S1. Decrease in white matter integrity of motor cortex and visual cortex after SCI is also reported.[57] However, these results have not been consistent with the past literature, where

some studies report no differences in cortical GMV after SCI.[20,58] A more recent study showed an association between decreased GMV in S1 and presence of neuropathic pain in SCI.[59] While, Yoon and colleagues reported decreased metabolism in dorsolateral and medial frontal cortex and decreased GMV in anterior insula and anterior cingulate cortex in individuals SCI and neuropathic pain. [60] These differences between studies may be attributed to differences in age, level of injury, completeness of injury, duration of therapy, secondary deficits etc. For example, Villiger and group demonstrated an increase in cortical GMV after a mere 4 weeks of rehabilitation in Chronic SCI individuals, clearly indicative of the effect rehabilitation may have on brain structure.[14]

The work of Bruehlmeier (1998) revealed that the magnitude of cerebral activation during hand movement measured using positron emission tomography is affected by lesion level with higher lesion levels causing greater activation.[61] Moreover, as the extent of sensorimotor and autonomic impairments are greater in cervical SCI when compared to thoracic or lumbar injury simply due to greater number of enervations received at these spinal cord locations; a difference between paraplegia and tetraplegia types of SCI is expected. However, no studies have demonstrated cortical structural differences between paraplegia and tetraplegia types of SCI.

The present study sought to investigate group differences while accounting for factors other than rehabilitation that could influence GMV and white matter volume (WMV) in SCI. By studying complete SCI within the first two years of injury, we expect to mitigate any possible effects from between subject differences in completeness of injury or long post injury durations that other studies may have encountered. Here, we hypothesized that individuals with complete SCI would demonstrate decreased GMV and

decreased WMV reflecting the level of function retained, with higher injury levels causing greater loss of sensory and autonomic afferents and therefore greater GMV loss. To test the hypothesis we applied VBM technique using high resolution MRI on complete SCI individuals within two years of injury in comparison to HC while adjusting for age and total GMV [62,63] .

3.2 Methods and Materials

3.2.1 Participants

Twenty-three healthy participants and thirty-six age matched individuals with complete traumatic SCI (24 paraplegia, 15 tetraplegia) were recruited in this study. All participants were right handed with no history of psychiatric disorders or brain trauma and were in a stable, chronic clinical condition. Further, a comprehensive neurological examination was performed on all participants to exclude accompanying neurological disorders of the peripheral and central nervous system. The level and extent of SCI were assessed based on the International Standards for Neurological Classification of Spinal Cord Injury (ISNCSC) that allows performing semi-quantitative assessment of motor (10 muscles on each side of the body) and sensory deficits (pin prick and light touch) in the lower and upper extremities. These scores were used to clinically characterize the type (paraplegia or tetraplegia) and extent (complete or incomplete) of injury. All the procedures were performed in accordance to the guidelines approved by the Ethics Committee of Third Hospital of Hebei Medical University and all participants gave their written consent to participate in the study.

3.2.2 MRI Acquisition and Preprocessing

High resolution structural images were acquired using magnetization-prepared rapid gradient echo sequence (MPRAGE). The imaging parameters for anatomical images were as follows: FOV = 240 mm, 512×512 matrix, TR = 2300 msec, TE = 2.91 msec, flip angle = 90°. The whole brain was imaged in an axial configuration where 176 slices were collected, and each slice was 1 mm thick.

The data processing was performed using CAT12 toolbox (http://dbm.neuro.uni-jena.de/cat/) an extension of Statistical Parametric Mapping (SPM12) (http://www.fil.ion.ucl.ac.uk/spm/) software under MATLAB R2012b environment (http://www.mathworks.com/). The origin of anatomical images was manually centered to anterior commissure of the brain for all subjects to reduce local maxima problem during normalization. The reoriented images were corrected for bias field in-homogeneities and normalized using an affine transform. The bias-field corrected images were segmented to grey matter, white matter and cerebrospinal fluid probability maps using segment tool of CAT12 toolbox of SPM12, which is an extension of the default unified segmentation algorithm. The segmented grey matter images with a resolution of 1.5×1.5×1.5 mm were normalized to MNI template using Diffeomorphic Anatomical Registration Through Exponentiated Lie algebra (DARTEL) [64] technique and were accounted for individual brain size (modulated). The template used for DARTEL registration was pre-generated from the T1 images of 550 healthy adults available in CAT12 toolbox. As part of the quality check process, the normalized bias corrected anatomical images were visually inspected for all subjects to make sure there are no apparent registration errors. Next, the mean overall correlation and weighted image quality measures available in CAT12 toolbox were

investigated to identify outliers. Subjects with mean correlation (or weighted image quality) measure that was 1.5 times the intra-quartile range or more than the third quartile or less than the first quartile were considered as outliers. One healthy subject and one paraplegic SCI subject had mean correlation and weighted image quality measure in the suspected outlier range. Two subjects (1 healthy control and 1 paraplegic SCI) with poor image quality and 15 patients (7 paraplegic SCI and 8 tetraplegic SCI) with incomplete sensory motor scores information were removed from subsequent analysis. The segmented and normalized images of remaining 45 subjects (22 HC, 16 paraplegia and 7 tetraplegia subjects) were smoothened using an 8mm full width at half maximum Gaussian kernel. The normalized, modulated and smoothed GMV maps of 45 subjects were used for statistical analysis. The demographic information of the 23 patients is presented in Table 3.1.

Table 3.1 Demographic Information of Patients with Paraplegia and Tetraplegia included in the Current Study

Subject ID	Age	Gender	Duration of Injury (Days)	ASIA Motor scores (Total: 100)	ASIA Sensory scores (pin prick + light touch) (Total: 224)
P001	45	F	53	50	97
P002	45	F	62	50	92
P003	34	M	268	50	96
P004	31	F	113	51	160
P005	34	M	61	50	136
P006	40	M	132	40	136
P007	40	M	300	40	136
P008	25	M	152	54	192
P009	44	M	83	50	136
P010	28	M	88	60	152
P011	25	M	619	70	209
P012	40	M	324	57	162
P013	36	M	72	54	174
P014	25	M	206	65	189
P015	35	M	90	40	132
P016	24	M	329	63	144
T001	27	M	186	30	72
T002	31	M	45	26	96
T003	34	M	58	16	78
T004	42	M	73	20	124
T005	56	M	228	13	18
T006	39	M	55	16	128
T007	27	M	73	7	26

Note: Subject ID P-- and T-- denote paraplegia and tetraplegia subjects respectively.

3.2.3 Tissue Volumetric Analysis (Aim 1a)

Statistical analysis was performed to identify voxels with significantly altered tissue volume in paraplegic SCI and tetraplegic SCI when compared with HC.

i) Voxel Based Morphometry Analysis: Regional tissue volume differences between HC, paraplegia and tetraplegia groups were computed using one-way ANCOVA with SPM12's second level model for each grey matter and white matter tissue probability maps.[65] After checking for orthogonality, TIV, age and gender were added as covariates in the model to account for inter-subject differences. Total intracranial volume was calculated from AC aligned MPRAGE images using CAT12 toolbox. Issue regarding multiple comparison was corrected by applying an extended threshold using false discovery rate (FDR) approach at uncorrected $p<0.001$.

ii) Region of Interest (ROI) Based Analysis: We further performed post-hoc analysis using ROI based approach on the clusters identified from the above method. Using the peak F-value coordinates obtained from voxel-wise ANCOVA, a ROI of 5 mm radius was generated for each of the clusters identified. The underlying volume of all the ROI's was extracted for all subjects. A partial-correlation using linear regression was first applied to remove the effect of total intracranial volume, age and gender on the average tissue volume of all ROI's. A two-sample t-tests was performed on the regressed tissue volume to compare a) HC vs. paraplegia, b) HC vs. tetraplegia and c) paraplegia vs. tetraplegia. A corrected p-value after FDR correction was used to identify ROIs of significant GMV or WMV differences for each of the three comparisons.

3.2.4 Effect of Post-Injury Duration (Aim 1b)

As both spontaneous and treatment induced recovery in SCI is expected to be time dependent, effect of injury duration on mean a) GMV and b) WMV was computed using a voxel-wise one sample t-test with effect of injury as covariate of interest and TIV, age and gender as covariates of no interest. Issue regarding multiple comparison was corrected by applying an extended threshold using FDR approach at uncorrected $p<0.001$.

3.3 Results

3.3.1 Tissue Volumetric Analysis (Aim 1a)

i) Voxel-based morphometry analysis: Output of voxel-wise ANCOVA for grey matter probability maps was threshold at FDR-corrected $p<0.05$ (uncorrected $p<.001$ with FDR extended threshold of 637 voxels). As displayed in Figure 3.1, one-way ANCOVA comparing the groups resulted in altered GMV in 2 clusters.[66] The peak difference between the three groups was observed in cluster 1 centered at right olfactory cortex extending dorsally to the right inferior frontal gyrus pars orbitalis and cluster 2 centered at right mid-orbital gyrus extending laterally to left mid-orbital gyrus, left ACC and ventrally to right rectal gyrus. A total of 2 clusters with peak activation in 5 regions survived the statistical threshold and their coordinates are presented in Table 3.2. Voxel-wise ANCOVA comparing WMV between the three groups resulted in no significant effects after FDR correction, therefore the subsequent ROI based analysis was performed only for the results from GMV comparison. These findings are also presented in the recent publication[63].

ii) ROI based analysis: ROI based analysis was performed on the five regions listed in Table 3.2. HC and paraplegia in general appear to have greater GMV than tetraplegia in all

five ROI's (shown in Figure 3.2). Two sample t-test comparing the GMV of the five ROI's between HC and paraplegia revealed no significant difference ($p>0.05$) between the two groups after multiple comparison correction. However, two sample t-tests comparing the GMV of the five ROI's between a) HC and tetraplegia and b) paraplegia and tetraplegia revealed significant difference in all five ROI's at FDR-$p=8.97x10^{-5}$ and FDR-p=0.0.0398 respectively.

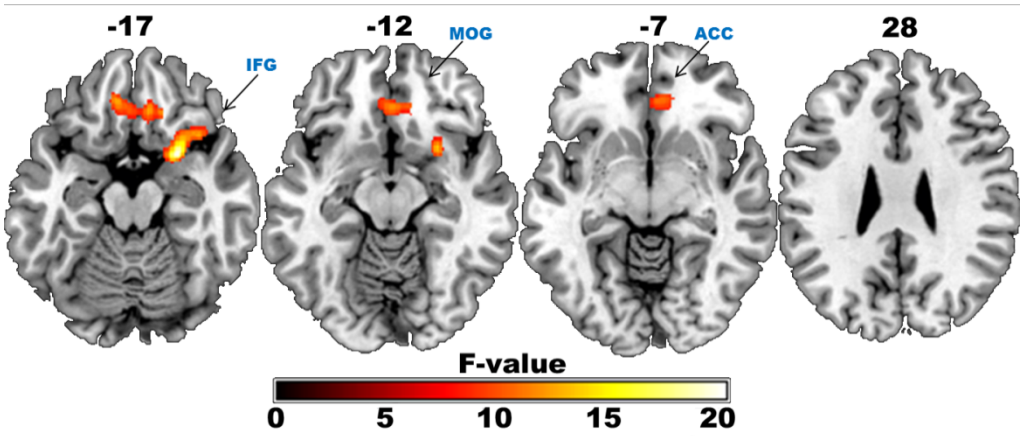

Figure 3.1 T-statistics map showing regions of right inferior frontal gyrus and bilateral mid orbital gyrus extending to anterior cingulate cortex with significantly altered GMV between the three groups at FDR corrected $p<0.001$, $k=637$ voxels. Z values on top represent the Z coordinate in MNI space. The color bar represents F-values shown in the f-statistics maps.

Table 3.2 List of Regions with Altered GMV between the three groups

Cluster	Cluster Size (Voxels)	MNI ANAT Regions*	F-value	x, y, z (mm)*
1	637	Right Olfactory Cortex (R.OC)	20.51	+26 +9 -15
		Right Inferior Frontal Gyrus Pars Orbitalis (R.IFG)	15.23	+36 +18 -18
2	744	Right Mid Orbital Gyrus (R.MOG)	12.90	+10 +33 -15
		Left Rectal Gyrus (L.ReG)	12.75	-8 +38 -18
		Left Mid Orbital Gyrus (L.MOG)	12.24	+0 +33 -14

Note: Results shown at FDR-corrected $p<0.05$ and their peak F-values. * indicates coordinates of the peak voxel in each cluster based on MNI Macro Anatomical label.

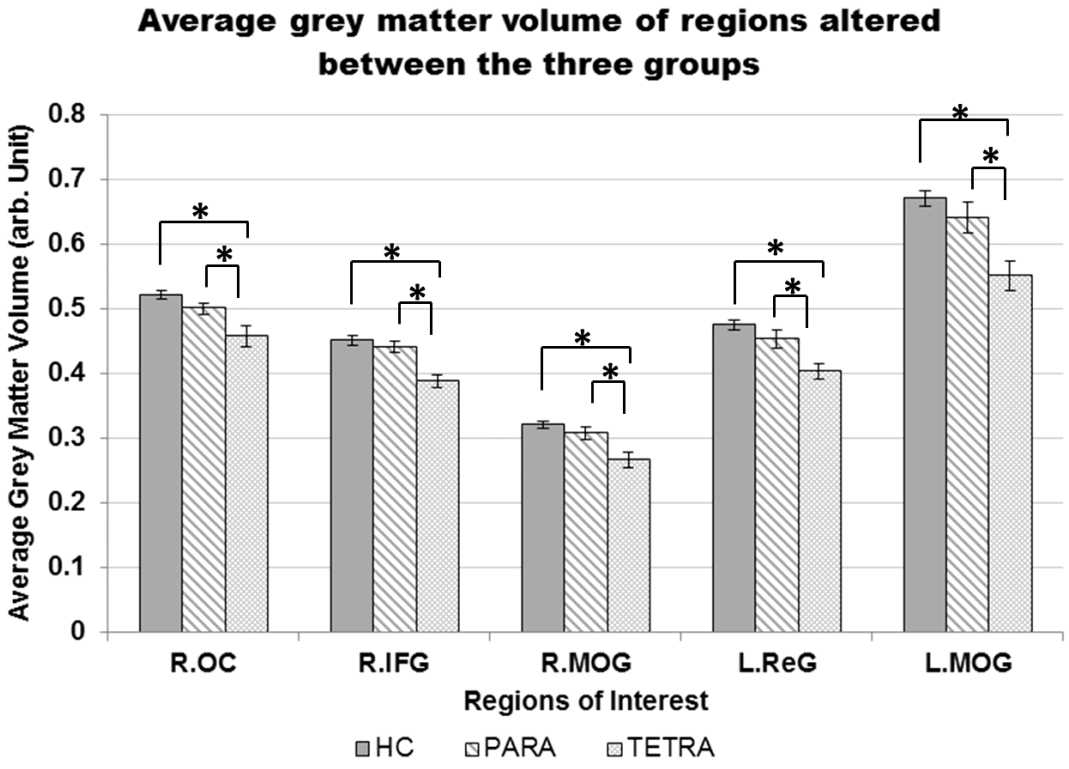

Figure 3.2 ROI based analysis of regions obtained from voxel-wise ANOVA: Bar plots of average GMV of the five clusters for HC, Paraplegia and Tetraplegia groups. * indicates a statistical significance of FDR-corrected $p<0.05$ between the groups. Error bars indicate standard error of mean.

3.3.2 Effect of Post-Injury Duration

Voxel-wise one sample t-tests for mean effect of injury duration on GMV at a lenient threshold of $p<0.005$ with $k=1443$ voxels resulted in numerous areas that were positively correlated with injury duration. The GMV of left middle frontal gyrus (MFG), left inferior frontal gyrus/anterior insula (IFG/INS), bilateral mid orbital gyri (MOG), right superior frontal gyrus (SFG) and right superior temporal gyrus (STG) extending to right intraparietal lobe in SCI group appears to decrease immediately post-injury and increase in the months after injury. As seen in Figure 3.3b, increasing the threshold to $p<0.001$ with $k=1549$ voxels resulted in only one cluster with peak T-value in L.IFG pars triangularis, centered at L.MFG that demonstrated a positive correlation with duration of injury. The Pearson's correlation between average GMV (after accounting for TIV, age and gender) of L.MFG/L.IFG with duration of injury was + 0.844 (shown in Figure 3.3). The list of significant clusters and their coordinates are summarized in Table 3.3.

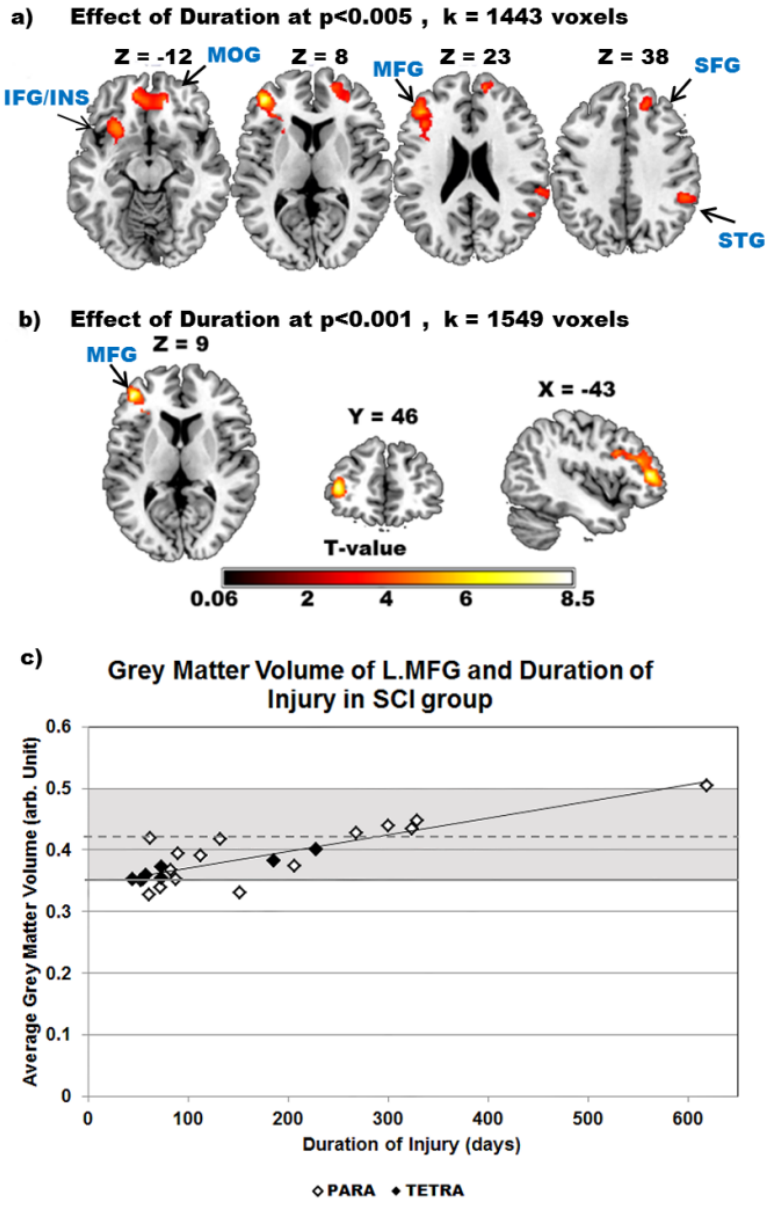

Figure 3.3 Effect of duration of injury on GMV: a) At a lenient threshold of uncorrected-p<0.005 with k=806 voxels, regions of left middle frontal gyrus (MFG), left inferior frontal gyrus/anterior insula (IFG/INS), bilateral mid orbital gyri (MOG), right superior frontal gyrus (SFG) and right superior temporal gyrus (STG) are positively correlated with duration of injury in SCI group. b) At uncorrected-p<0.001 with k=1549 voxels, a cluster with peak T-value at L.IFG pars triangularis and centered at left MFG, is positively correlated with duration of injury in SCI group. c) Scatter plot demonstrates the relationship between average GMV of left MFG cluster (1549 voxels) from plot b and duration of injury (in days) in SCI group. For reference, the dashed line and the shaded area indicates the mean and standard deviation of GMV of left MFG cluster in HC. The values on top of T-maps represent the Z coordinate in MNI space. The color bar represents the T-values of the map shown.

Table 3.3 List of Regions with Significant Positive Correlation between Grey Matter Volume and Duration of Injury in SCI group

Cluster	Cluster Size (Voxels)	MNI ANAT Regions*	T-value	x, y, z (mm)*
1	3750	Left Middle Frontal Gyrus	8.62	-42 +45 +10
		Left Middle Frontal Gyrus	5.62	-44 +34 +22
		Left Posterior Orbital Gyrus	5.39	-27 +22 -10
2	1443	Right Superior Temporal Gyrus	5.49	55 -38 +15
		Right Middle Temporal Gyrus	4.93	+51 -48 +10
		Right Angular Gyrus	4.56	+56 -54 +20
3	3721	Left Medial Frontal Cortex	5.15	-10 46 -14
		Right Superior Frontal Gyrus	4.89	14 56 21
		Right Superior Frontal Gyrus	4.84	15 42 32

Note: Results shown at uncorrected voxel wise threshold of $p<0.005$, FDR cluster=1443 voxels * indicates Coordinates of peak statistical difference in each cluster based on MNI Macro Anatomical label. T-value column represents the t-value of peak coordinates.

3.4 Discussion

3.4.1 Cortical Grey Matter Atrophy after SCI

In the first analysis comparing GMV of HC, paraplegia and tetraplegia, 2 cortical clusters were significantly altered at FDR-corrected $p<0.05$, that too predominantly extending to IFG/aINS, olfactory cortex, bilateral MOG and ventral ACC. In contrast, no regions showed significantly altered WMV between the three groups. Although several studies have observed grey matter differences within the sensorimotor regions, only a small number of studies have shown GMV differences in secondary motor related regions after SCI. Even fewer studies have reported decrease in white matter volume of bilateral pyramids and cerebral peduncle after SCI [19]. Our results overlap with Wrigley, P.J. (2009), where they show decreased GMV in regions associated with emotion such as medial prefrontal cortex, anterior cingulate cortex along with insula and hypothalamus in complete thoracic SCI at an average post-injury duration of 12 years. [56] In addition to disrupting motor and sensory pathways, SCI also causes deafferentation of visceral and skin interoceptive afferents to the neocortex. Interestingly, orbito-frontal cortex, ACC, insula and operculum, are also the major locations of interoceptive and affective processes. Orbito-frontal cortex is believed to be involved in emotional executive functioning by conveying the affective value of external sensory information to the autonomic nervous system through reciprocating connections to both the amygdala and sensory cortices (as seen in primate tracing studies).[67] The level of interoception sensitivity has been shown to positively correlate with extent of emotions experienced in healthy individuals. [68] In fact, Pistoia, F. and colleagues have shown decreased interoceptive awareness in patients with

SCI while responding to an emotional stimulus. [69] Therefore, we could argue that lack of interoceptive inputs could have influenced alterations in GMV of these regions.

Furthermore, it is known through several studies that regions of orbito-frontal cortex, ACC, pre-frontal cortex, insula along with subcortical regions present with decreased GMV as a pain signature in certain pain conditions. [70,71] Though it is well established that chronic pain is a common comorbidity of SCI, the lack of information regarding the pain status of the current cohort makes it difficult to conclude these GMV changes as neural correlates of acute or chronic pain.

While patients with SCI frequently experience impairments of physiological, nociceptive and affective nature; olfactory dysfunction, is rather an under explored but not atypical consequence of SCI. [36,72-74] Loss of GMV in the orbitofrontal cortex and insular cortex regions is common to both idiopathic olfactory dysfunction and chronic rhinosinusitis conditions with olfactory deficits [75,76]. A similar decrease in GMV of these regions after complete SCI suggests possible effect of cortical grey matter atrophy on olfactory functioning in these patients. For that reason, further studies are required to comment on the dynamic relationship between interoception and affective processing in SCI to identify whether lack of interoceptive inputs could consequently alter emotion, pain and olfactory processing that further depreciates the quality of life for these individuals.

While these outcomes contradict the findings of the studies that report no grey matter structural changes after SCI, it is also interesting that we did not observe significant GMV differences within sensorimotor regions as majority have reported. [19-21,58,77] These studies have shown significant decrease in GMV of M1 and S1 areas representing lost motor function. Different rehabilitation techniques could have contributed to this disparity;

though, it is important to note that GMV differences interpreted as grey matter loss could also occur due to underlying cellular differences in cell size, axonal sprouting, dendritic pruning, angiogenesis as well as non-neuronal changes that all contribute to some of the opposing observations between VBM studies. [78]

All ROI's showed a similar trend in difference between the subgroups where tetraplegia had greater GMV loss than paraplegia. It would be safe to assume that higher cord level injuries are expected to result in greater loss of cortical GMV although the magnitude of GMV may not necessarily be proportional to the severity of the injury. Greater decrease in cortical GMV after tetraplegia when compared to paraplegia could simply be due to greater functional retention in paraplegia. For example, injury to C8 results in 22 disconnected segments, 12 thoracic, 5 lumbar and 5 sacral segments as compared to an injury to T7 resulting in 15 disconnected segments, 5 thoracic, 5 lumbar and 5 sacral segments. In addition, the cross-sectional area of C2 level is reported to be smaller in the anterior-posterior direction of tetraplegia group than paraplegic group likely suggestive of wallarian axonal degeneration following tetraplegic SCI [79]. Furthermore, IFG including pars triangularis (BA 45) and dorsal lateral prefrontal cortex (BA 46) has been shown to be associated with resolving incongruence between intention and sensory feedback of motor movements.[80] It is agreed upon that SCI patients lack proprioceptive information to successfully initiate feedforward or feedback pathways and rely heavily on visual relay. Such conflict between intention of movement and sensory feedback is expected to be substantially higher in tetraplegia due to greater loss of body representation.

3.4.2 Effect of Post-Injury Duration

Mean effect of duration of injury on the GMV revealed GMV of prefrontal cortex, orbitofrontal cortex, INS and temporo-parietal regions increased with increasing post-injury duration in SCI group. Spontaneous plasticity following SCI could result in decreased GMV during the first few months of injury that may improve with time in response to therapy or residual musculature. [61] Neuroplasticity due to residual musculature or rehabilitation causing increase in afferents could either present as a protective mechanism from further GMV loss or increase the susceptibility of the individuals to spurious neural rewiring leading to maladaptive outcomes. A recent study by Ionta and colleagues have shown impaired body representation with increased dependency on visual information (*body image)* over sensorimotor information (*body schema)* in complete SCI [81]. Inferior frontal regions along with temporoparietal regions are known to be involved in generation of visually-guided movements. Collectively, all these allow us to speculate if the decrease in GMV shortly after injury in cortical structures involved in multi-sensory integration could be a consequence of imbalanced sensory inputs received after SCI.[82] Nevertheless, increase in cortical GMV with increasing injury duration indicates the importance of injury window in studying cortical reorganization following SCI. Due to lesser GMV loss and greater residual musculature, patients with paraplegia may remain more receptive to therapy than patients with tetraplegia during the first year of injury.

3.4.3 Conclusion

The present study used VBM technique to delineate grey matter alterations in complete SCI within two years of injury. Although preliminary in nature, many observations are made in this study. This study demonstrates cortical atrophy associated with complete SCI and its

subtypes. We show that cervical level injury when compared to thoraco-lumbar level injury is associated with greater loss of cortical GMV in non-motor related regions.

A positive association was also observed between cortical GMV and injury duration in both paraplegia and tetraplegia signifying improved GMV with increased injury duration is likely due to spontaneous recovery over time. It also supports the notion that both injury level and duration since injury could be potential contributors to extent of brain reorganization. In conclusion, VBM could provide useful structural markers in SCI about injury, recovery and secondary outcomes, though it may require both longitudinal and well-designed cross-sectional studies that account for both injury level as well as window of disease condition to minimize the variability between subjects.

CHAPTER 4

INTRINSIC FUNCTIONAL CONNECTIVITY AFTER SPINAL CORD INJURY (AIM 2)

4.1 Introduction

4.1.1 Background

Injury-induced reorganization is the complex process of molecular events contributing to the evolution of adaptive and maladaptive pathological changes at both the site of injury and the multi-systemic level of the brain [42,44,83]. The previous chapter summarized the anatomical brain changes observed after complete SCI. However, considering the complexity of brain pathology, a multi-modal approach to examine the concomitant functional alterations becomes fundamental to the understanding of the brain mechanisms involved with SCI. Functional cortical reorganization after SCI in humans is well-documented using non-invasive functional imaging techniques. Specifically, task-based fMRI studies have demonstrated an expansion in the somatotopic cortical representation of the body rostral to the level of injury in SCI patients [19,41,56,84,85]. Numerous researches have now implemented task-based fMRI in people with SCI where the BOLD signal changes during passive tactile stimuli or motor movement task is used to study the functional changes in the sensorimotor cortex and related regions [20,85-94] (list of task studies utilizing sensorimotor tasks are summarized in Table 4.1).

Table 4.1 Demographics and Clinical Characteristics of the Main fMRI Studies over the last Two Decades on Patients with SCI

Authors	N	Age [83]	Gender	Level	Degree	Time since SCI
Lotze et al. [95]	4	41–66	3 M, 1 F	3 Thoracic, 1 Lumbar	3 Complete 1 Incomplete	6–1456 weeks
Moore et al. [5]	12	33–76	M	Thoracic	Complete	4–8 yrs
Curt et al. (2002)	9	30.3±6.9	6 M, 3 F	4 Thoracic, 5 Lumbar	8 Complete 1 Incomplete	4–106 mo
Jurkiewicz et al. [84]	6	28±9	5 M, 1 F	Cervical	3 Complete 3 Incomplete	1,3,6,12 mo
Wrigley et al. [56]	20	22–63	18 M, 2 F	Thoracic	Complete	2–37 yrs
Duggal et al. (2010)	12	49.6±12.8	8 M, 4 F	Cervical	Incomplete	18±26 d 204±34 d
Jurkiewicz et al. (2010)	4	20–42	3 M, 1 F	Cervical	Complete	1,3,6,12 mo
Freund et al. [19]	10	47.1±10.7	M	Cervical	2 Complete 8 Incomplete	7–30 yrs
Lundell et al. [20]	19	46±12	18 M, 1 F	15 Cervical, 3 Thoracic, 1 Lumbar	Incomplete	1–18 yrs
Lundell et al. (2011b)	19	46±12	11 M, 3 F	15 cervical, 3 Thoracic,1 lumbar	Incomplete	1–18 yrs
Jutzeler (2015)		24	22 M, 2 F	11 Cervical, 15 Thoracic and Lumbar	11 Complete 13 Incomplete	
Awad A (2015)	1	59	1 M	Cervical	Complete	29 yrs
Stroman (2016)	16	50.1±16	13 M, 3 F	14 Cervical 2 Thoracic	5 Complete 11 Incomplete	5-37yrs
Wrigley (2018)	23	43±13	19 M, 4 F	Thoracic	Complete	
Chen Q (2019)	13	51.3±6.4	10 M, 3 F	Cervical	Incomplete	11.5±15.2d
* N: Number of Patients; M: Male; F: Female; Complete: total loss of sensory/motor function						

The study by Henderson and colleagues using task-based FMRI during passive brush stroke in complete thoracic SCI showed expansion of the finger region of the somatosensory cortex to medial cortical regions that encode for lower limb function[41]. Such

cortical reorganization is assumed to play a critical role in decelerating the grey matter and white matter atrophy that may have resulted otherwise. The majority of SCI research on functional recovery has focused on cortical reorganization, even though reorganization is known to occur at subcortical structures[44]. A study on monkeys with unilateral corticospinal tract lesion showed that the monkeys were able to recover voluntary control of limbs when red nucleus found in tegmentum was intact[96]. Presence of cortico-rubrospinal tract indicates a functional redundancy but red nucleus activating both during extension and flexion may indicate reorganization. This supports the presence of somatotopic remapping in subcortical structure with redundant connections. Lenz et al. revealed that ventral thalamic cells that normally receive input from upper extremities began responding to inputs from neck and occiput in humans with complete SCI[97].

However, it is believed that subcortical regions (in addition to the thalamus) may directly or indirectly impact changes in the cortical regions. The role, if any, played by subcortical plasticity in functional recovery is yet to be fully understood. Besides, not all cortical/subcortical reorganization leads to function recovery as it also occasionally leads to misfiring causing spasticity, phantom sensations and neuropathic pain, a major downfall in some SCI cases[9]. Moore and colleagues using tactile stimuli demonstrated that somatosensory regions responding to referred sensations co-activate with non-adjacent motor regions that are being stimulated, indicating a sub-cortical reorganization driving the cortex[5]. In fact, reports from over a century ago show that SCI pain may be associated with abnormal activity in thalamus [23]. Unfortunately, subcortical plasticity is often ignored due to lack of non-invasive techniques that can reliably study the changes in these regions following SCI. Hence, cortical/sub cortical reorganization, a dynamic phenomenon

initiated by SCI requires a well-controlled approach that will enable an understanding of the pattern of reorganization and consequently help in preventing unwanted outcomes.

The aforementioned is due to the nature of the technique where the type of task paradigm limits the regions of interest that can be examined by the technique [98]. For example, a task involving tactile stimuli is predominantly limited to S1 cortex and secondary sensory integration regions[99]. Other limitations of the task-based fMRI technique include 1) difficulty performing tasks when the participant is cognitively or functionally impaired, 2) low signal usability (only ~30% with majority as noise), and 3) confounding factors such as subject specific differences in task strategy, individual effort, adaptation, disease abnormality etc[100]. A promising alternative is the **resting-state fMRI (RS-fMRI)** technique that warrants the measurement of brain activity in the absence of an explicit stimulus[28,101]. This can be advantageous to the study of SCI due to its ability to analyze multiple networks using a single resting-state scan at a high signal to noise ratio while eliminating the confounding factors introduced by tasks.

4.1.2 Resting-State functional Magnetic Resonance Imaging

fMRI detects brain activity on the basis of neurovascular coupling where a change in neuronal activity is indirectly reflected as a change in local perfusion measured in the form of blood-oxygenation level dependent signal [102]. Increase in neuronal/synaptic activity increases the metabolic consumption of glucose, releases vasoactive ions and releases vasoactive neurotransmitters causing an inflow of blood flow and blood volume to replenish the consumed oxygen[102]. The resulting disparity in the magnetic environment due to differences in concentration of paramagnetic (deoxyhemoglobin) and diamagnetic (oxyhemoglobin) molecules of a tissue creates a contrast in the BOLD signal. For example,

during a directed task, the brain regions associated to the task exhibit a transient decrease (reflecting increasing deoxyhemoglobin) followed by an increase (reflecting incoming blood flow) in the BOLD signal of that region known as hemodynamic response [103]; whereas regions unrelated to the task show no significant change in BOLD signal. Fascinatingly, the hemodynamic response of the brain in the absence of an explicit stimulus or resting-state is thought to reflect the inherent baseline activity of neurons across the whole brain.

The significance of inherent fluctuations in the BOLD signal was first demonstrated by Biswal and colleagues[28], where, by using a standard fMRI acquisition on subjects performing no particular task the authors concluded that the brain is still highly active during rest. The authors specifically demonstrated that the low frequency fluctuations (<0.1 Hz) of BOLD signal of the motor cortex in the two hemispheres are highly correlated. Since then numerous studies have validated the method to be a robust technique to reliably identify the resting-state functional connectivity (RSFC) of different regions forming networks known as resting-state networks [24,104-106]. The RSFC of two regions is defined as the statistical measure of the level of synchronization between the BOLD time series of those two regions. The standard resting-state networks include sensorimotor, visual, auditory, salience, central executive, dorsal attention and default mode networks [24].

4.1.3 Application of Resting-state Functional Magnetic Resonance Imaging in SCI

Given the success of RS-FMRI in studying the functional architecture of the brain, both animal and human research have applied RS-fMRI to SCI population[16-18,107-110]. RS-fMRI studies in humans mostly report a decrease in RSFC of cortical sensorimotor regions after SCI [16-18], though alterations in the lower motor centers such as the basal ganglia, thalamus,

and cerebellum have also been reported[16,17,109-112]. Findings from alternative approaches such as graph analysis have provided evidence for preserved small-world-ness with reduced local efficiency and greater network modularity and characteristic path length in the network architecture of SCI patients [110,113]. Such alterations in resting state properties hold significant implications for the prognosis of SCI as RSFC measures of sensorimotor regions have been shown to be positively correlated with recovery at six months post-injury [18]. Furthermore, RS-fMRI has shown capable of measuring short-term cortical plasticity after a mere 4-week locomotor training in people with incomplete SCI[114]. Relatedly, a clinical case study of a patient with chronic cervical SCI also reported good agreement between RS-fMRI measures and the clinical presentation of the patient[107]. Collectively indicating the potential of RS-fMRI in optimizing therapies for individuals with SCI as well as aiding in better diagnosis and prognosis. However, the translation of RSFC patterns into clinically adaptive or maladaptive biomarkers is yet to be established and demands a better understanding of the subcortical substrates of SCI.

Maladaptive complications of SCI such as neuropathic pain and dysesthesia are prevalent in ~53% of population with SCI [115]. Neuropathic pain in particular has been associated with impairment along the spinothalamocortical axis. A longitudinal study on SCI rat model showed that SCI pain is associated with aberrant functional connectivity between thalamus and cortical regions of nociceptive processing[116]. Thalamic dysrhythmia as a result of deafferentation is also associated with decrease in alpha activity of the cortex after SCI [97,117,118]. Research also illustrates a reduction in grey matter volume, perfusion, and concentration of N-acetyl aspartate and gamma-aminobutyric acid in thalamic nuclei of SCI patients and neuropathic pain compared to HC [72,119].

Outside the role of the thalamus in pain, research suggests that body movement related cortical reorganization may be mediated by reorganization within the thalamus and brain stem to recalibrate the integration of multisensory information appropriate to the altered body state [12,15,120]. Evidence from primate and human anatomical studies corroborate the possible roles of the thalamus in synchronizing spatially distinct cortical areas [121] allowing fast multisensory interplay through thalamic sub-nuclei [122] and even providing a feed-forward circuit through the cortico-thalamic-cortical relays [123,124]. Given the large-scale changes in cortical connectivity after SCI, the new perspective of the thalamus as both a relay and modulator in cortico-cortico processing leads us to hypothesize that a compound alteration must occur in the thalamocortical pathways of different sub-nuclei after SCI. Reorganization in the connectivity of different sub-nulcei may uniquely contribute and compensate towards the adaptive or maladaptive cortical changes observed after SCI. Despite the evidence in the literature, the consequences of SCI on different thalamic sub-nuclei in humans remain mostly unexplored.

Hence, the goal of this study is to investigate the extent of whole brain cortical and sub-cortical reorganization in individuals with paraplegic and tetraplegic types of SCI using resting-state fMRI and explore the use of data-driven approach to demonstrate cortical reorganization of thalamic sub-nuclei corresponding to different functions in SCI patients. Related findings of different thalamic nucleus in the literature are also discussed to understand the possible roles of thalamic sub-nuclei in SCI.

4.2 Methods and Materials

4.2.1 Participants

Participants recruited for the anatomical study were also used for this study. Refer to Section 2.1.1 of Chapter 2 for inclusion criteria, exclusion criteria of the participants. The demographics of the SCI group is provided in Table 3.1.

4.2.2 Imaging Parameters

High-resolution structural images were acquired using magnetization- prepared rapid gradient echo sequence (MPRAGE). The imaging parameters for MPRAGE were as follows: FOV = 240 mm, 512x512 matrix, TR = 2300 ms, TE = 2.91 ms, flip angle = 90. The whole brain was imaged in the sagittalconfiguration where 176 slices were collected, and each slice was 1 mm thick. The spatial resolution of all the anatomical scans was 1 mm x 0.469 mm x 0.469 mm. The functional images were acquired using echo planar imaging sequence (EPI) with the following imaging parameters: FOV = 240 mm, 64x64 matrix, TR = 2000 ms, TE = 27 ms, and flip angle = 90. The whole brain was scanned in an axial configuration where 20 slices were collected, and each slice was 6 mm thick. The spatial resolution was 3.75mm x 3.75 mm x 6 mm for all functional scans. During the scan duration, the subjects were instructed to remain motionless and avoid falling asleep. A total of 195 volumes were collected over a period of 390 s during the scan.

4.2.3 Data Processing:

The data processing was performed using Statistical Parametric Mapping 12 toolbox [125] within the MATLAB environment (Mathworks Inc, Massachusetts, USA). Before preprocessing the first five time points were removed to reduce transient scanner artifacts

and the origin of the functional and anatomical images of all participants was manually reoriented to the anterior commissure of the brain. Preprocessing workflow included the following procedures. First, head motion correction using a least squared approach and 6 parameters (rigid body) spatial transformation with respect to the first image of the scan was performed; a total of 43 subjects (19 HC, 17 paraplegic SCI, 7 tetraplegic SCI) were used for the following steps after eliminating subjects with more than 1 mm head motion in any direction and individuals with no sensory-motor impairment score. Second, co-registration of anatomical image to the mean functional image of each subject was performed. Third, segmentation of anatomical images into grey matter, white matter, and cerebrospinal fluid tissue probability maps was conducted. Fourth, spatial normalization was done using deformation vector obtained from the segmentation procedure of each subject and resampling to isotropic voxel size of 3x3x3 mm^3. Fifth, regression of the average white matter and average cerebrospinal fluid time series was extracted from voxels of white matter and cerebrospinal fluid probability maps with probability>0.98. Sixth, regression of head motion noise using Friston 24- parameter model was performed (6 head motion parameters, 6 head motion parameters from previous time point, and their 12 corresponding quadratic parameters) [126]. Last spatial smoothening was conducted on the data using a Gaussian kernel of 8 mm full-width at half maximum followed by a temporal filtering between 0.01 to 0.1 Hz.

4.2.4 Whole Brain Connectivity Analysis (Aim 2a)

Whole brain RSFC differences between SCI group and HC were examined using ROI based analysis. The ROI's were generated using the MNI coordinates of 160 seeds defined by Dosenbach and colleagues [127] using meta-analysis. A seed of 5 mm radius was generated

for each ROI using the dimensions of the functional images. The average BOLD signal of every ROI was then extracted resulting in 160 extracted ROI time series for every subject. Three ROI's from the cerebellar network was removed from the analysis as they were present outside of the brain mask in few subjects. Hence, a 157x157 correlation matrix was obtained for every subject using Pearson's r correlation. To identify differences between HC and the two subgroups of SCI, a one-way ANCOVA accounting for age and gender was performed on the 12,089 unique ROI pairs. ANCOVA results were threshold at uncorrected-$p<0.001$. Resultant ROI pairs were entered into a post-hoc analysis to compare a) HC vs. paraplegia, b) HC vs. tetraplegia and c) paraplegia vs. tetraplegia. An FDR-correction was performed to account for multiple comparison problems.

4.2.5 Thalamocortical Connectivity Analysis (Aim 2b)

Abnormal thalamic connectivity based on RSFC in SCI group were first identified using a data driven independent component analysis. A hypothesis driven approach was later applied to identify cortical regions differentially connected to the abnormal thalamic nuclei.

i) Thalamus Parcellation Using Independent Component Analysis: Thalamus was parcellated into sub-nuclei using the method applied by Rui and colleagues[128]. The method first calculates the whole brain voxel wise connectivity map of every voxel in the thalamus for all participants. A thalamus mask obtained from Harvard- Oxford cortical and subcortical structural atlas was down sampled to 3x3x3 mm to use for this analysis. Next, spatial independent component analysis decomposition was performed on the 4-D dataset created by concatenating voxel wise functional connectivity maps of all thalamic voxels from all subjects to generate 20 spatially independent components. Independent component

analysis was performed using FSL's MELODIC function[129]. Out of the 20 spatially independent components, 10 known resting state networks (primary visual, dorsal attention, anterior and posteriors default mode network, sensorimotor, left and right frontoparietal network, salient, auditory, andventral attention metworks) were chosen manually for the next steps of the analysis. To identify the thalamic voxels associated to each of the 10 networks, a spatial linear regression model was employed to measure the contribution of each independent network component to the whole brain functional connectivity of each voxel. A linear regression model was executed for every voxel of the thalamus, repeating for every subject. Beta parameter estimates for each of the 10 independent components from the linear regression model was back projected to the corresponding voxels of every subject. For each of the ten thalamic sub- nuclei beta maps, FSL's *randomise* was used to perform non- parametric voxel wise Two sample t-test and one-way Analysis of Covariance (ANCOVA) to assess differences in the spatial boundaries of thalamic sub-nuclei between the two groups and its subtypes (Paraplegia, and Tetraplegia). Finally, the probability maps using threshold free cluster enhancement representing difference among the three groups were corrected for family wise error at $p<0.05$. A spatial mask, comprising of only the voxels in the thalamus, was used.

ii) Seed Based Analysis: Based on the results obtained from thalamus parcellation, thalamocortical functional connectivity maps of different thalamic sub-nuclei were generated using seed-based analysis technique. Six 3-D spherical seeds of 5mm radius were generated using MNI coordinates of bilateral pulvinar (±15, 31, 5), bilateral mediodorsal (±6, 16, 9) and bilateral ventrolateral (±15, 13, 9) nucleus [130]. Average time series of each of the six thalamus seeds were extracted as the reference time series for each of the

participants. Using AFNI's 3dfim+ function, the whole brain voxel-wise connectivity map of all six seeds in the thalamus were computed for all participants [131]. Each of the connectivity maps were then converted to z-score maps using r to z fisher transformation. For next steps of the analysis a 4-D dataset for each of the six seeds were generated by concatenating the z maps of all subjects. For each of the six thalamic seeds, FSL's *randomise* was used to perform non- parametric voxel wise two-sample t-test using 5000 permutations to assess connectivity differences between the two groups [132]. The statistical design included gender and age as covariates of no interest. Significant effects were obtained by thresholding the voxel-based probability maps at uncorrected $p<0.002$ with multiple comparison correction. A Monte-Carlo simulation was performed using AFNI's *3dClustSim* with the autocorrelation function to compute cluster-size threshold for each of the six thalamic seeds to correct for the multiple comparison problem. Furthermore, to exclude regions outside of the brain from statistical analysis, a spatial mask comprising of only the voxels present across all subjects was used as an inclusive mask.

Lastly, average connectivity measure of all clusters that survived the statistical threshold was further extracted and correlated with motor and sensory index scores (pinprick and light touch) of SCI patients using a one-way ANCOVA in MATLAB. The ANCOVA model was tested for the following: a) mean effect of the motor score on FC measures and b) mean effect of the sensory score on FC measures while accounting for age and gender as covariates.

iii) Effect of Post-Injury Duration: For each of the six thalamic seeds, FSL's *randomise* was used to model the effect of injury duration on FC measures utilizing a non-parametric voxel wise estimation using 5000 permutations. The general linear design included

duration of injury as a covariate of interest and gender and age as covariates of no interest. Significant effects were obtained by thresholding the voxel-based probability maps at FWE-corrected $p<0.05$.

4.3 Results

4.3.1 Whole Brain Connectivity Analysis

Mean correlation map of HC, paraplegia tetraplegia (shown in Figure 3.1a) indicates increased positive functional connectivity in tetraplegia group when compared to healthy control and paraplegia groups. The increased connectivity can be seen between regions of sensorimotor network and occipital and cingulo-opercular network. One-way ANCOVA comparing 12,089 ROI pairs resulted in 808 unique ROI pairs altered between the three groups at $p<0.05$. Further thresholding at $p<0.001$ resulted in 30 ROI pairs that were significantly different between the three groups. Post-hoc analysis using two-sample t-tests revealed 27 out of 30 ROI pairs to be significantly altered between HC and paraplegia whereas only 1 out of 30 ROI pairs (post occipital gyrus and insula) was significantly altered between HC and tetraplegia at p-value<9.4e-05. Lower number of significant differences between HC and tetraplegia could be attributed to the smaller sample size in tetraplegic group. Two sample t-test comparing paraplegia and tetraplegia revealed 15 out of 30 ROI pairs to be significantly different between the two subtypes of SCI. Five out of the 30 ROI pairs corresponded to regions in non-sensorimotor networks, while 10 ROI pairs consisted of regions in the sensorimotor network. Functional connectivity maps and average connectivity measures are displayed in Figure 4.1b and Figure 4.1c. Average

functional connectivity bar plots show greater connectivity in these ROI pairs for tetraplegia group when compared to HC or paraplegia.

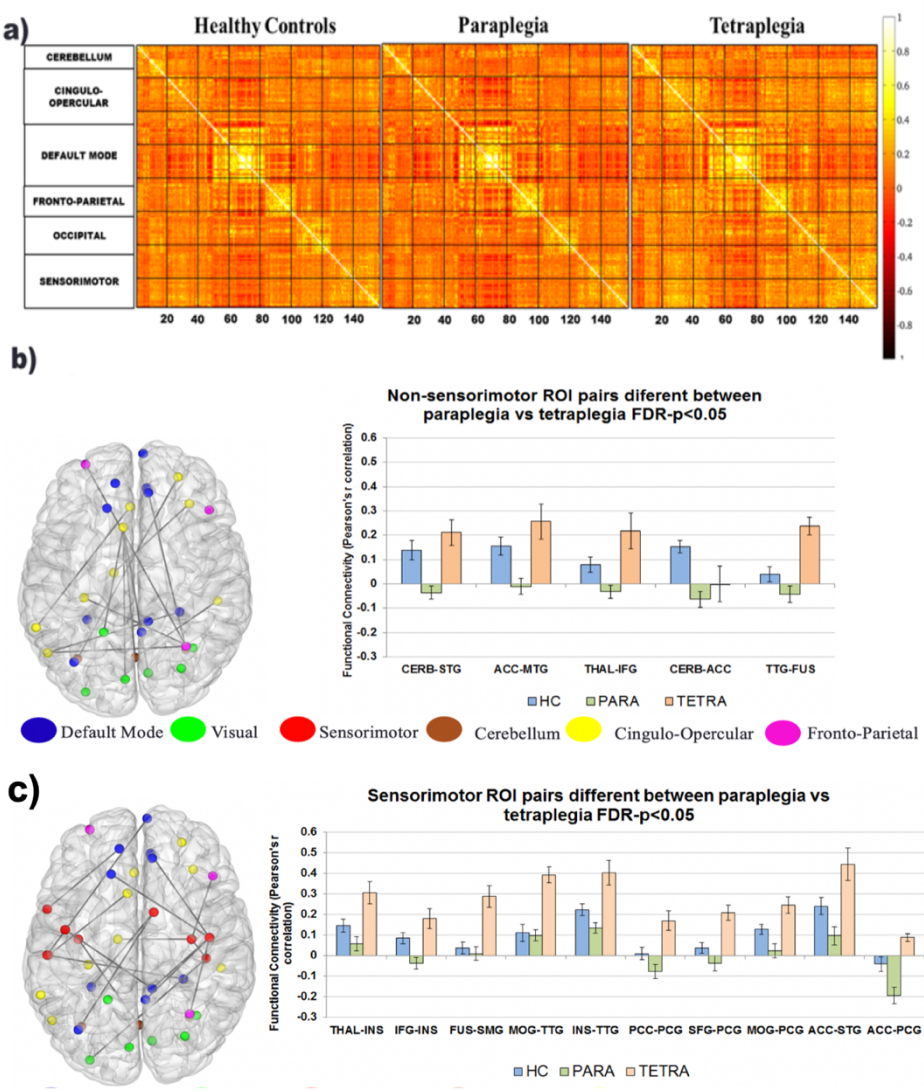

Figure 4.1 ROI based connectivity analysis: a) Mean correlation matrix in HC, paraplegia and tetraplegia groups. b) Connectivity between 5 non-sensorimotor ROI pairs that are significantly different between paraplegia and tetraplegia at FDR-p<0.05. c) Connectivity between 10 sensorimotor ROI pairs that are significantly different between paraplegia and tetraplegia at FDR-corrected p<0.05. Average bar plot indicates mean functional connectivity for each ROI pair in each group. The color indicates the network of the ROI. (CERB-cerebellum, STG-superior temporal gyrus, MTG-middle temporal gyrus, THAL-thalamus, IFG-inferior frontal gyrus, ACC-anterior cingulate cortex, TTG-transverse temporal gyrus, FUS-fusiform gyrus, INS-insula, SMG-supramarginal gyrus, MOG-middle occipital gyrus, PCC-posterior cingulate cortex, SFG-superior frontal gyrus, PCG-precentral gyrus, STG-superior temporal gyrus).

4.3.2 Thalamocortical Connectivity Analysis

i) Parcellation Of the Thalamus Using ICA: Spatial ICA on thalamic functional correlation maps across all subjects (control and patients) generated 40 ICs, of which 10 independent components belonging to standard brain networks were visually identified to use in subsequent steps[133,134]. The 10 networks shown in Figure 4.2 belong to auditory, posterior default mode, left fronto-parietal, right fronto-parietal, medial visual, dorsal attention, sensorimotor, salient, lateral visual and anterior default mode networks. The beta maps of the thalamus obtained for specific resting state networks denote the connection strength of each of the voxels to that particular network. A one sample t-test on the thalamus beta maps resulted in group maps of different functional thalamic sub-nuclei. The parcellation of these sub-nuclei and their boundaries were confirmed with the thalamus maps obtained by Rui et al. and the morel template[128]. For example, the sub-nuclei of default mode network comprised of the medial dorsal nucleus, left anterior nucleus, intralaminar nucleus and left ventral lateral nuclei. Likewise, the sub-nuclei corresponding to sensorimotor network comprised of ventral posterior lateral nucleus of the thalamus. Next, one-way ANOVA comparing paraplegic and tetraplegic SCI to HC at FDR-corrected $p<0.05$ resulted in significant alteration of sub-thalamic boundaries belonging to auditory and salient network (shown in Figure 4.3). Voxels corresponding to auditory thalamic nuclei (MD nucleus) shows decreased network strength with cortical auditory regions in paraplegic group. Similarly, thalamic voxels corresponding to salient thalamic nuclei (MD nucleus) is decreased in paraplegic group and increased in tetraplegic group.

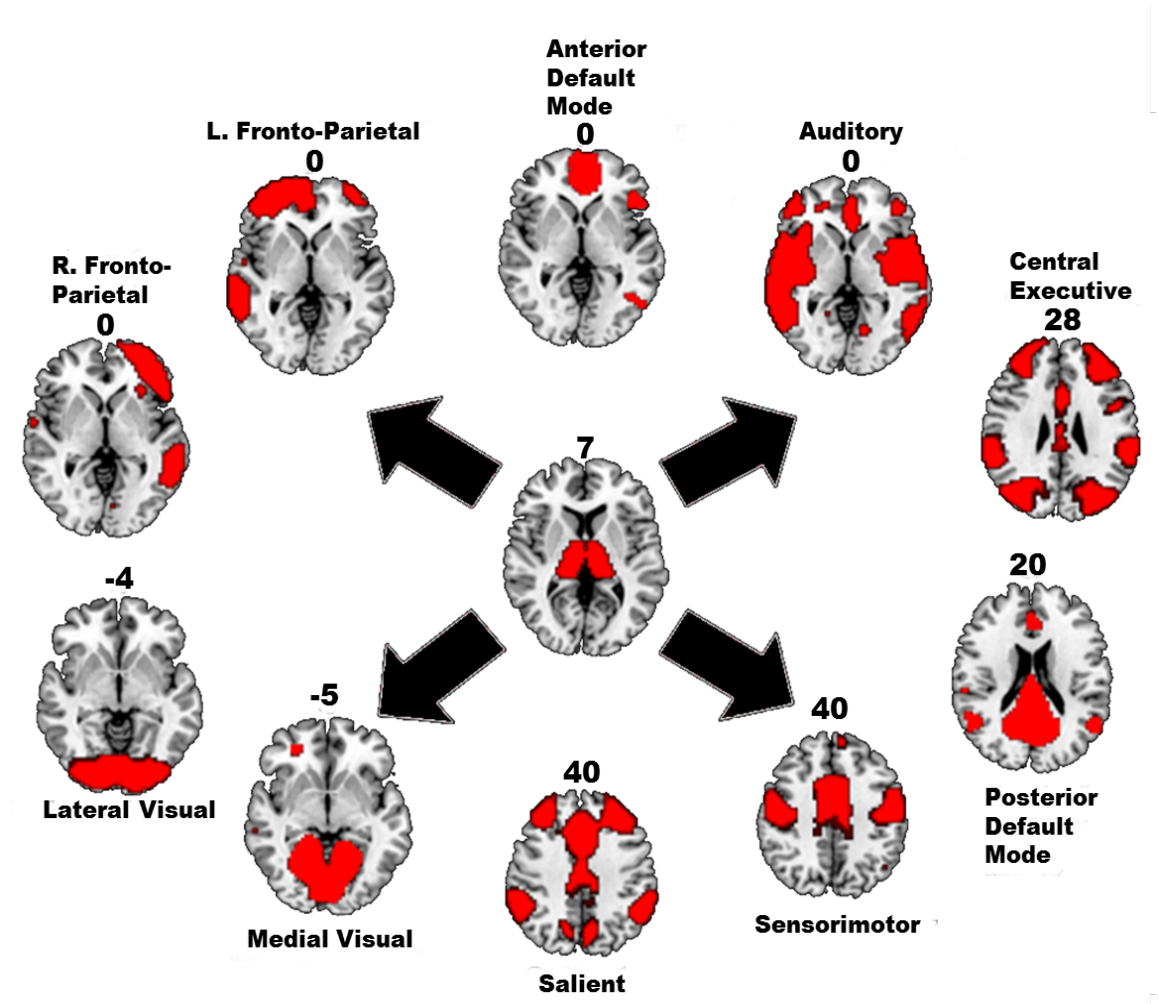

Figure 4.2 Mask of bilateral thalamus and the 10 spatially independent components obtained from whole brain voxel-wise functional connectivity maps of the voxels inside the thalamus. The index indicates the MNI z coordinate of the slices.

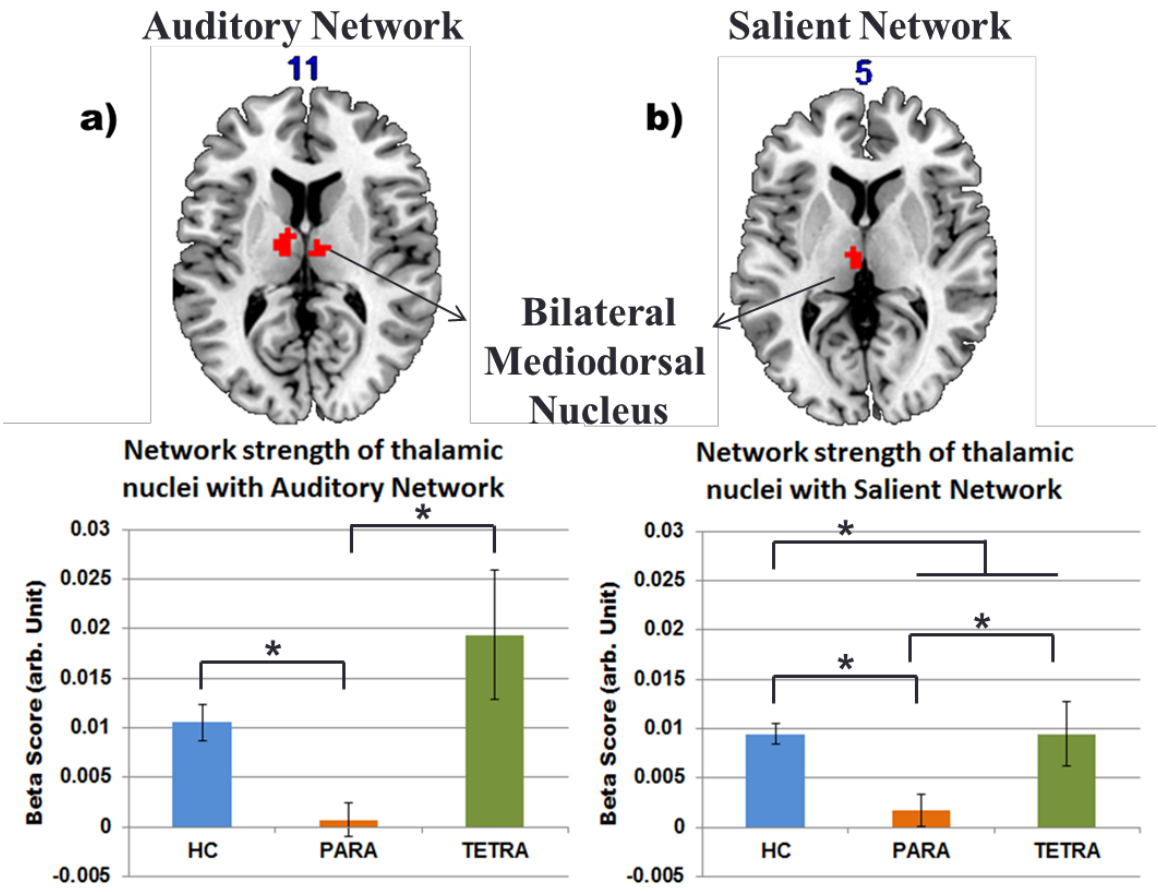

Figure 4.3 Sub-regions of the thalamus corresponding to a) auditory network and b) salient network altered in SCI in comparison to HC at FWE corrected $p<0.05$. Bar plot shows the average network strength of the thalamic sub-regions in HC and SCI (Paraplegia and tetraplegia).

ii) Seed Based Analysis: Based on thalamus parcellation using independent component analysis, paraplegia shows the greatest decrease in thalamic functional connectivity. Hence, the statistical analysis of seed-based analysis of thalamic seeds was performed only between HC and paraplegia. Figure 4.4 displays the group functional connectivity maps of the six thalamus seeds in HC and SCI group. The mean FC of left and right PUL nucleus in both groups is localized to areas of bilateral PUL nucleus, bilateral hippocampus, bilateral precuneus and posterior cingulate cortex regions. The mean FC map of left PUL nucleus in SCI also extends to additional areas in bilateral angular gyrus.

On the contrary, the mean FC of MD nucleus in HC subjects is spatially widespread, where it extends to regions of the bilateral superior frontal gyrus, inferior parietal cortex, basal ganglia, insula, anterior cingulate cortex, medial prefrontal gyrus, middle cingulate gyrus, and precuneus. Whereas, the mean FC of MD nucleus in SCI appears to be spatially limited to regions of the basal ganglia, medial prefrontal gyrus, and precuneus areas. Similarly, the mean FC of VL nucleus in HC encompasses regions of pre-motor cortex, middle cingulate cortex, prefrontal cortex, basal ganglia, intraparietal cortex and posterior-cingulate cortex. However, the FC of VL nucleus in SCI subjects is once again sparse with mean connections mostly extending to basal ganglia, frontal gyrus, and cingulate gyrus.

Statistical tests comparing the voxel-wise connectivity maps between the SCI and HC groups resulted in significant effects in five out of the six seeds investigated (shown in Figure 4.5). The two-sample t-test at a lenient threshold of uncorrected at $p<0.002$ (not shown in the Figure) revealed a widespread increase in functional connectivity of left PUL nucleus to regions of the left inferior frontal gyrus, right precuneus, anterior thalamus and left middle occipital gyrus (intraparietal cortex) in SCI group. However, as seen in Figure 4.5a, only one cluster in the left inferior frontal gyrus-pars triangularis survived multiple comparison corrections. Likewise, the result of two-sample t-test for the right PUL nucleus shown in Figure 4.5b displayed one cluster centered in left middle temporal gyrus that was significantly different between the two groups. Next, comparing the connectivity of MD nucleus between the two groups revealed decreased connectivity of left MD with regions of left putamen extending to the insula, left anterior cingulate cortex and right superior temporal gyrus in SCI group (shown in Figure 4.5c). In the same way, right MD

demonstrated significantly decreased connectivity with right rolandic operculum extending to insula and right superior temporal gyrus in SCI group. Further, at a lenient threshold of uncorrected-p<0.002 (not shown in the Figure), both left and right MD displayed decreased FC with regions of the bilateral temporal gyrus, insula, and dorsal anterior cingulate cortex. Lastly, the result of the Two sample t-tests comparing FC of VL nucleus between the two groups demonstrated a significant decrease in FC of left VL nucleus with left superior temporal gyrus in SCI group with no significant difference in FC of right VL nucleus. A list of all the regions with significantly altered FC to the thalamus in SCI group is summarized in Table 4.2.

Figure 4.6 displays the average connectivity measures of all regions that exhibited significantly altered FC with the six thalamic seeds in SCI group when compared with HC group. Except for connectivity of left PUL nucleus with left inferior frontal gyrus, the HC group has a mean positive FC between the thalamus and different cortical regions whereas the SCI group has decreased positive FC in same regions.

A one-way ANOVA examining the correlation between sensory-motor scores and FC measures of significant clusters revealed a significant correlation between FC of R.MD-R.STG with motor scores (r=-0.366, p=0.02) and FC of L.PUL-L.IFG with sensory scores (r=-0.543, p=0.02). However, no significant correlation between sensory scores (pin-prick + light touch) or motor scores with FC measures was observed for SCI group after correcting for multiple comparison problems (p>0.05).

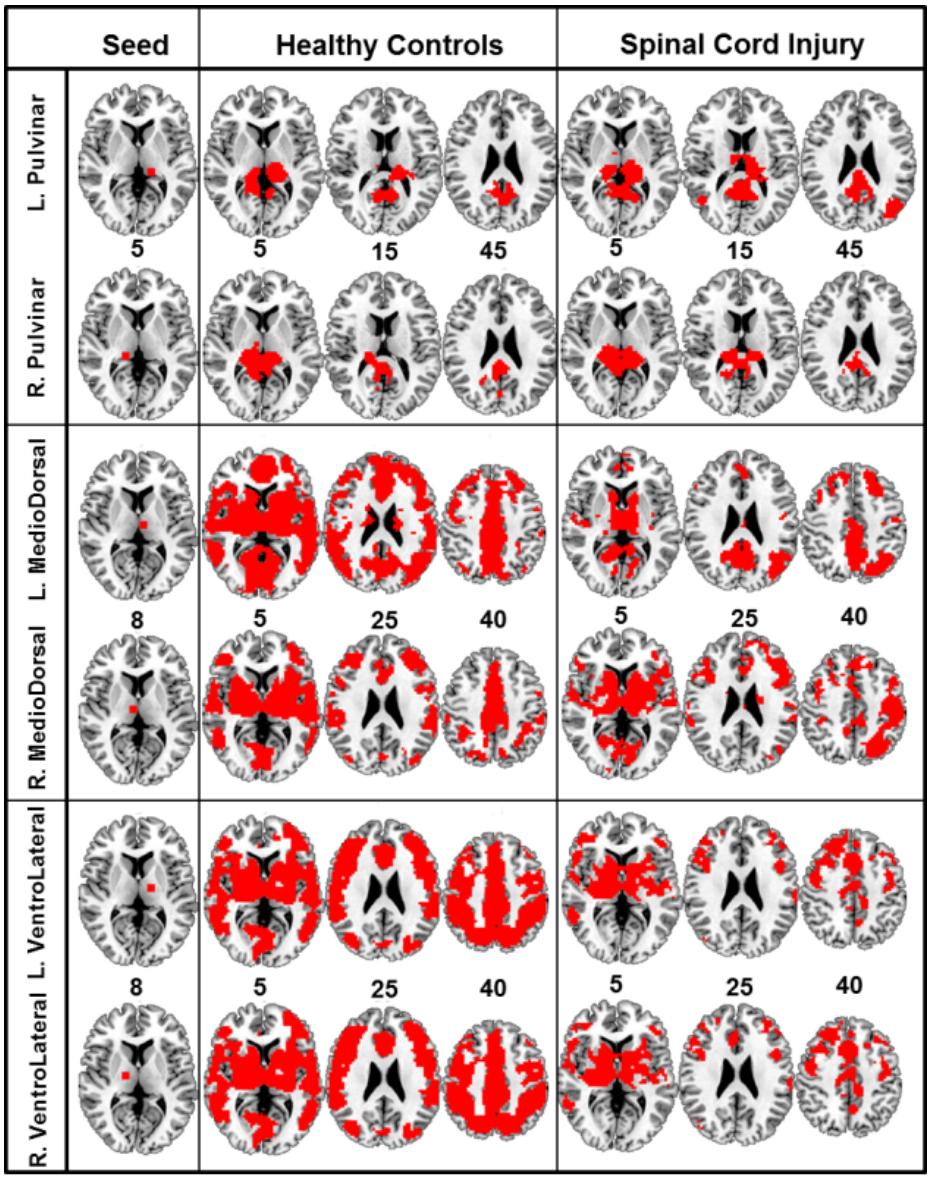

Figure 4.4 Panel displays mean group connectivity map of left and right pulvinar nucleus, left and right mediodorsal nucleus (middle) and left and right ventrolateral nucleus for HC and SCI group. All functional connectivity maps are a result of mean group effect threshold at voxel-based family-wise error corrected at $p<0.05$ with threshold-free cluster enhancement and an extended cluster size of 20 voxels. Seed columns on the left indicate the thalamic seed used to perform each row of seed-based analysis. The number indicates the z coordinates of the slices given.

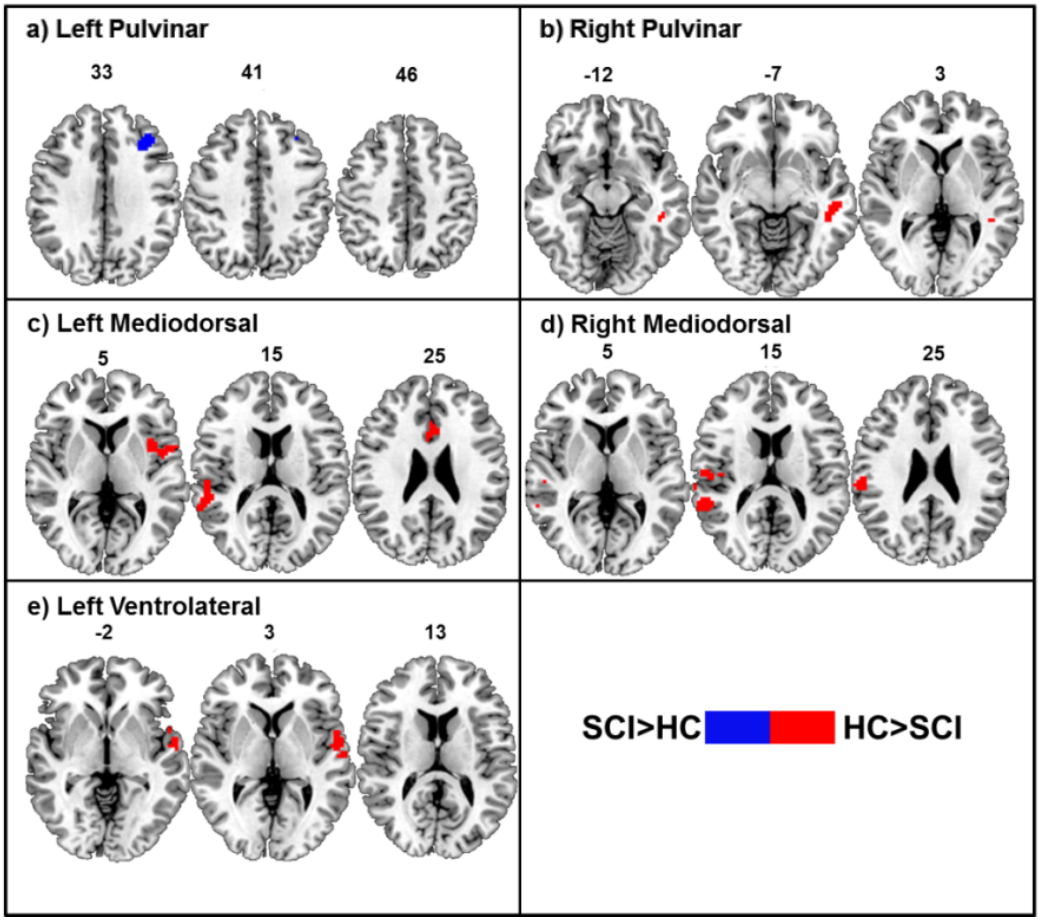

Figure 4.5 Result of two-sample t-test displaying regions with altered functional connectivity to the different thalamic sub-nuclei in SCI when compared to HC. a) A single cluster with peak activation at left inferior frontal gyrus pars triangularis exhibits increased FC with left PUL nucleus in SCI at uncorr-p<0.002 and cluster size=51 voxels. b) Single cluster with peak activation at left middle temporal gyrus exhibits decreased FC with right PUL nucleus in SCI at uncorr-p<0.002 and cluster size=50 voxels. c) Three clusters with peak activation at the left anterior cingulate cortex, left putamen and right superior temporal gyrus exhibit decreased FC with left MD nucleus in SCI at uncorr-p<0.002 and cluster size=51 voxels. d) Two clusters with peak activation at right rolandic operculum (insula) and right superior temporal gyrus exhibit decreased FC with right MD nucleus in SCI at uncorr-p<0.002 and cluster size=53 voxels. e) A single cluster with peak activation at left superior temporal gyrus exhibits decreased FC with left VL nucleus in SCI at p<0.002 and cluster size=51 voxels. Red indicates regions that are decreased in SCI in comparison to HC; blue indicates regions that are increased in SCI in comparison to HC. The number represents the z coordinates of the slices shown. Note: Right VL nucleus showed no statistically significant differences between the two groups (p>0.05).

Table 4.2 List of Regions with Altered FC to different Thalamus Sub-Nuclei

Seed	Cluster Size (Voxels)	Region of Interest (MNI Atlas)	MNI Coordinates		
			x (mm)	y (mm)	z (mm)
Left PUL (L.PUL)	60	Left Inferior Frontal Gyrus pars triangularis (L.IFG)	-36	27	30
Right PUL (R.PUL)	56	Left Middle Temporal Gyrus (L.MTG)	-45	-39	-6
Left MD (L.MD)	97	Left Putamen (L.PUT)	-30	0	-3
	82	Left Anterior Cingulate Cortex (L.ACC)	-3	21	24
	57	Right Superior Temporal Gyrus (R.STG)	60	-45	15
Right MD (R.MD)	111	Right Rolandic Operculum (R.ROPE)	51	-21	12
	53	Right Superior Temporal Gyrus (R.STG)	60	-45	12
Left VL (L.VL)	71	Left Superior Temporal Gyrus (L.STG)	-60	0	-6

Note: Seed column denotes the thalamic sub-nuclei with connectivity changes to the particular ROI. The coordinates of each of the clusters are presented in Montreal neurological institute (MNI) space in left-posterior-inferior orientation.

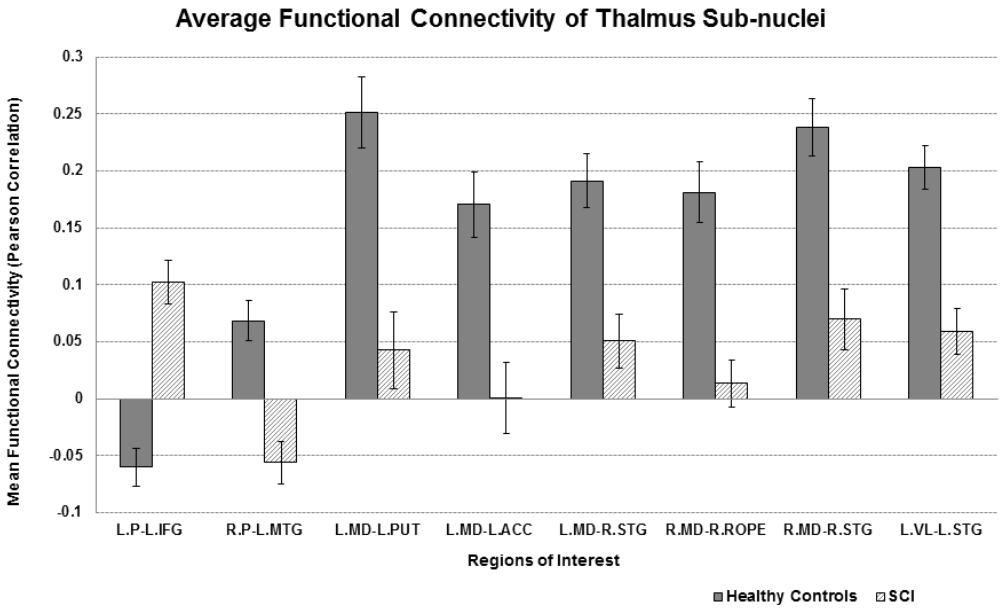

Figure 4.6 Average functional connectivity measures of the regions with significantly altered connectivity to the different thalamic sub-nuclei in HC and SCI groups. Statistical significance was computed at uncorrected-$p<0.002$ with cluster-based thresholding using Monte-Carlo simulation. Error bars given here indicate standard error of the mean.

4.3.3 Effect of Post-Injury Duration

Randomization process to model the mean effect of injury duration on FC of the thalamus in SCI resulted in statistically significant effect in three out of the six nuclei studied, namely, the left MD, right MD and right PUL nucleus. Figure 4.7a presents the regions whose FC with left MD (shown in red), right MD (shown in blue) and right PUL nucleus (shown in green) are significantly associated to the duration of injury in SCI patients. The significant regions whose FC strength with L.MD is associated with the duration of injury include left superior occipital gyrus (L.SOG), right cuneus (R.CUN) and left middle cingulate cortex (L.MCC). Similarly, the regions whose FC strength with R.MD is significantly associated to the duration of injury include left superior frontal gyrus (L.SFG), right inferior temporal gyrus (R.ITG) and left calcarine gyrus (L.CAL). Lastly, FC of R.PUL nucleus as shown in Figure 4a -right displays significantly high negative correlation

with duration of injury for multiple regions including right postcentral gyrus (R.PoCG), left calcarine gyrus (L.CAL), right precuneus (R.PCUN), right postcentral gyrus (R.PoCG), left cuneus (L.CUN), left inferior parietal lobule (L.IPL) and right superior occipital gyrus (R.SOG). In general, as shown in Figure 4.7b, the FC of the thalamic sub-nuclei to regions of the visual cortex, pre-motor cortex, and secondary somatosensory cortex appears to be dynamic and progressively decreasing with time following the injury in patients with SCI.

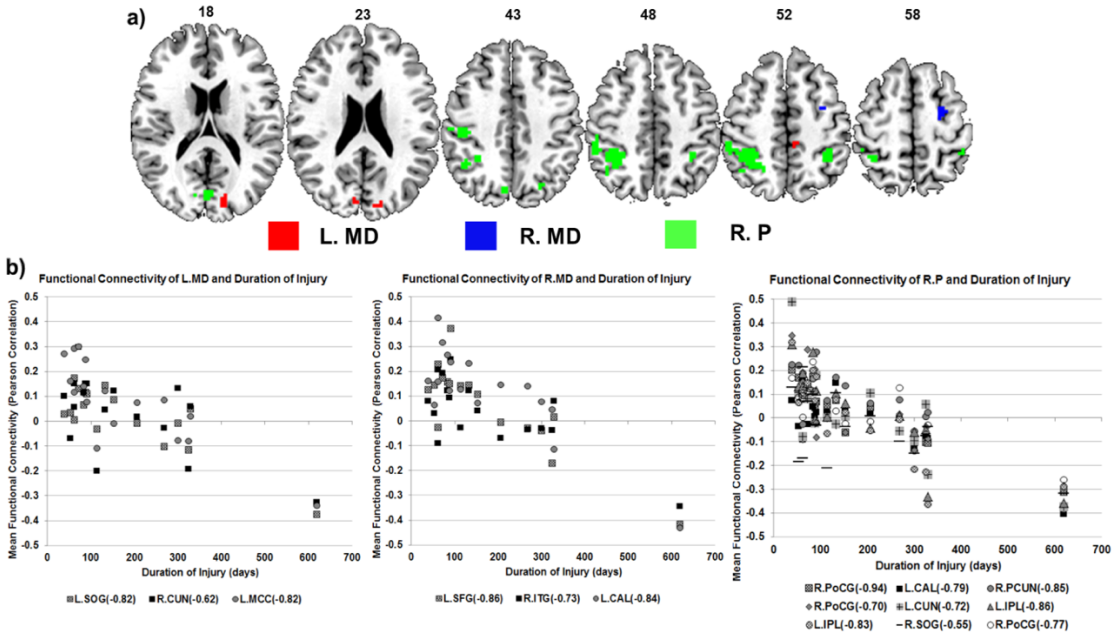

Figure 4.7 Effect of duration of injury on functional connectivity of the different thalamus sub-nuclei in SCI group. a) Result of f-test displaying clusters whose FC to the thalamus sub-nuclei is significantly correlated to the duration of injury. Statistical maps were thresholded at voxel-based FWE corrected $p<0.05$ with threshold-free cluster enhancement. Red indicates clusters whose FC to the left MD nucleus is significantly associated with the injury duration in SCI patients; similarly, blue indicates clusters whose FC to the right MD nucleus is significantly associated to the injury duration in SCI patients and green indicates clusters whose FC to the right PUL nucleus is significantly associated to the injury duration in SCI patients. The number represents the z coordinates of the slices shown. b) Left: Negative relationship between duration of injury and FC measures of left MD nucleus with L.SOG, R.CUN, and L.MCC. Middle: Negative relationship between duration of injury and FC measures of right MD nucleus with L.SFG, R.ITG, and L.CAL. Right: Negative relationship between duration of injury and FC measures of right PUL nucleus with R.PoCG, L.CAL, R.PCUN, R.PoCG, L.CUN, L.IPL, and R.SOG. Pearson r correlation values of the relationship between FC and duration of injury is given in parenthesis in the legend of each plot next to the region of interest.

4.4 Discussion

4.4.1 Whole Brain Connectivity after SCI

Right precentral gyrus of the sensorimotor cortex showed significantly greater connectivity to posterior cingulate cortex, superior frontal gyrus, middle occipital gyrus and ACC in tetraplegia when compared to HC and paraplegia. M1 located in the precentral gyrus is highly interconnected to other frontal motor areas, including SMA, cingulate motor cortex, premotor cortex and parietal regions for the planning and execution of highly complex movements. Initiation, planning or suppression of movement, requires sensorimotor feedback from corticospinal neurons as well as from the secondary somatosensory regions, frontal gyrus and visual regions in order to generate a perception, action and reaction. Parietal regions interplay with sensory sources including somatosensory, visual and auditory sources to aid motor planning and execution. Increased functional connectivity between supramarginal gyrus and fusiform gyrus, middle occipital gyrus, heschls gyrus and temporal gyrus supports the notion that tetraplegia due to greater loss of afferents, is likely to experience an imbalance in sensory weighting. Hawasli and colleagues report decrease in connectivity of sensorimotor region simultaneous with a compensatory increase in connectivity between visual cortex and intraparietal region [135] Therefore, an increase in functional connectivity with the sensory areas, such as supramarginal gyrus, visual cortex and cuneus, could be a compensatory mechanism in tetraplegia.

Additionally, the connectivity between cerebellum and ACC is the only ROI pair where tetraplegia shows decreased connectivity when compared to HC. Interestingly left MD nucleus of the thalamus also show increased connectivity to insula and inferior frontal gyrus, regions that show decreased GMV in the same cohort. Hence accounting for the

effects of GMV atrophy on functional connectivity of these regions would be beneficial to the interpretation of functional connectivity results. Animal and human brain imaging studies on SCI, have reported decrease in grey matter volume, movement related M1 potentials, fractional anisotropy and spine density during the aftermath of deafferentation. Some RS-fMRI and task studies report increased RSFC of primary motor cortex with SMA, basal ganglia [111] and premotor areas to be associated to better motor recovery [18]. However, no past reports of significant increase in connectivity of motor region with temporal gyrus or heschls gyrus regions exist in SCI literature. But, increase in effective connectivity of M1 with ipsilateral temporal gyrus and middle frontal gyrus has been seen in stroke patients with complete and partial paralysis[136]. The increased functional connectivity to regions of multisensory association regions in tetraplegia could be a result of reorganization induced due to deafferentation and loss of sensory inputs from upper and lower limb in tetraplegia.

Based on the somatotopic organization (or homunculus) of the primary motor cortex, the regions encoding the torso, head and neck regions anatomically overlap with temporal regions[134]. As the study involves only complete SCI, it is possible that, tetraplegic group may receive no sensory or motor efferents from the corticospinal pathways causing an imbalance in the feedforward and feedback motor pathways at the cortex. This "all or none" system, where HC receive all necessary signals and tetraplegia receive no inputs may initiate a more rigorous compensatory mechanism than paraplegia that in theory receives only half the amount of signaling pathways as HC. Then, it could be argued that our observations are either a compensatory mechanism of tetraplegia to preserve M1

functionality or a compensatory mechanism of tetraplegia to rely greater on integrating sensory inputs (such as auditory and visual information).

4.4.2 Thalamocortical Connectivity after SCI

An overwhelming proportion of the SCI population develops chronic pain manifested in the form of nociceptive or neuropathic pain, often unresponsive to conventional pharmacological treatment [36]. Previous research in SCI suggests an association between thalamus dysfunction and chronic pain [97,119,137]. Owing to the variation in type, location and magnitude of pain experienced in SCI patients, the role of the thalamus whether in generation or maintenance of central pain condition in SCI is yet to be established.

Classically, the thalamus is a major relay while the modern view suggests a modulatory and an indirect transthalamic role with numerous pathways between the cortex, thalamic nuclei, and lower motor centers [138,139]. Identifying the functional alterations of the thalamus at a sub-nuclei level in response to an imbalance in cortical computation and peripheral reactions (as in the case of SCI) could provide insight into the neuroplasticity following SCI. In this study, we performed resting-state functional connectivity based parcellation followed by a voxel-wise seed-based analysis to identify reorganization in cortical connectivity of the following three major nuclei, the PUL as well as the MD and MD nucleus in SCI. Using resting-state FC of the thalamus to the whole brain, we identified specific alterations in connectivity of left PUL, bilateral MD nucleus and left VL nucleus. Furthermore, the FC of bilateral MD and right PUL nucleus to regions of the visual cortex and sensory cortex was found to have a negative relationship with injury duration.

Parcellation of the thalamus using a data-driven technique such as independent component analysis with spatial regression accounts for some of the selection bias involved

with other techniques. Parcellating the thalamus also allows to study the thalamus segregated based on function rather than the conventional anatomical boundaries. The drawback, however, is the appropriate interpretation of the beta estimates as indirect measure of functional connectivity. Methodological limitations such as number of independent components also limit the application this technique on a neurological condition and necessitate a seed-based analysis to identify specific cortical correlates. Nevertheless, the parcellation into sub-nuclei conforms to thalamic sub-nuclei demonstrated in literature.

Functional connectivity findings indicated decreased connectivity between left MD nucleus and L.ACC, L.PUT and R.STG, and decreased connectivity between right MD nucleus and R.ROPE and R.STG in SCI. Also at a lower threshold, the right MD nucleus displayed reduced connectivity with dorsal ACC and left insula in SCI group. The MD nucleus consisting of medial and lateral subdivision is known to influence cognitive processes including working memory, executive function, emotional perception, and decision-making [140,141]. Rodent and non-human primates show extensive reciprocal connections between the MD nucleus and PFC with ablation of one resulting in dysfunction of the other [142-145]. Furthermore, some literature suggests that sympathetic and parasympathetic afferents from the tissues in the body project to the insular cortex and dorsal ACC through the ventromedial and MD nucleus, respectively [146]. Taken together, disconnection of autonomic afferents from lower motor centers to the thalamus in SCI could explain the hypo-connectivity of the MD nucleus with the ACC, and insula. Furthermore, the dorsal ACC, insula, striatum, amygdala along with the PFC constitute the salience network responsible for integrating internal sensory information (interoception

and visceromotor signals) with external sensory information to generate meaningful neural responses including emotional awareness [147].

The salience network is also posited as the pain matrix of the brain where the occurrence of central pain condition is considered as a behavioral response to an event of imbalance in the internal and external sensory information or bodily states [148]. So, if the same cortical regions represent the visceral, emotional and pain states of the body, an alteration in connectivity of MD thalamus to these cortical regions could be associated to both emotion and pain processing deficits observed in SCI. Impairment of emotional perception in SCI although subtle is greatly debated and is still overlooked due to the overbearing psychological consequence of a life-altering injury. Emerging evidence in SCI indicates impaired emotional perception [69] and enhanced activity in dACC, temporal gyrus, and periaqueductal grey regions during an emotional fear conditioning task [149]. A disorder that is comparable with SCI is Pure Autonomic Failure (PAF). Unlike SCI that may withstand both autonomic and sensorimotor denervation, PAF is a disorder of the autonomic ganglia adjacent to the spinal cord leading to autonomic denervation with intact sensorimotor afferents. Interestingly, individuals with PAF report similar difficulty in identifying their own emotions but accompanied by increased activity in ACC and decreased activity in the right insula during a stressor task [150]. Intriguingly, neuropathic pain is rarely reported in PAF cases suggesting that although impaired emotion and central pain are an aspect of autonomic function, their cortical or subcortical correlates might differ. The cortical basis of pain as postulated by the thermosensory-inhibition theory states that the pain could result from the lack of descending signals emerging from dorsal ACC to the homeostatic sites regarding thermoregulatory behavior (parabrachial nucleus and

periaqueductal grey) [151]. If the above is true, we could debate whether the decreased connectivity observed between ACC and L.MD could perhaps contribute to reduced connectivity to the brainstem. However, we do not have information regarding the pain status of the SCI patients, and therefore no direct conclusion of the results can be drawn regarding pain.

Results also revealed an increase in functional connectivity between left PUL nucleus and L.IFG and at a lower threshold demonstrated increased FC with the left superior occipital gyrus, right precuneus and anterior thalamus in the SCI group. The PUL is a higher order nucleus that receives the majority of the inputs from the cortex and sends efferent connections to the cortex [152]. It is also an important component of the visual attention network with connections mostly extending to regions of multi-sensory association cortices [153]. Example, PUL nucleus connects to posterior parietal lobe and frontal gyrus for visuo-somaesthetic processing and superior temporal gyrus for visuoauditory processing. Besides, the PUL is believed to regulate and facilitate large-scale synchronization of cortical regions through cortico-pulvinar-cortical pathways [154]. Therefore, a lack of afferents from lower motor centers could create an imbalance in sensory-weighting, initiating a compensatory increase in synchronization between the multisensory association cortices through PUL. After all, the accuracy of spontaneous or goal-directed movements depends on the accurate and continuous processing of visual information updated by body's spatial representation through proprioception. Hence, an increase in connectivity between the left PUL and the regions of the frontoparietal network in SCI patients could be a compensatory mechanism contributing to spatial awareness and body image in individuals with a lack of proprioceptive feedback.

Additionally, an increased connectivity between the left PUL and anterior thalamus was observed at a lower threshold supports the above explained lack of proprioception as the anterior thalamus has been shown to contain head direction cells that encode the direction of the head with respect to the environment for spatial navigation [155]. Similarly, SCI patients rely more on visual, vestibular and auditory sources for spatial navigation. However, the same differences were not observed for the right PUL nucleus as it presented with decreased FC with L.STG in SCI group when compared to HC group. The significance of this is unclear although animal and human studies suggest that the pulvinar, depending on its connection to the parietal region, may allocate attention to the occipitotemporal stream or the ventral stream that is associated to the recognition of an object in space [156,157].

Seed based analysis resulted in decreased connectivity of the left VL nucleus to R.STG with no changes in the FC of right VL nucleus. The VL nucleus along with other ventral subnuclei are the motor thalamic nucleus that receives afferent signals from lower motor centers and relays sensory information to the cortical layers of M1, SMA, and premotor cortex [158]. The lack of significant differences in the FC of VL nucleus was unanticipated considering the large number of reports on the reorganization of motor components after SCI. Maybe, examining the FC of the sensorimotor network in the same cohort would benefit from the interpretation of these results. Additionally, it could also be a consequence of the seed selection as the effects of SCI can be greater in the ventroposterior lateral nucleus (sensory nuclei) rather than the motor nucleus of the thalamus. Furthermore, since the right PUL and right VL nucleus result in few or no significant differences in FC, it raises the question of whether the thalamus dysfunction in

SCI patients manifests in the left hemisphere due to asymmetrical thalamic function. Evolutionarily, the lateralization of the thalamus function is expected to reflect the asymmetric organization of the cortex; where the left hemisphere majorly dictates language processing and the right hemisphere implements visuospatial attention processing [159]. But again, the notion that almost all thalamic relays to the neocortex are likely regarding ongoing cortical and subcortical activity related to efferent motor commands has been previously established [160]. Hence, a left-lateralization of thalamus dysfunction observed in this study could merely be the result of investigating right-handed or left hemisphere motor dominant individuals with complete SCI.

Lastly, a significant association between FC measures of different thalamic nuclei and duration of injury indicates that the functional alterations of the thalamus are likely dynamic and vary through the recovery process after SCI. Specifically, the FC of the left MD, right MD and right PUL nucleus with the regions of the dorsal visual attention stream and visual cortex appears to vary depending on duration since the time of injury. Our findings indicate that the average FC of thalamic nuclei is positive and higher in individuals with shorter post-injury duration (~3 months) that gradually declines and approaches the HC level in individuals with longer disease duration (~12 months). The immediate increase in FC post-injury could be attributed as a compensatory response to deafferentation though it is unclear if this would always contribute to recovery or lead to long-term spurious cortical rewiring. Hou et al. show a similar increase in FC of M1 and cerebellum to anterior and MD portions of the thalamus respectively, in incomplete SCI at ~12 weeks post-injury. In contrast to our findings, Rao et al. report observing a decrease in FC between the thalamus and parieto-occipital association cortex of rhesus monkeys with right

hemitransection at 8 weeks post-injury. Though, it is possible that the completeness of the injury could explain the inconsistency in our results, inter-subject variability in residual functionality, rehabilitation techniques, comorbidities and non-linear recovery patterns emphasize the need for longitudinal studies in humans with SCI. A more recent study in individuals with complete SCI report a decrease in FC between the visual cortex and the motor cortex simultaneous with a compensatory increase in FC of visual cortex with sensory parietal cortex [135]. Perhaps this compensatory increase between the visual and sensory parietal cortex is reflected by or is a reflection of alterations in the potential visuo-thalamo-parietal pathways.

4.4.3 Conclusion

The present study uses resting state fMRI in order to demonstrate functional connectivity changes in cortical and subcortical brain networks after SCI. Although, preliminary in nature, a number of novel observations are made in this study. We report differences in functional connectivity of sensorimotor regions between the subtypes of SCI. We also successfully parcellated the thalamus and demonstrated widespread decrease in thalamic functional connectivity in SCI patients using resting-state fMRI.

The study has few limitations, first, the lack of patient information on pain status and rehabilitation limits our understanding of the functional implications of the current findings. Next, by performing a priori selection of regions for the functional analysis, the scope of the study was limited to the pre-defined regions of interest. The functional analysis does not also account for structural changes present in this population as a result of the injury. Alternatively, future studies could investigate the resting state properties using a data-driven approach. It is also recommended that the effects of grey matter changes are

taken into account while examining the functional connectivity of cortical or sub-cortical structures after SCI.

Nevertheless, this is the first study to investigate and quantify resting state FC patterns of the whole brain as well as the different sub-nuclei after complete paraplegic SCI when compared to HC. We demonstrate significant changes in the FC of the pulvinar and MD nucleus in complete SCI in comparison to HC. We also show variation in FC of higher order nuclei to visual attention regions depends on the duration since injury in these individuals. Our study provides a new outlook to the role of thalamus in SCI and can advance our understanding of the pathophysiology leading to successful clinical recovery in SCI patients.

CHAPTER 5

FUNCTIONAL NEAR-INFRARED SPECTROSCOPY IN SPINAL CORD INJURY (Aim 3)

5.1 Introduction

5.1.1 Background

Neuroplasticity after SCI is often facilitated by means of physical therapy either involving a conventional physical therapy or using targeted interventional therapy [161-163]. Research has shown that repetitive physical training stimulates neuroplasticity by inducing neural rewiring, sprouting and upregulation of brain derived neurotrophic factors and neurotransmitters within the central nervous system[164]. Such activity dependent neuroplasticity is anticipated to manifest as altered activity in brain regions associated with lost function, as well as in areas of intact function to compensate and accommodate the lost functionality[165]. Functional MRI has laid the foundation for identifying, formulating and understanding the mechanisms of such neuroplastic changes in humans in the form of changes in functional connectivity and task evoked activity [11,16,18,43,109,110,112]. Studies have repeatedly confirmed an expansion in the somatotopic representation of the body rostral to the area of injury in the brain in individuals with SCI. That is, people with paraplegia for example, report exhibiting an expansion of the functional representation of hand region towards the affected leg region in M1 and S1 regions[12,41,42]. As previously described in Chapter 3, resting-state studies also report decrease in the intrinsic functional connectivity of the sensorimotor cortex, specifically between a) bilateral primary motor cortices [17], b) bilateral supplementary motor area (SMA)[18] and M1, and c) primary sensory cortex (S1) and other sensorimotor regions[16]. Such alterations in resting state properties have emerged

to hold significant implications for functional recovery after SCI. However, MRI suffers from the major shortcoming of limiting large movements inside the scanner making it unsuitable for testing the cortical correlates associated to dynamic naturalistic movements such as gait-training or upper extremity manipulation training or even simple movements such as sit to stand etc. A non-invasive neuroimaging technique that is alternatively suited for investigating the neural underpinnings of cortical reorganization and recovery in people with SCI in a real-world setting is the **continuous wave fNIRS**[166]. fNIRS offers a unique and cost-effective approach to quantify changes in the hemoglobin concentration proximal to the surface of the cortex during dynamic tasks such as gait training, which is not possible with fMRI[167,168].

5.1.2 Functional Near-Infrared Spectroscopy

Continuous wave fNIRS is a promising technique to non-invasively and reliably measure the hemodynamic response of the brain at a high temporal resolution[168,169]. fNIRS utilizes the same concept of neuro-vascular coupling as fMRI to indirectly quantify brain activity[31,168]; fNIRS however takes advantage of the optical properties of the oxy-hemoglobin (HbO) and deoxy-hemoglobin (HbR) molecules in the visible and near-infrared frequency range[170]. Specifically, the absorption properties of the chromophores (HbO and HbR) in the 700-1000 nm range that is typically transparent to biological tissue and water is targeted. This is performed by introducing near-infrared light at the abovementioned frequency (also known as the optical window) such that the light penetrates through the scalp, skull and the cortex and becomes absorbed, scattered and reflected in all directions. Using the appropriate placement of sources and detectors, the reflected signal is then captured by the detectors. Depending on the amount of light that is

reflected the concentration of the chromophores are quantified using a modified Beer-Lambert's law. The modified Beer-Lambert's law essentially describes the relationship between change in light attenuation and chromophore concentration[168]. For instance, an increase in neuronal activation during task increases the demand of cerebral metabolites causing a cascade of changes in the cerebral blood flow, cerebral blood volume and metabolic rate of oxygen consumption [171-173]. The overcompensation of blood flow results in changes in HbO and HbR concentration that is reflected and recorded as optical intensity values at the near-infrared range (650-950nm) of the electromagnetic spectrum[174].

Even though fNIRS does not rectify all shortcomings of fMRI and holds few inherent limitations by itself, it still offers key methodological advantages[175,176]. First, the hemodynamics measured using fNIRS is less prone to head-motion noise. Next, it allows hemoglobin concentration changes at a temporal resolution of 1-2 milliseconds. And lastly, even though fNIRS do not permit recording of secondary physiological measures such as perfusion, oxygen extraction fraction or cerebral metabolic rate of oxygen consumption, short-source separation channels enable removal of physiological noise by recording hemodynamic activity from non-brain regions such as meninges and skull[177].

5.1.3 Application of Functional Near-Infrared Spectroscopy in SCI

There is ample evidence encouraging the use of fNIRS in neurorehabilitation and neurofeedback of the SCI population[169,172,178]. fNIRS originally gained popularity in the study of cognition and sensory development in infants due to its ability to test brain function in a natural setting that is less susceptible to motion artifacts[179,180]. But the aforesaid also opens opportunities for the study of motor behavior in SCI population, specifically to examine cortical mechanisms underlying real-world movements involved in

rehabilitation. fNIRS studies using motor paradigms report region-specific differences in the spatiotemporal characteristics of hemodynamic response to different movements[181]. Investigators of a clinical trial report using fNIRS to successfully monitor the real-time cortical activity during robot-assisted gait training in three people with SCI[178]. This ability to investigate cortical correlates common and distinct to the variations of motor or sensory tasks in a real-world setting makes fNIRS an excellent tool for both prognostication of SCI as well as formulation of effective treatment strategies after SCI. With advancements in the mechanical design of the fNIRS system, a more compact, portable and even laser-less systems could offer rehabilitation studies a simpler and economical imaging technique to record simultaneous cortical activity during regular gait training or with advanced robot assisted physical therapy[182]. Plus, the simplicity of the fNIRS system makes it suitable for longitudinal studies, for example, to monitor brain changes during the rehabilitation phase. However, no studies have thus far applied fNIRS to systematically investigate cortical reorganization after SCI [166].

Furthermore, impairment of the sympathetic control after SCI results in cardiovascular deficits such as supine hypotension, orthostatic hypotension, cardiac arrhythmia and autonomic dysreflexia [183]. Especially injuries above T6 level result in the impairment of dynamic cerebral autoregulation, cerebrovascular reactivity and neurovascular coupling properties of cerebrovascular control [30]. Dong-Il Kim and colleagues proposed that SCI patients will experience decreased perfusion in response to increase in arterial CO_2 or metabolic demand when compared to healthy counterparts[184]. Based on their model, it is suggested that the imbalance in cerebrovascular control may in turn influence the inference of task-induced hemodynamic response in SCI patients[184].

Cerebrovascular impairment in other populations such as stroke typically require the removal of cerebrovascular differences to understand true neuronal effects. However, differences in cerebrovascular reactivity after SCI is often not examined in neuroimaging studies measuring brain activity after SCI.

Therefore, the objective of this study is to validate the use of fNIRS in identifying cortical reorganization following SCI specifically within the sensorimotor cortex while accounting for differences in cerebrovascular reactivity. It was first hypothesized that the hemodynamic response measured using fNIRS is sensitive to differential patterns of activation in the sensorimotor cortex including regions of close proximity. We hypothesized that this hemodynamic response reflects the somatotopic reorganization previously reported after SCI resulting in paraplegia. Our final hypothesis was that accounting for cerebrovascular reactivity will ensure that the hemodynamic response measured using fNIRS reflect true neuronal differences after SCI.

The proposed hypotheses were tested by comparing one of the most robust and well-studied motor paradigms in fNIRS studies [185], finger tapping, in healthy participants and people with paraplegic SCI. An expansion or alteration in the representation of the unaffected limb in the cortex after paraplegic SCI was demonstrated by comparing finger tapping movement with the movement of the affected limb (by means of an attempted ankle tapping movement). Additionally, to ensure the cortical differences are in fact a result of abnormal brain activity from the injury, finger tapping movement was also compared with an intact motor action (finger tapping imagery) as a control paradigm. Cerebrovascular reactivity measured using a simple and non-invasive breath hold task was then used to calibrate task-based fNIRS measures to identify neuronal differences after paraplegic SCI

[32]. The findings of this dissertation using fNIRS in the SCI population could prove as a benchmark for future studies employing flexible task designs to study cortical correlates of movements in neurological population with lower-body paralysis. Advanced signal processing strategies in combination with longitudinal recordings could also expand the application of fNIRS as a therapeutic tool. Furthermore, the ability to account for vascular effects could expand the implementation of fNIRS to patient populations involving conditions with vascular impairments.

5.2 Test-Retest Reliability of Cortical Activity using fNIRS (Aim 3a)

For the first part of this study, a total of 42 young healthy participants were recruited, 16 of the 42 were scanned during two separate sessions/visits were examined to compute the test-retest reliability of cortical activity measures from task-based and resting-state fNIRS data.

5.2.1 Participants

Sixteen healthy participants (24.9 ± 5.6 years, 3 females) were recruited to participate in two session performed at least a week apart (demographics shown in

Table 5.1). Exclusion criteria included the use of orthopedic devices, neuromuscular or neurological disorders, chronic medical illness, history of psychosis, experiencing symptoms of depression or pregnant. Participants also had no history of brain trauma, psychiatric or neurological disorders. All procedures were performed in accordance with the guidelines approved by the institutional review board of New Jersey Institute of Technology. Each participant was informed, and consent was obtained before their participation in the study.

5.2.2 Instrument and Setup

A continuous wave 32 channel fNIRS system manufactured by Tech En Inc. with 690 and 830 nm lasers was used to measure HbO, HbR and total hemoglobin (HbT) concentration changes at a sampling frequency of 50 Hz. A custom designed 26 channel layout shown in Figure 5.1 was used to place the optodes on the scalp. The optodes were placed with the help of *Brain Sight (Rouge Research Inc.'s Neuronavigation System, Canada)* neural navigator such that channels recorded hemoglobin concentration changes from bilateral prefrontal, bilateral pre-motor and bilateral sensorimotor areas of the cortex. The *Brain Sight* neural navigator deformed the standard MNI template into the expected brain template of each individual subject, which was then used to place the optodes on the scalp. The optode placement was guided by pre-defined regions of interest (ROI) from fMRI literature, such that channel 3 (Source B to Detector 2) and channel 8 (Source D to Detector 5) measured Hb concentration changes from the ROI in right and left primary motor cortex (M1), channels 21 (Source F to Detector 3) or 22 (Source F to Detector 4) measured Hb concentration changes from supplementary motor area (SMA) and channels 7 (Source A to Detector 7) and 20 (Source E to Detector 12) measured from right and left lateral SMN.

Out of the 26 channels used, 25 channels were placed at a distance of 30 mm from the source to record cortical hemoglobin concentration changes whereas 1 channel was placed at a distance of 8.4 mm [177] from the source to record the physiological hemoglobin concentration changes from the meninges. A pictorial representation of optode placement and the respective channels are shown in Figure 5.1b.

Table 5.1 Demographics of the Healthy Participants Recruited in the Test-Retest Reliability Study

Subject	Age (years)	Gender
01	27	M
02	21	M
03	27	M
04	24	M
05	26	M
06	19	M
07	25	F
08	20	M
09	18	M
10	26	M
11	41	F
12	31	F
13	18	M
14	24	M
15	27	M
16	25	M

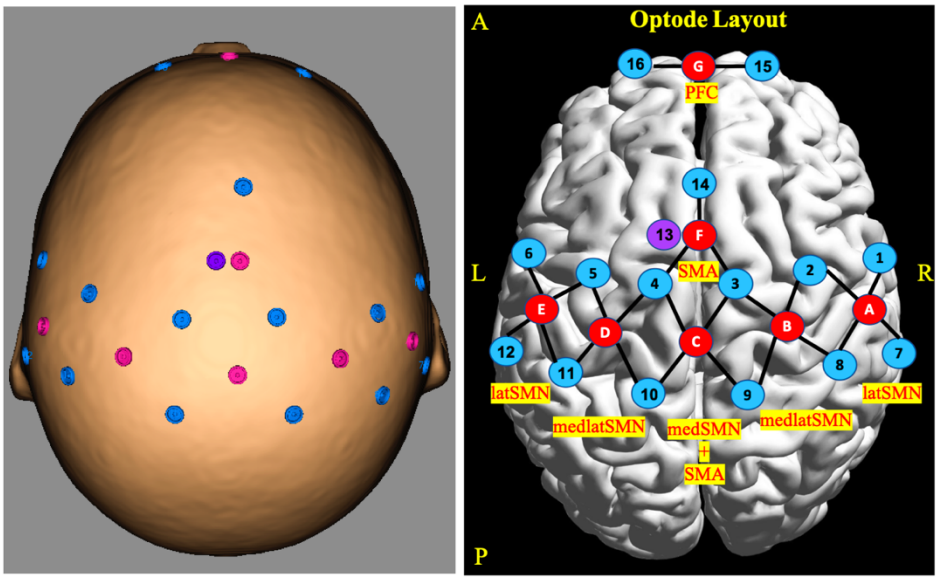

Figure 5.1 a) Optodes as placed on the scalp of the subject where blue indicates the detectors 1 to 16 except 13, pink indicates the sources A to B and violet indicates detector 13 measuring physiological signal. b) Twenty-six channels (represented by black connections) divided into 7 regions of interest namely, A-right lateral SMN (latSMN), B-right medial SMN (medSMN), C-SMN+SMA (medSMN+SMA), D-left lateral SMN, E-left lateral SMN, F-SMA, G-prefrontal cortex. A-P indicate anterior-posterior orientation, L-R indicate left-right orientation.

5.2.3 Task Protocol

The task protocol proceeded in the following order i) 7-minute rest scan, ii) 4 runs of 6.5-minute motor scan and iii) 5.5-minute breath hold scan. For this study, only the motor and breath hold data were analyzed and therefore the resting state scans will not be discussed further. Every motor run consisted of 9 blocks of 20 second rest period alternated by 20 second task period. The motor tasks comprised of three different movements; bilateral finger tapping (FT), imagination of bilateral finger tapping by mental imagery (FTI) and bilateral ankle tapping (AT). The tasks appeared in randomized order through the four runs to avoid habituation (as shown in Figure 5.2

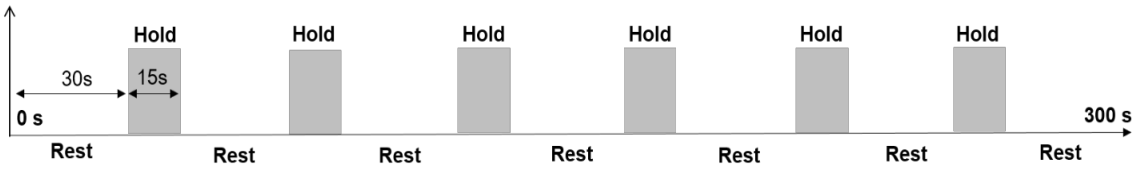

a). The breath hold task comprised of 30 seconds of relaxed breathing alternated by 15 seconds of breath holding for a total of 5.5 minutes (shown in Figure 5.2

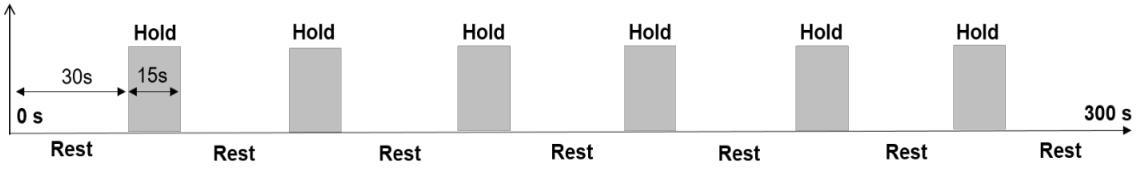

b). The total duration of the experiment included 30 minutes of setup and 38 minutes of scan time. The same protocol was repeated during the second visit.

5.2.4 Data Analysis

Intensity values acquired in the NIRS format was analyzed using MATLAB R2012a with the help of in-house scripts. A schematic of the preprocessing pipeline is displayed in Figure 5.3. Conversion of raw intensity values to optical density was performed using the equation *Absorbance* $A = -\log(I/I_o)$, where I is the intensity of the light measured and I_o is the initial light intensity (in this case the mean of I over the entire duration). Head motion seen as abrupt spikes in the optical density data was removed using wavelet-based correction technique introduced by Molavi B and colleagues [186]. The motion-corrected optical density values were bandpass filtered (0.008-0.1 Hz for rest and 0.008-0.15 Hz for task) and converted into concentration values using modified beer-lambert law through HomeR2 function *hmrOD2Conc*. The concentration values included HbO, HbR and HbT concentration changes in 26 channels (including physiological channel). Next, the high pass filtered (with a cut-off of 0.1hz) physiological channel was removed from the

concentration values of remaining 25 channels using simple linear regression [187]. The residuals of the regression model were used to perform quality control, where, the total power of the first principal component of HbO concentration changes in the low-frequency range (0.002-0.03 Hz) was computed for all participants from all four motor runs. Participants with total power more than 1.5 times the interquartile range away from the first or third quartile was considered as outliers. Based on this criteria, four subjects were excluded as outliers from the remainder of the analysis.

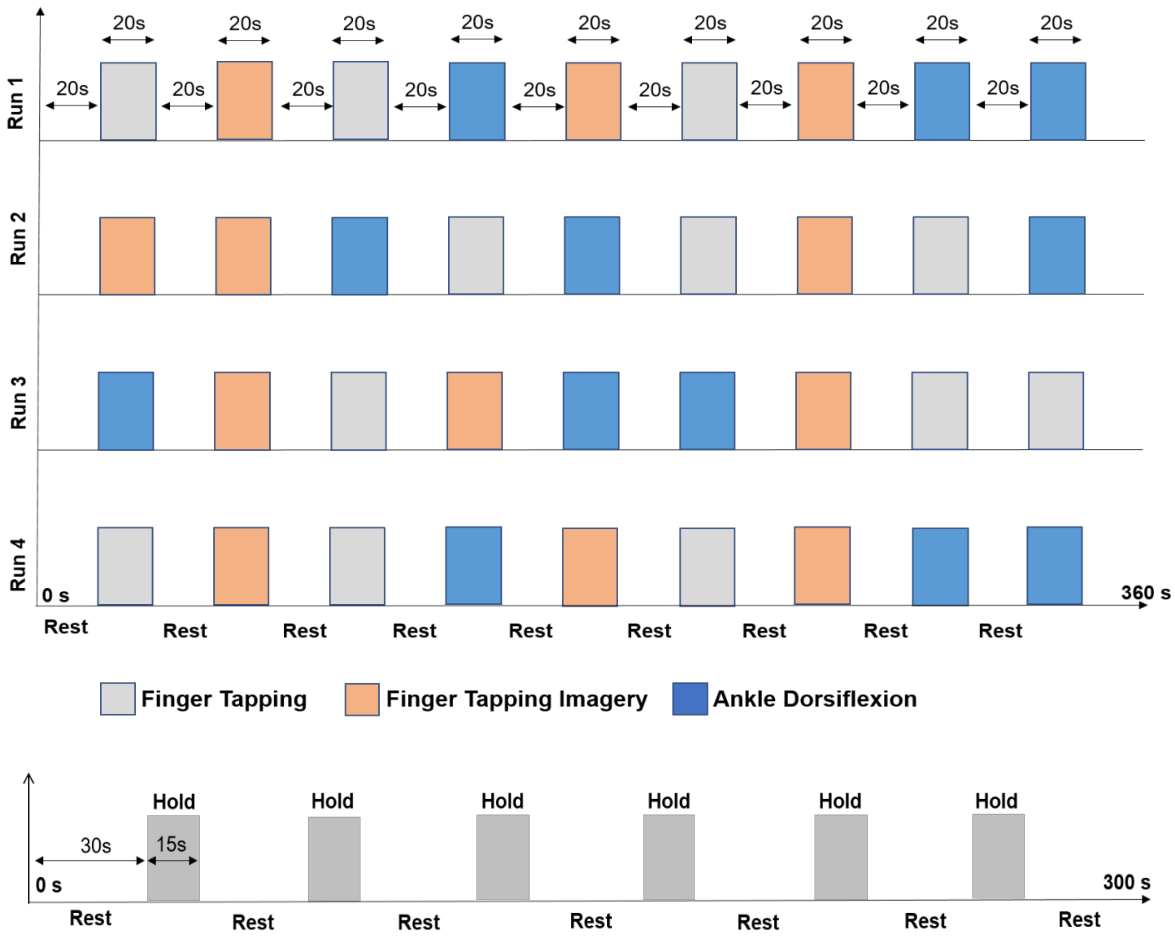

Figure 5.2 Task protocol for four runs of motor task and one run of breath hold task: a) Each run of motor task includes a boxcar design of 20 second rest period alternated with 20 second motor task period for a total duration of 380 seconds and b) breath hold task includes a boxcar design of 30 second rest period alternated with 15 second breath hold period for a total duration of 300 seconds.

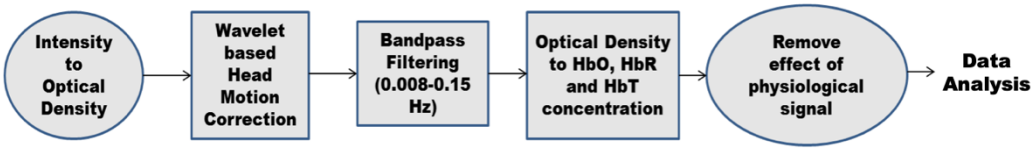

Figure 5.3 Preprocessing pipeline of raw intensity data in NIRS format to obtain processed concentration changes of HbO, HbR, HbT for data analysis.

5.2.5 Test-Retest Reliability Measurement

Intraclass correlation coefficient (ICC) was computed to test the reliability of fNIRS metrics within session as well between the two sessions. A two-way random model with single measure ICC was computed using Equation 5.1.

$$ICC = \frac{Variance_{betweensubject} - Variance_{withinsubject}}{Variance_{betweensubject} + (k-1) * Variance_{withinsubject}} \quad (5.1)$$

Where, k=1 and $Variance_{betweensubject}$ and $Variance_{withinsubject}$ are the between subject and within subject variance of the data[188]. All ICC calculations were performed using the IPN toolbox available in MATLAB[189]. ICC measures were evaluated based on the criteria that ICC of 0 to 0.25 is poor, 0.25 to 0.4 is low, 0.4 to 0.6 is fair, 0.6 to 0.75 is good and 0.75 to 1 is excellent reliability[190].

5.2.5.1 Resting-State Activation. The test-retest reliability of resting-state data was computed on the resting-state functional connectivity measure of 300 channel pairs obtained during session 1 and session 2 in 16 participants. This was obtained by performing a Pearson's correlation between HbO concentration changes in every channel with the remaining 24 channels of every subject in each session. ICC was then computed for the 300 functional connectivity measures of each subject in session 1 with session 2.

5.2.5.2 Motor Task Activation. The test-retest reliability of task data within-session (cap was never removed) and between-session was computed on the area under the HbO curve (AUC) measure of different motors tasks. The AUC was computed as the integration of HbO concentration during the stimulus duration, i.e., n=0 to 20 seconds. The AUC was calculated on the rescaled average hemodynamic response (rescaled to 0 and above) using

trapz algorithm in MATLAB. The average hemodynamic response of a channel to the different motor tasks, FT, FTI and AT within a session was estimated by averaging all the blocks corresponding to a particular motor task in a channel during a given run. For example, block of motor task is defined was the 5 seconds before the start of stimuli, the 20 seconds of continuous stimuli and the 20 seconds of rest following stimuli (total duration: 45 seconds). Every run consists of 3 blocks of FT, FTI and AT each and therefore an average of the three blocks in each run was used to perform within-session reliability analysis of each task. Similarly, for between-session reliability analysis, the average hemodynamic response was obtained from all 12 blocks of a session and was used to perform between-session reliability analysis of each task. ICC measures were computed for within-session reliability during session 1 and between-session reliability i.e., between session 1 and session 2 for each of the channels during each of the tasks.

5.2.5.3 Breath Hold Activation. The same analysis described in 5.2.5.2 was repeated for breath hold task, where a block was defined as the 5 seconds before the start of stimuli, the 15 seconds of continuous stimuli and the 30 seconds of rest following stimuli (total duration: 50 seconds). The average hemodynamic response was calculated by averaging the 6 blocks of every channel in every subject in session 1 and 2. The AUC was computed using the *trapz* algorithm by rescaling the average hemodynamic response (to 0 and above) for the interval of n=10 to 30 seconds. ICC measures were computed for the AUC of every channel in subjects in session 1 with session 2.

5.3 Application of fNIRS in Spinal Cord Injury (Aim 3b-Aim3d)

For the second part of this study, the proposed hypotheses were validated by comparing the task-based and resting-state fNIRS measures from 13 males with paraplegic SCI with 13 age-matched healthy male participants.

5.3.1 Participants

Fourteen healthy males (47.6 years) and thirteen males with paraplegic spinal cord injury (48.4 years) were recruited in this study (demographics shown in Table 5.2). Exclusion criteria included a history of brain trauma, neuromuscular or neurological disorders, chronic medical illness, history of addiction, history of psychosis, symptoms of depression or pregnancy. Participants with SCI were excluded if they had an injury to the cervical level of the spinal cord. All procedures were performed in accordance with the guidelines approved by the institutional review board of New Jersey Institute of Technology. Each participant was informed, and consent was obtained before their participation in the study.

Table 5.2 Demographics of Participants with SCI Recruited in this Study

ID	AGE	LEVEL OF INJURY	#Disconnected segments	Complete/Incomplete	CAUSE	NEUROPATHIC PAIN	Duration Of Injury (years)
S01	42	T7	15	C	Elevator accident	Yes	8
S02	73	T3	19	C	Automobile	No	33
S03	32	T8	14	I	Automobile	Yes	5
S04	45	T4	18	C	Construction accident	No	15
S05	53	T10	12	C	Tree fall	Yes	2
S06	68	T3	19	I	Automobile	No	40
S07	59	T3-4	18	C	Air bubble in the spine	Yes	14
S08	43	T11	11	I	Fall	Yes	8
S09	38	T10	12	C	Gunshot	Yes	11
S10	42	T2	20	C	Automobile	Yes	12
S11	55	T10	12	C	Construction accident	Yes	11
S12	30	T12	10	C	Fall	Yes	5
S13	50	T1	21	I	Diving accident	Yes	22

5.3.2 Instrument and Setup

A continuous wave 32 channel fNIRS system manufactured by Tech En Inc. with 690 and 830 nm lasers was used to measure HbO, HbR and total hemoglobin (HbT) concentration changes at a sampling frequency of 50 Hz. A custom designed 26 channel layout shown in Figure 4.1 was also used for this study. The optode placement and regions of interest are explained in Section 4.4. A pictorial representation of optode placement and the respective channels on a person with paraplegic SCI is shown in Figure 5.4.

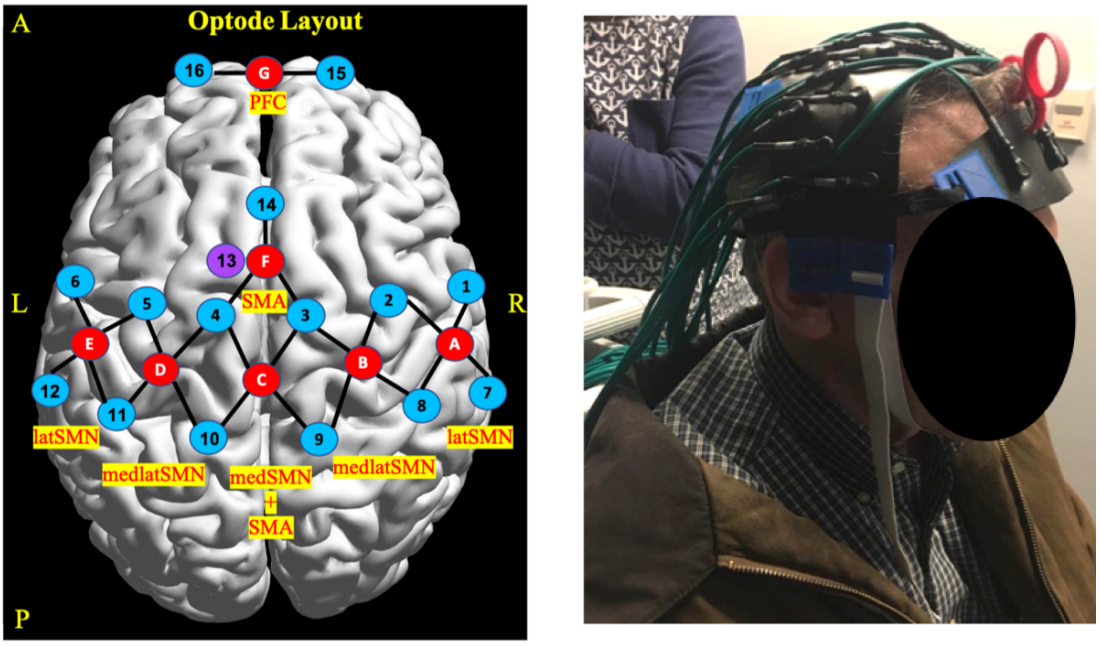

Figure 5.4: a) Optode layout where, red indicates the sources A to B, violet indicates detector 13 measuring physiological signal from the meninges and blue indicates the detectors 1 to 16 except 13. A total of twenty-six channels were recorded (represented by black edges). The channels were divided into 7 regions of interest namely, source A-right lateral SMN (latSMN), B-right medial SMN (medSMN), C-SMN+SMA (medSMN+SMA), D-left lateral SMN, E-left lateral SMN, F-SMA, G-prefrontal cortex. A-P indicate anterior posterior orientation, L-R indicate left and right orientation. b) Optode cap setup as seen in a participant.

5.3.3 Task Protocol

Similar to the task protocol in the Chapter 3, the task protocol for this study proceeded in the following order i) 7-minute rest scan, ii) 4 runs of 6.5-minute motor scan and iii) 5.5-minute breath hold scan. During rest, the subject was instructed to stay still with eyes open. Every motor run consisted of 9 blocks of 20 second rest period alternated by 20 second task period. The motor tasks comprised of three different movements; bilateral finger tapping (FT), imagination of bilateral finger tapping by mental imagery (FTI) with action observation and bilateral ankle tapping (AT). During action observation participants watched a 20 second animated video of bilateral finger tapping at 2Hz frequency created using Unity 3D. The tasks appeared in randomized order through the 4 runs to avoid habituation (as shown in Figure 5.5a). The breath hold task comprised of 30 seconds of relaxed breathing alternated by 15 seconds of breath holding for a total of 5.5 minutes (shown in Figure 5.5b). The total duration of the experiment included 30 minutes of setup and 38 minutes of scan time.

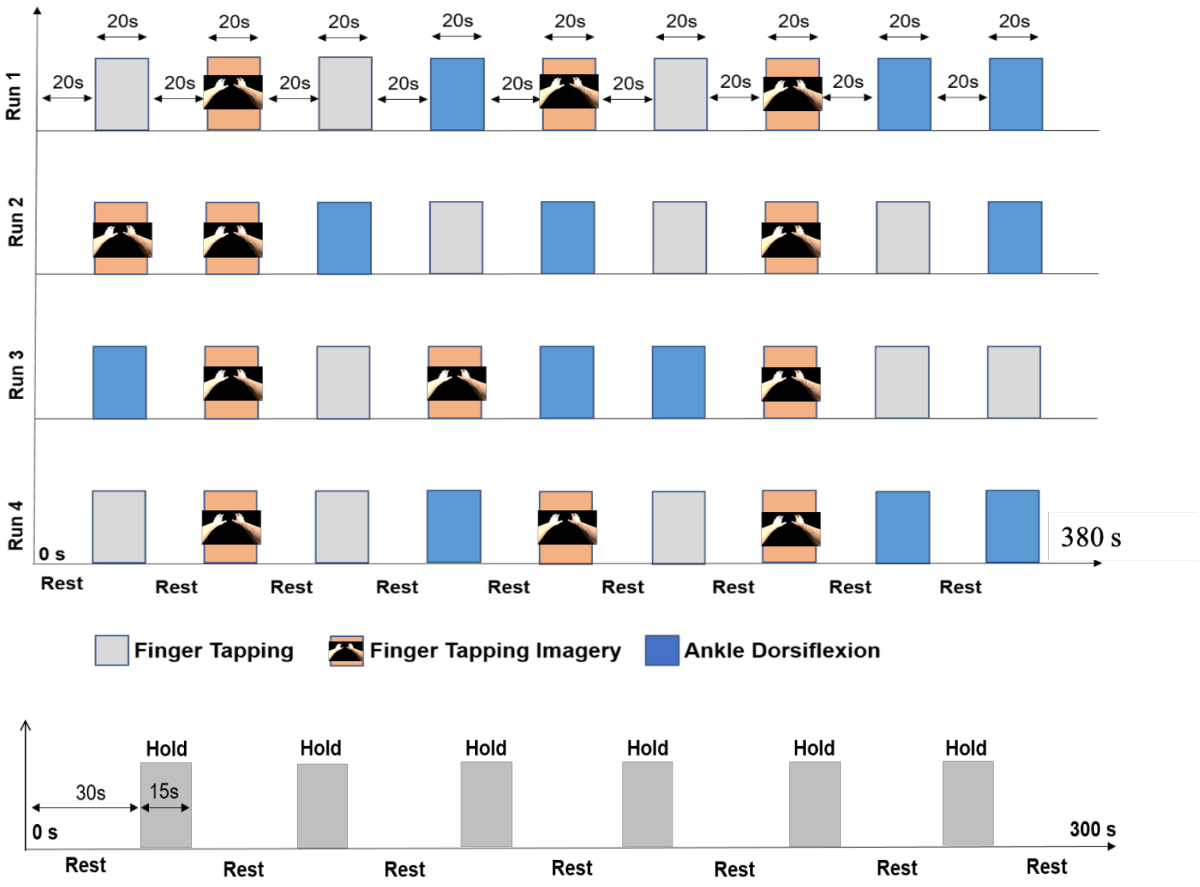

Figure 5.5 Task protocol for four runs of motor task and one run of breath hold task: a) Each run of motor task includes a boxcar design of 20 second rest period alternated with 20 second motor task period for a total duration of 380 seconds and b) breath hold task includes a boxcar design of 30 second rest period alternated with 15 second breath hold period for a total duration of 300 seconds.

5.3.4 Data Analysis

All preprocessing steps were performed using in-house scripts in MATLAB R2012 platform. Preprocessing included optical density measurement, head-motion correction, bandpass filtering (0.008-0.1 Hz for rest and 0.008-0.15 Hz for task), conversion to concentration and regression of physiological channel. Each of the preprocessing steps are explained in greater detail in the data analysis Section 4.2.4.

5.3.5 Resting-State Functional Connectivity Analysis (Aim 3b)

Resting-state functional connectivity was computed by performing a Pearson's r correlation between the HbO time-series of every channel with all the other 24 channels resulting in a 25x25 correlation matrix. A two-sample t-test was performed for every channel pair to identify significant differences in functional connectivity between the two groups. Functional connectivity measures of significant channel pairs were extracted and correlated with post-injury duration and number of disconnected segments to identify significant relationship between resting-state functional connectivity and SCI characteristics.

Further, to measure the lateralization of functional connectivity within the motor cortex, a lateralization index was computed for the 11 homologous channel pairs (or 22 channels) placed on the sensorimotor cortex. Ten out of the 11 channel pairs were placed on the bilateral sensorimotor cortex, while one pair was located on the SMA. The lateralization index (L.I) was computed using Equation 5.2.

$$L.I = \frac{R-L}{|R|+|L|} \tag{5.2}$$

where, R is the mean functional of the right channel in a channel-pair and L is the mean functional connectivity of the left channel in the channel pair[191]. The mean functional connectivity was calculated as the average connectivity of a channel to all other 22 channels in the SMN. The L.I measures of the 11 channel pairs were then compared between the two groups using a two-sample t-tests. Multiple comparison correction was performed using false-discovery rate correction.

5.3.6 Motor Task-Evoked Hemodynamic Measurement (Aim 3d)

i) Oxy-hemoglobin Concentration During Task: The block-average technique described in Section 4.2.1 was also applied to the task-data to compute the block-averaged hemodynamic response to different tasks. In brief, the hemoglobin changes to FT, FT imagery +action observation and AT were estimated for every channel to qualitatively compare the HDR curve between the tasks. A block of motor task was defined as the 5 seconds before the start of stimuli, the 20 seconds of continuous stimuli and the 20 seconds of rest following stimuli (total duration: 45 seconds). A total of 12 blocks of FT, FT imagery + action observation and AT from the four runs of motor task was used to calculate the average HbO and HbR for every channel. The channel-wise HDR were further categorized and averaged to quantify the average net change in HbO and HbR concentration in 7 ROI's viz. ROI 1 (channels 1-4), ROI 2 (channels 5-8), ROI 3 (channels 9-12), ROI 4 (channels 13-16), ROI 5 (channels 7-20), ROI 6 (channels 21-23) and ROI 7 (channels 24-25). Each block of HbO and HbR was normalized using the HbO and HbR concentration from the 5 seconds prior to the start of the stimuli in a given block.

Task activation was quantified as 1) maximum increase in HbO concentration during the duration of stimuli and 2) area under the HbO (AUC) curve during the duration of task. The AUC was calculated on the rescaled HbO time series (scaled to 0 and above). The task-activation measures (maximum increase in HbO and AUC) during a) FT, b) FT imagery +action observation, c) AT, d) FT-FT imagery + action observation and e) FT-AT were compared between the two groups using a two-sample t-tests.

A one-way ANOVA was also performed on the AUC measures of each of the three tasks in SCI group to identify main effects of duration since injury, level of injury,

neuropathic pain and and completeness of injury. Multiple comparison correction was performed using FDR-correction.

ii) Task-based Functional Connectome: Task-based functional connectome was calculated for every task type: FT, b) FT imagery + action observation and AT. The HbO timeseries from the task blocks corresponding to each of the task types during the fours run along with the 20seconds of rest period following the task block were concatenated together to generate a single HbO time series for each of the task types. The single HbO time series for each of the task types was generated for every channel in every subject. A Pearson's r correlation was then performed between the HbO time series of every channel with other 24 channels to generate a 25x25 correlation matrix corresponding to each of FT, FT imagery + action observation and AT per subject. A two-sample t-test was performed for each of the channel pairs to compare task-based functional connectivity during FT, AT and FT imagery +action observation in the two groups. Multiple comparison correction was performed using false-discovery rate correction.

5.3.7 Cerebrovascular Reactivity from Breath Hold (Aim 3c)

A block averaged technique described in Section 4.2.1 was also repeated for breath hold task, where a block was defined as the 5 seconds before the start of stimuli, the 15 seconds of continuous stimuli and the 30 seconds of rest following stimuli (total duration: 50 seconds). Six blocks from the breath hold scan was used to generate the average net change in HbO and HbR concentration for the 7 ROI's for all subjects. An average of the maximum increase (across the 6 blocks) in HbO concentration after breathing was resumed (was calculated as cerebrovascular reactivity in all subjects. Further to identify changes in the latency of breath hold activation, the time of maximum increase in HbO concentration was

estimated. The initial dip was quantified as the maximum decrease in HbO concentration in the first 10 seconds of breath holding. A two-sample t-test at alpha=0.05 was performed for all the breath hold measures to identify significant differences between HC and SCI group.

5.3.8 Calibration of Motor Activity using Cerebrovascular Reactivity (Aim 3d)

Maximum increase in HbO concentration during breath hold was used to calibrate the a) maximum increase in HbO concentration and b) area under the curve measures of each of the task types. The calibration was performed by regressing the breath hold activation from the task-activation measures across the 25 channels using a simple spatial linear regression model[192]. The residuals of regression were used to repeat the two-sample t-tests between HC and SCI group at alpha=0.05 for each of task types: FT, FT imagery + action observation, AT, FT-FT imagery +action observation and FT-AT. Multiple comparison correction was performed using false-discovery rate correction.

5.4 Results (Aim 4a)

5.4.1 Test-Retest Reliability of Resting-State Functional Connectivity

The ICC and Pearson's r correlation matrix of resting-state functional connectivity (Figure 5.6) indicates that the reliability during rest is mostly fair (0.3-0.5) but also high (>0.75) across the different channel pairs of the sensorimotor cortex and pre-frontal cortex[193]. Least reliable measures were observed within and between channels 21 to 23 and channels posterior to them, namely, 9-13. The most reliable connections (>0.75) were between sensorimotor channels in the two hemispheres, namely, 1-14, 1-17, 7-16, 14-20.

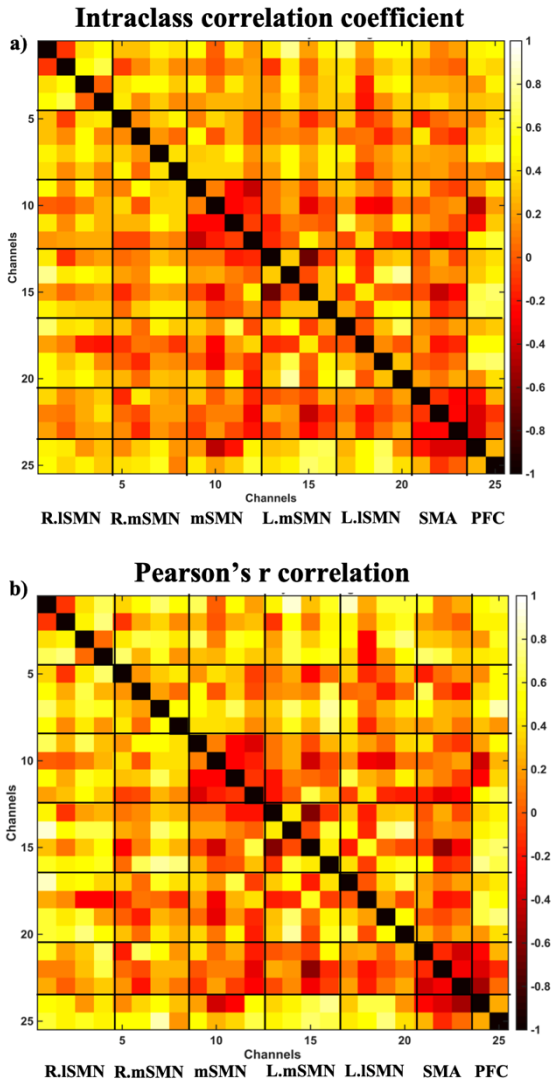

Figure 5.6 Test-Retest reliability measures of resting-state functional connectivity in 16 participants during 6.5 minutes of rest scan from session 1 and session 2: a) Intraclass correlation coefficient of RSFC between session 1 and session 2. The color bar indicates the ICC values with lighter colors denoting high positive ICC measures. b) Pearson's r correlation coefficient of RSFC between session 1 and session 2. The color indicates Pearson's r correlation values with lighter color denoting higher correlation coefficient. Note: the lower diagonal of the matrix is a mirror-image of the upper half of the matrix.

5.4.2 Test-Retest Reliability of Motor Task-Evoked Activation

Five out of the 16 participants had incomplete data in the motor run of session 1 and therefore had to be removed from the reliability analysis of motor tasks. The within-session reliability of AUC measures from the three motor tasks using the remaining 11 participants

(shown in Figure 5.7) was high in majority of the channels. A global ICC of 0.72,0.76 and 0.77 was achieved for FT, FTI and AT tasks, respectively. For the same 11 participants, the between-session ACC was only average (above 0.4) in 9 out of the 25 channels for FT task, 8 out of the 25 channels for FTI task and 13 out of the 25 channels for AT task. Additionally, Pearson's r correlation of the AUC measures from the 25 channels between-sessions for FT, FTI and AT were 0.41, 0.45 and 0.48 respectively.

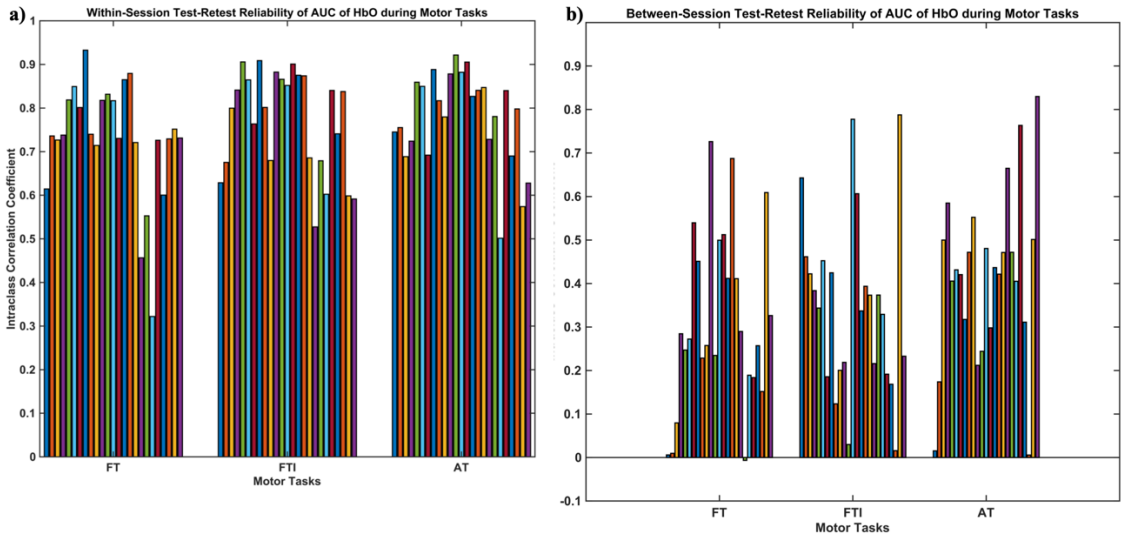

Figure 5.7 Test-Retest reliability of motor activation in 11 participants from session 1 and session 2: a) Within-session ICC (during the four runs) of the three different tasks, where each of the bars indicate a channel, b) Between-session ICC of the three different tasks, where each of the bars indicate a channel. The total number of channels is 25.

5.4.3 Test-Retest Reliability of Breath Hold Activation

The ICC measures of AUC measures during breath hold in 16 participants from session 1 and session 2 is shown in Figure 5.8. The reliability appears to be poor to good across the 25 channels. Surprisingly, the least reliability is observed in channels 1-4 and channels 23-25. The global reliability between the sessions was 0.435 and the Pearson's r correlation between the two session was 0.5 s

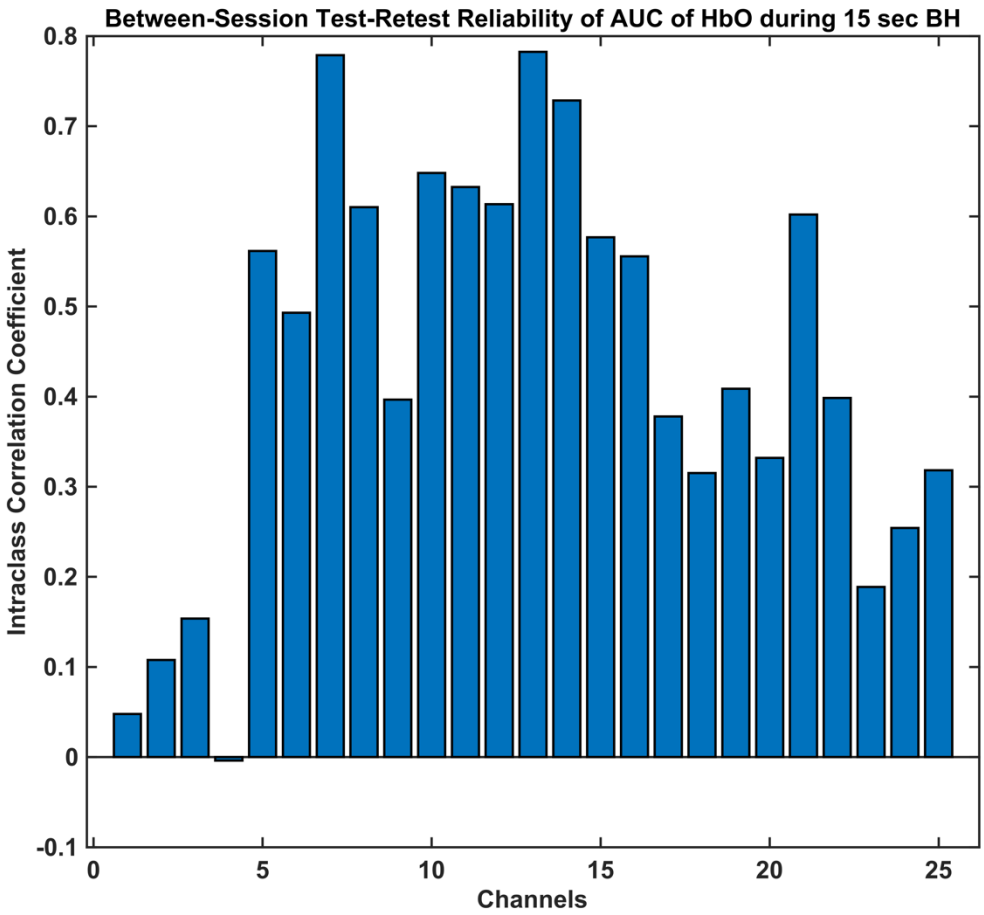

Figure 5.8 Test-Retest reliability of breath hold activation in 16 participants during session 1 and session 2 scanned at least a week apart.

5.5 Results (Aim 4b- Aim 4d)

5.5.1 Altered Resting-State Functional Connectivity in Spinal Cord Injury (Aim 4b)

Mean functional connectivity of the 25 channels in the sensorimotor cortex, supplementary motor area and pre-frontal cortex showed an over-all decrease in positive connectivity in the SCI group when compared to HC (Figure 5.9). High positive correlation was observed along the channels in the diagonal corresponding to channels in close proximity; thus, exhibiting high positive connectivity with each other in both SCI and HC. While the interhemispheric connectivity and between-region connectivity represented by the channel pairs off-diagonal exhibit much lower connectivity in the SCI group when compared to HC (Figure 5.3). Result of two-sample t-tests comparing the functional connectivity measures of 25 channels between the two groups is displayed in Figure 5.10. Figure 5.10a maps the 14 channel pairs in the motor cortex that exhibit significantly decreased connectivity in SCI group at $p<0.01$. It is mainly observed that a) the intrahemispheric connectivity in the precentral gyrus is decreased after SCI (i.e., between channels 2 -5, channels14-17), b) interhemispheric connectivity of primary somatosensory cortex (i.e., channels 4-19) is decreased after SCI and c) connectivity between medial SMN/SMA region with left post-central gyrus regions (i.e., channel 9 -15, 9-16) exhibit decreased connectivity d) connectivity between (i.e., channel 1-3) exhibit decreased connectivity.

Relationship between number of affected segments (level of injury) and Resting state functional connectivity: The average Pearson's r correlation measure for the 14 channel pairs are plotted in Figure 5.10b, where, the connectivity trend for the different channel pairs are the same and positive between two groups but reduced in SCI group. The resting-state functional connectivity of channels 11 and 12 was positively correlated to the number

of affected spinal cord segments with higher level injuries having greater functional connectivity in the medial posterior SMN of left (channel 12) and right hemisphere (channel 11) (shown in Figure 5.10c). In contrast, the functional connectivity of channels 9 and 16 exhibit a negative relationship with number of affected spinal cord segments implying that higher levels of injury are associated with lower functional connectivity between medial SMN +SMA (channel 9) region and left posterior mediolateral SMN (channel 16).

Further, by computing the lateralization index of the 11 homologous channel pairs in the sensorimotor cortex we observed three key significant effects a) Increased left lateralization in the anterior lateral areas (pre-central gyrus) of sensorimotor cortex in SCI group, b) Increased right lateralization in the posterior lateral areas (post-central gyrus) of sensorimotor cortex in SCI group and c) Significantly reduced right lateralization of posterior medio-lateral regions (post-central gyrus) in SCI group. No other channel pairs showed any observable differences in lateralization of RSFC between the two groups. Figure 5.11 shows the average lateralization index for each of the channel pairs in the sensorimotor in both the groups.

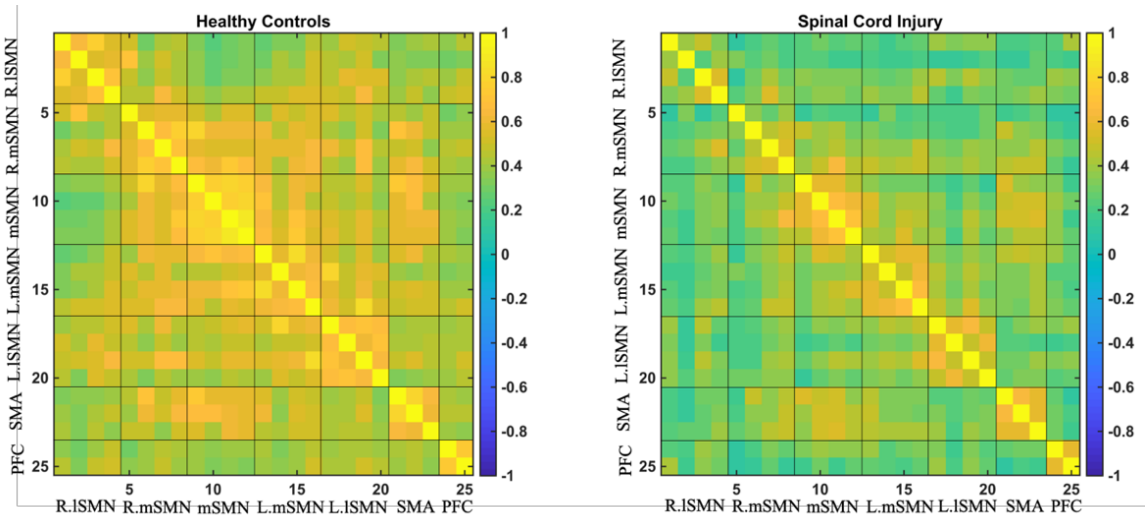

Figure 5.9 Mean functional connectivity maps of HC and SCI group. The 25 channel locations are labelled on the x and y axis. Color bar indicates the Pearson's r correlation measure of each channel pair.

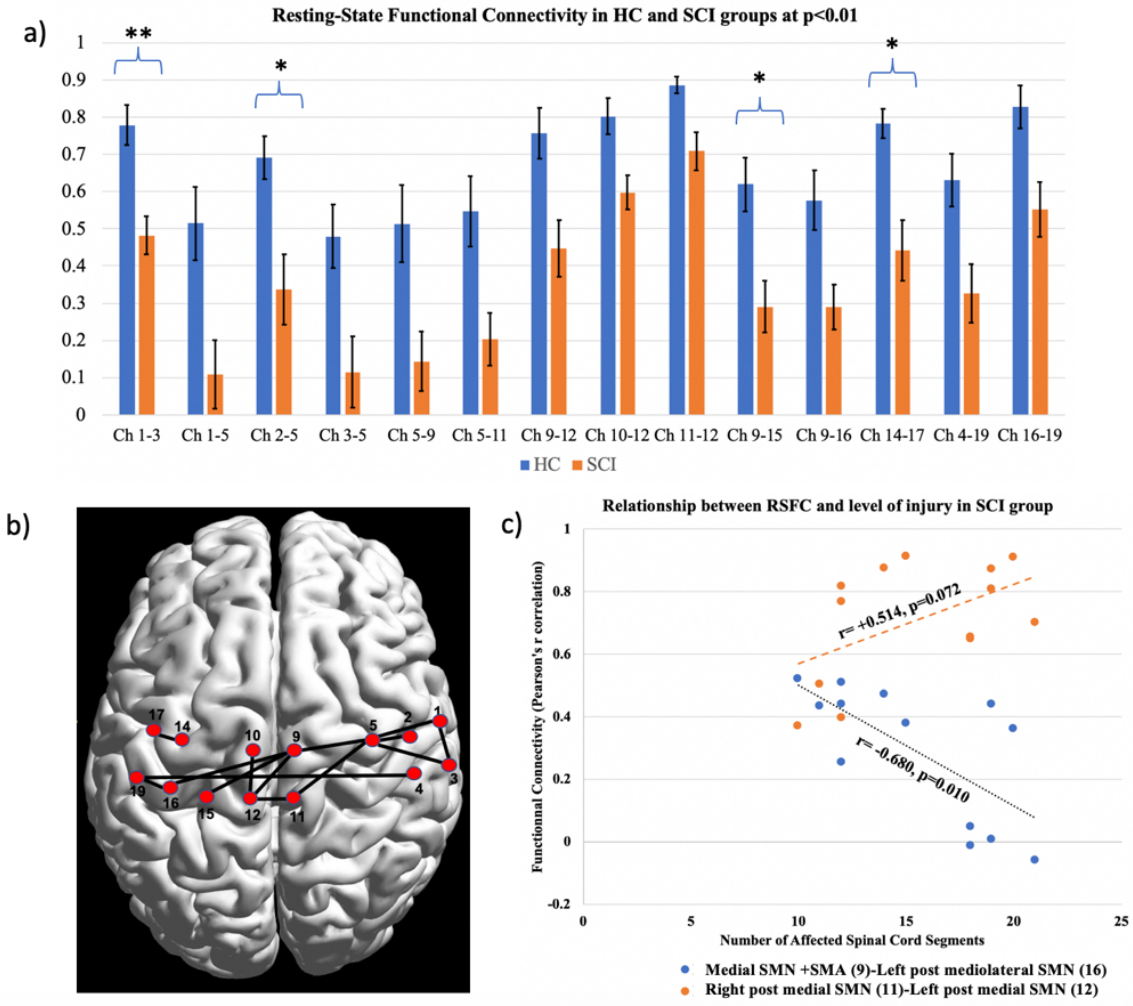

Figure 5.10 Result of two sample t-tests comparing the resting-state functional connectivity of the frontal and parietal cortex regions between healthy controls and SCI groups at $p<0.01$: a) Average functional connectivity in HC and SCI group in channels shown in b). The error bar indicates the standard error of mean. ** indicates $p<0.001$ and * indicates $p<0.005$. b) Channel-pairs showing significant differences in connectivity between the two groups. c) Relationship between resting state functional connectivity of 1) medial SMN + SMA (channel 9) with left posterior mediolateral SMN (channel 16) and 2) right posterior medial SMN (channel 11) and left posterior medial SMN (channel 12) with level of injury represented as number of affected spinal cord segments. The Pearson's r correlation measures are shown in the plot.

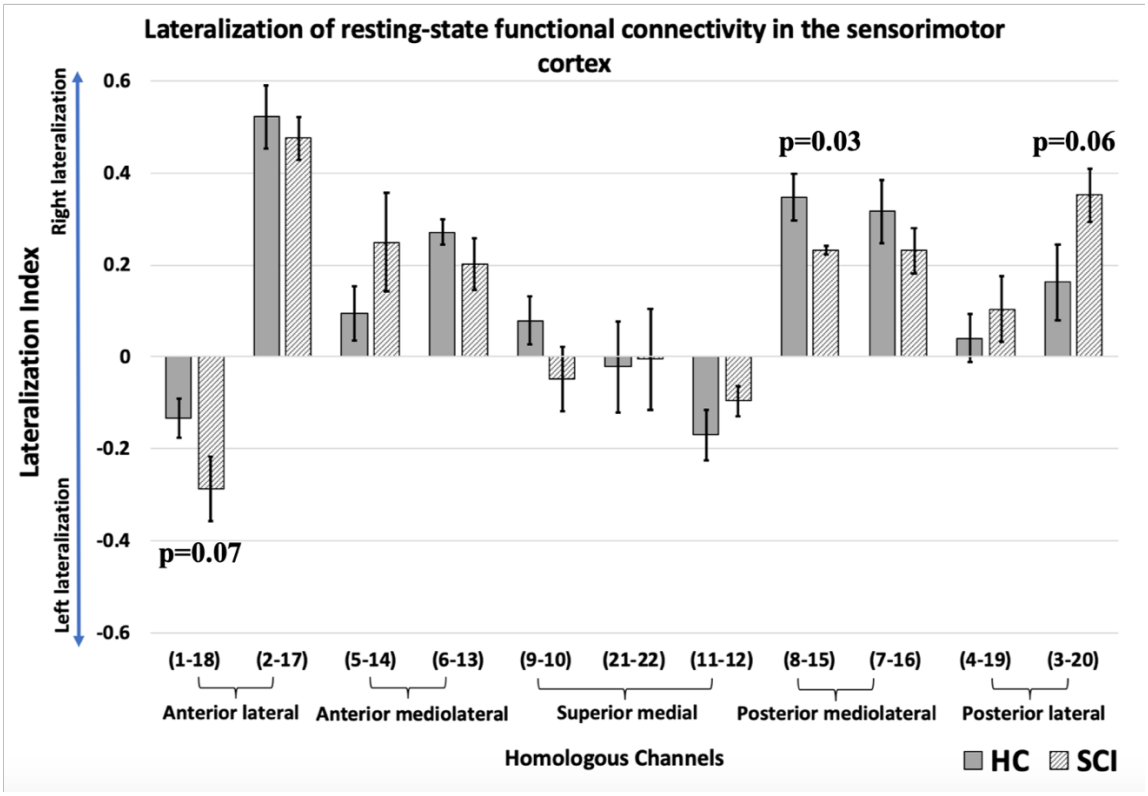

Figure 5.11 Lateralization of resting-state functional connectivity between 11 homologous channel pairs of sensorimotor cortices in HC and SCI. Only the channel pairs with low probability are indicated.

5.5.2 Altered Cortical Activation during Motor Tasks in Spinal Cord Injury (Aim 3d)

The group averaged hemodynamic response to the different motor tasks from the 7 sources are shown in Figure 5.12. Finger tapping task elicited a similar hemodynamic response in both HC and SCI groups (seen in Figure 5.12a). The HbO concentration increased shortly after task onset, peaked around 5 seconds after onset that started to decrease at task cessation. Both groups exhibited an onset and offset transient response although was less obvious in SCI group. The average hemodynamic response to finger tapping imagery with action observation (Figure 5.12b) on the other hand was unanticipated as both groups demonstrated an inconsistent HbO concentration change to stimulus. More interestingly, sources A, B, C, D and E in HC exhibited an increase in HbO concentration after the

stimulus period ended. Finally, the hemodynamic response to ankle tapping in HC exhibited a bimodal response in all sources with an onset and offset transient response. Whereas the SCI group demonstrated a sustained but smaller increase in HbO in all the sources, with the greatest increase in the prefrontal gyrus (Figure 5.12c).

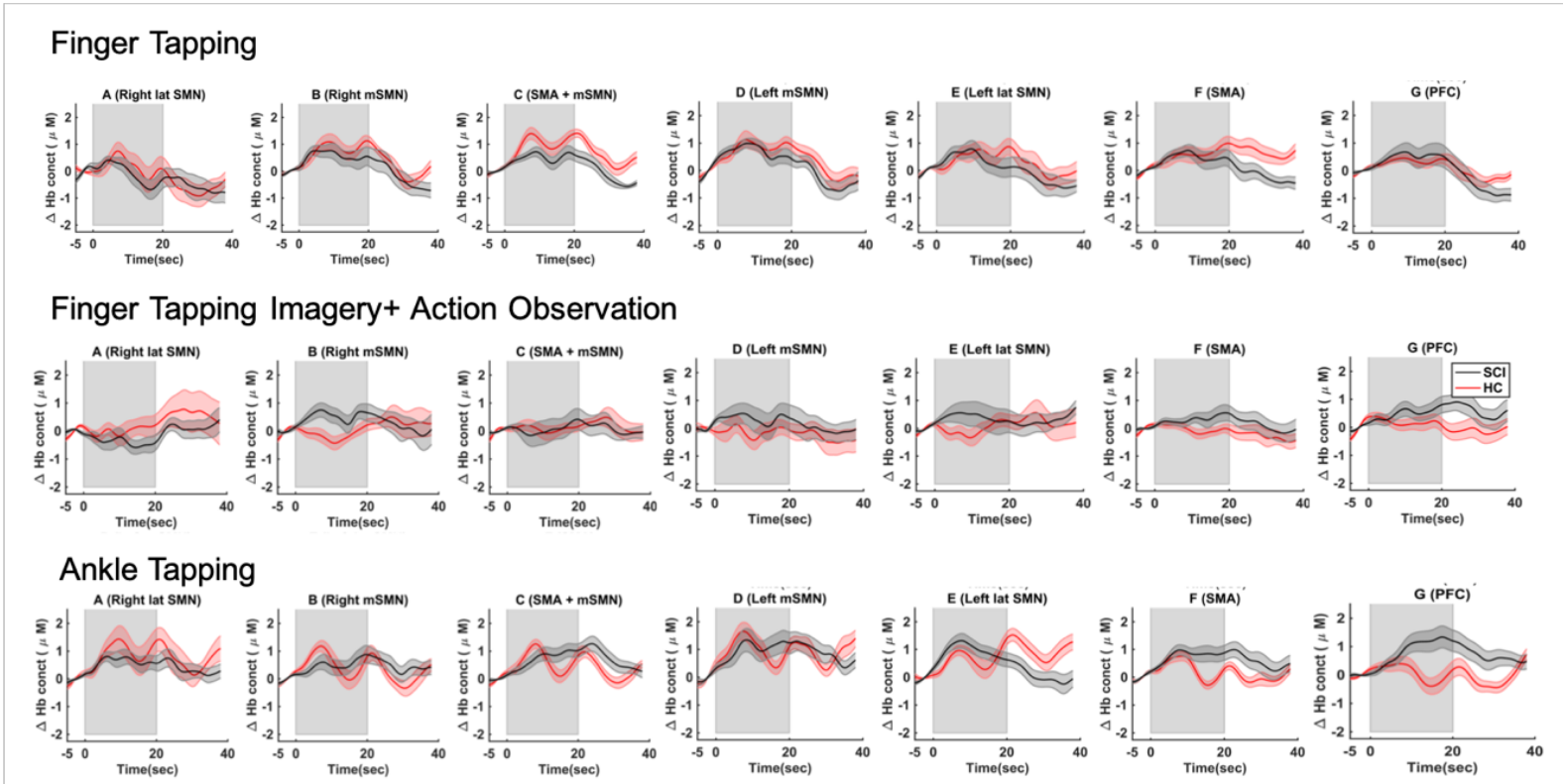

Figure 5.12 Group block averaged HbO concentration changes in the 7 ROI's in HC and SCI groups during a) finger tapping, b) finger tapping imagery with action observation and c) ankle tapping. Red curve indicates HC and black curve indicates SCI group. Error of time series represents the standard error of mean. Gray shaded area in the plot indicates the duration of task.

i) Oxy-hemoglobin Concentration during Motor Task: The maximum increase in HbO concentration for the different tasks resulted in no significant differences between the two groups for any of the task types. However, the area under the HbO curve for each of the motor tasks calculated for the duration of the task stimuli revealed differences between the two groups (Figure 5.13a) at $p>0.05$ but with medium effect size. Finger tapping execution in SCI group demonstrated a smaller AUC (effect size of 0.375) in medial SMN+SMA region in comparison to HC. No significant differences in AUC measures were found between the two groups during finger tapping imagery with action observation. Even though not statistically significant, the SCI group appeared to exhibit a greater AUC in PFC when compared to HC. Similar to FT, the AUC measures for ankle tapping revealed a smaller AUC in SCI group when compared to HC in right lateral SMN (effect size of 0.377). Further, comparing finger tapping vs. ankle tapping in the two groups revealed that the AUC during finger tapping is significantly greater than ankle tapping in the right lateral SMN region of SCI group while AUC during ankle tapping is significantly greater than finger tapping in the same region of HC during ankle tapping. Similarly, even though not significant at $p<0.05$, the same region, right lateral SMN showed greater AUC during finger tapping when compared to finger tapping imagery in SCI group while in HC is not significantly different between the two tasks. The effect size r of significant regions of interest (presented in the Figure 5.13a and Figure 5.13b range from medium (0.3) to high (>0.5) effect.

Results of ANOVA showed significant main effects of duration since injury and level of injury on the AUC measures of the three types of motor tasks (Figure 5.13c and Figure 5.13d). The relationship between AUC measures of FT, FTI and AT with duration

since injury was positive with longer post-injury durations associated with greater AUC measures during the three tasks. In contrast, the relationship between AUC measures of FT, FTI and AT with number of affected spinal cord segments was negative with higher levels injury was associated with smaller AUC in response to different motor tasks. Specifically, the AUC of left mediolateral SMN and SMA ROI's during FT task was significantly correlated to both duration since injury and level of injury. Likewise, the AUC of medial SMN and PFC regions during FTI task was significantly correlated to duration since injury and level of injury. And lastly, the AUC of medial SMN and SMA during AT task was significantly correlated to the injury characteristics.

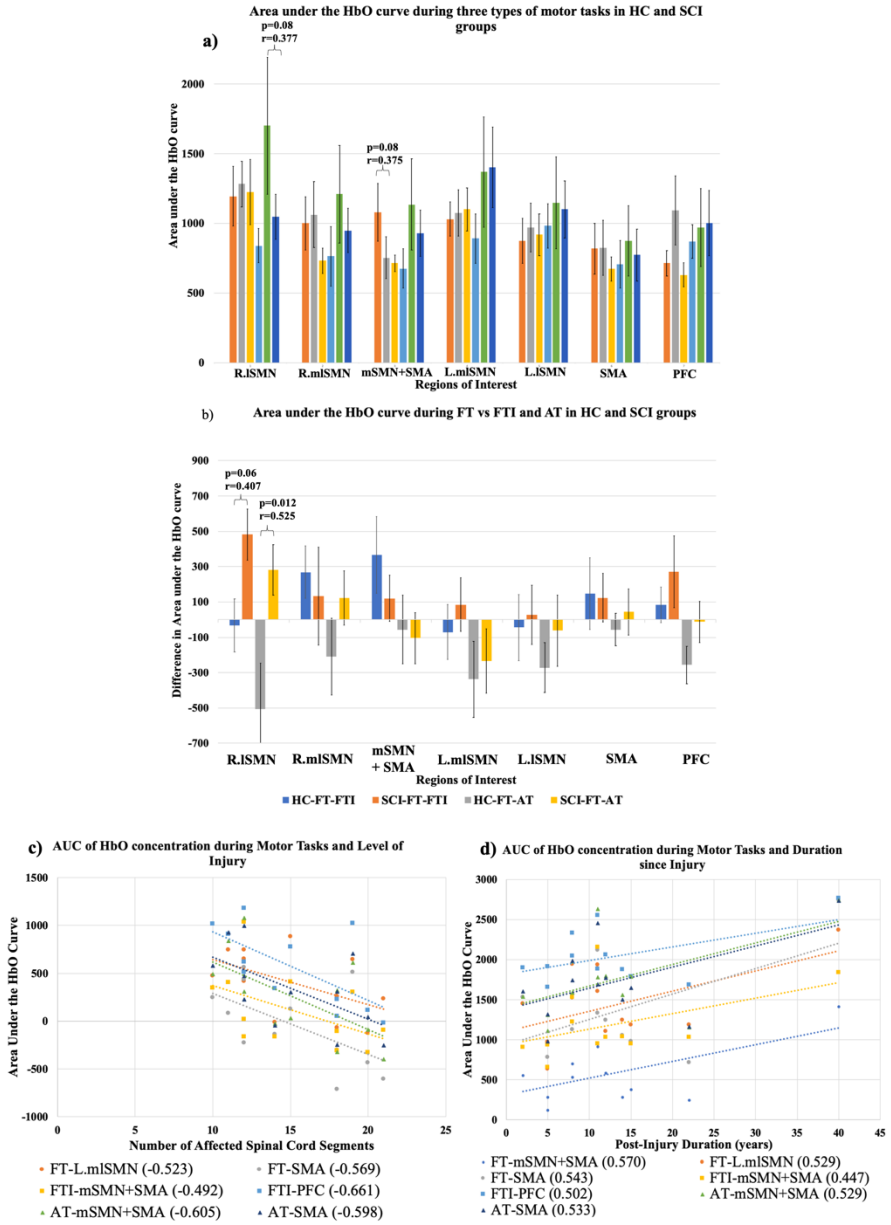

Figure 5.13 Area under the HbO curve measure for HC and SCI groups for a) FT, FTI and AT and b) FT vs. FTI and FT vs. AT. The regions of interest with low probability outcome from the two-sample t-test are specified. The r value indicates the effect size calculated using the t-statistics and degree of freedom. (R. lSMN-Right lateral sensorimotor network, R.mlSMN-Right mediolateral SMN, mSMN+SMA-medial SMN+SMA, L.mlSMN-Left mediolateral SMN, L.lSMN-Left lateral SMN, SMA-Supplementary motor area, PFC-Prefrontal cortex). Bottom Panel: Output of ANOVA for the mean effect of c) number of affected spinal cord segments (or level of injury) and d) duration since injury on the AUC measures of three motor tasks. The Pearson's r correlation measures of each of the regions with the injury characteristics are shown in the legend.

ii) Task-Based Functional Connectome: The task-based functional connectome for each of the motor tasks using a simple Pearson's r correlation resulted in distinct average connectome for HC and SCI group. Figure 5.14 shows the 25x25 mean connectivity matrix representing the correlation or similarity in the HbO concentration change during a) finger tapping, b) finger tapping imagery with action observation and c) ankle tapping between the different channels. Among the three motor tasks, the finger tapping imagery with action observation showed the maximum number of significant differences between the two groups (Figure 5.14b) as is denoted by the black boxes. In general, the functional connectivity between task-evoked hemodynamic responses is greater and more positive in healthy controls when compared to SCI group in all three motor tasks.

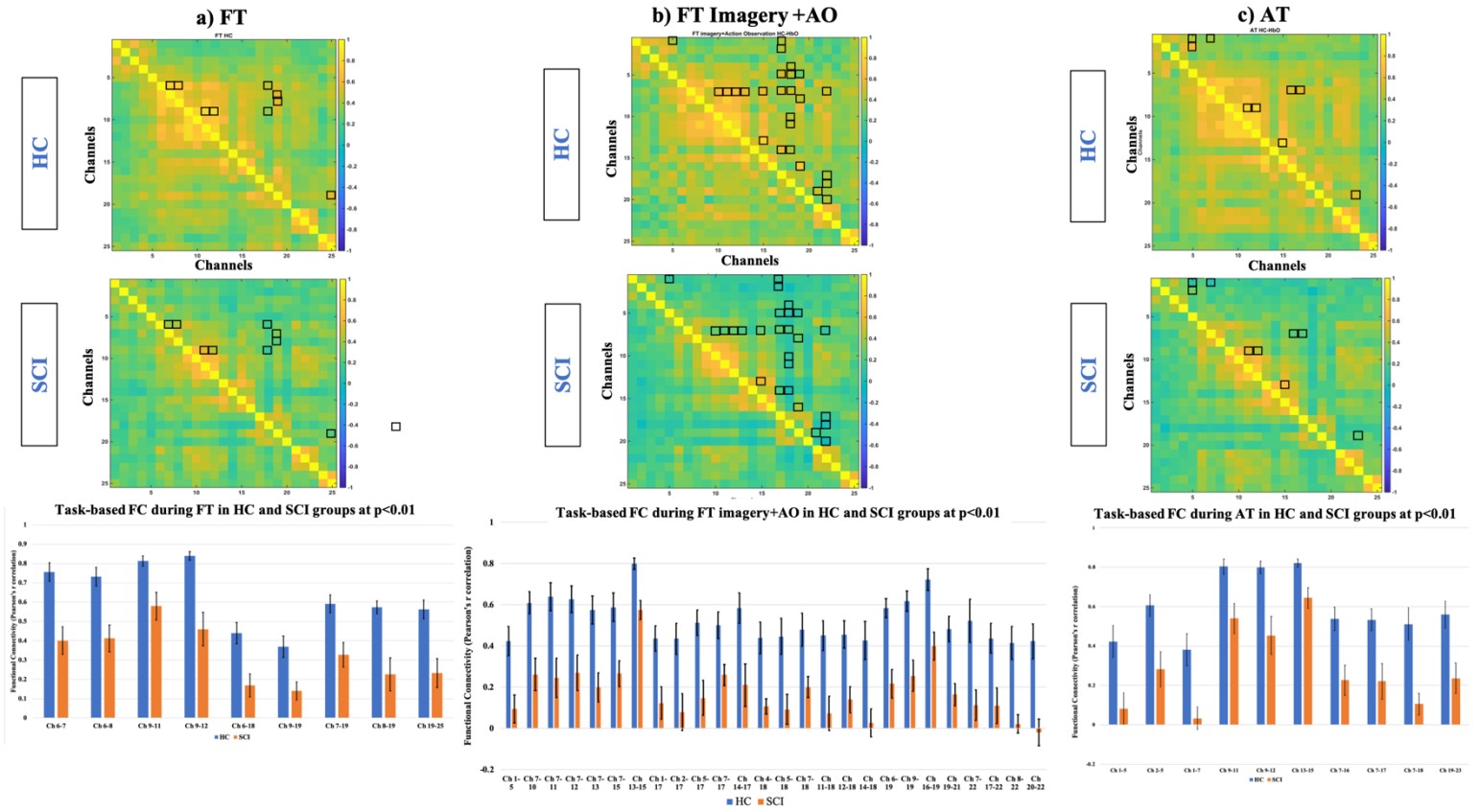

Figure 5.14 Task-based Functional Connectome in HC and SCI group: Mean connectivity matrix during a) finger tapping, b) finger tapping imagery with action observation and c) ankle tapping shown in the left and middle panel. The black boxes indicate the channel-pairs that show significant difference between the two groups at $p<0.05$. The right panel shows the average Pearson's r correlation for each of the channel pairs in the three tasks that show significant difference between the two groups.

As summarized in Table 5.3 the significant differences in connectivity of HbO changes during finger tapping was observed in 9 channel pairs located in medial SMN areas and left lateral SMN areas. The group mean functional connectivity seen in the bar plot shown in Figure 5.14a [74] show a positive and large connectivity for all channel pairs in healthy controls.

The task-based functional connectome of FT imagery with action observation task resulted in 26 channels significantly different between the two groups at $p<0.01$, with 9 surviving multiple comparison correction. Bar plots of the mean functional connectivity between the two groups showed a similar trend as FT task where SCI exhibited a smaller but positive mean functional connectivity. Most notably, the significant differences were observed between channels of left lateral SMN and SMA, where, SCI group show little to no functional connectivity in these channels. Other significant channels involve areas from the mediolateral area of SMN between the two hemispheres. Results from statistics on the functional connectome of AT resulted in 10 pairs (Table 5.3) that are significantly different between the two groups (SCI vs. HC). Out of the 10 pairs during AT, 2 channel pairs (9-11 and 9-12) were also found to be significantly different during FT. The channels corresponded to mediolateral SMN area between the two hemispheres as well as within medial SMN.

Table 5.3 Task-based Functional Connectome between HC and SCI groups

List of channel pairs with significantly different functional connectivity between HC and SCI at p<0.01		
Finger Tapping	**Finger Tapping Imagery + Action Observation**	**Ankle Tapping**
6-7	1-5	1-5
6-8	7-10	2-5
9-11	7-11	1-7
9-12	7-12	9-11
6-18	7-13*	9-12
9-19	7-15	13-15
7-19	13-15*	7-16
8-19	1-17	7-17
19-25	2-17	7-18
	5-17	19-23
	7-17	
	14-17	
	4-18*	
	5-18	
	7-18	
	11-18	
	12-18	
	14-18	
	6-19*	
	9-19*	
	16-19*	
	19-21*	
	7-22	
	17-22	
	18-22*	
	20-22*	
* indicates FDR-corrected p<0.05, where p is 0.0017 for alpha=0.05		

5.5.3 Breath-hold Activation (Cerebrovascular Reactivity) after Spinal Cord Injury (Aim 3c)

Block averaged hemodynamic response to 15-second breath hold in the two groups are displayed in Figure 5.15. The HC group in this study exhibited a delayed peak in HbO concentration followed by a post-stimulus undershoot. The SCI group also exhibited a delayed peak in HbO concentration but presented with a large initial dip and no obvious post-stimulus undershoot.

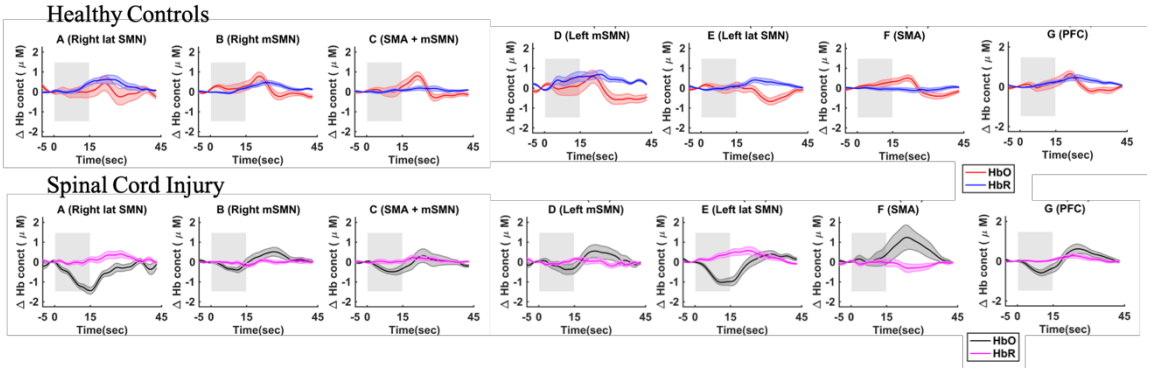

Figure 5.15 Group block averaged HbO and HbR concentration changes in the 7 ROI's in HC and SCI groups during breath holding paradigm. Error of time series represents the standard error of mean. Grey shaded area in the plot indicates the duration of breath holding.

The maximum HbO increase after resuming normal breathing in the two groups showed no significant differences (seen in Figure 5.16a). Although, the time taken to attain the maximum HbO increase was greater in SCI group when compared to HC in all sources. As shown in Figure 5.16b, Left and right lateral SMN (i.e., sources A and E) showed significant difference between the two groups. On average, SCI group appeared to be nearly 8-10 seconds slower to attain maximum HbO concentration after holding breath for 15 seconds. Further, the maximum decrease in HbO concentration during breath holding was quantified as the initial undershoot. The initial dip for the same regions, right and left lateral SMN (i.e., sources A and E) showed significantly large initial dip in SCI group when

compared to HC (Figure 5.16c). One-way ANOVA results computing the correlation between maximum HbO concentration and SCI characteristics revealed significant negative relationship between HbO increase in right lateral SMN and a) post-injury duration, where longer durations of injury was associated with smaller peak response, b) level of injury, where higher levels of injury were associated with smaller peak response, c) interaction between post-injury duration and level of injury, where higher level injury with long post-injury durations showed the least peak response and d) interaction between level of injury and presence of neuropathic pain, where people with lower levels of injury and neuropathic pain showed greater peak response than people with lower levels of injury without neuropathic pain. The scatter plots and their Pearson's r correlation estimates are demonstrated in Figure 5.17.

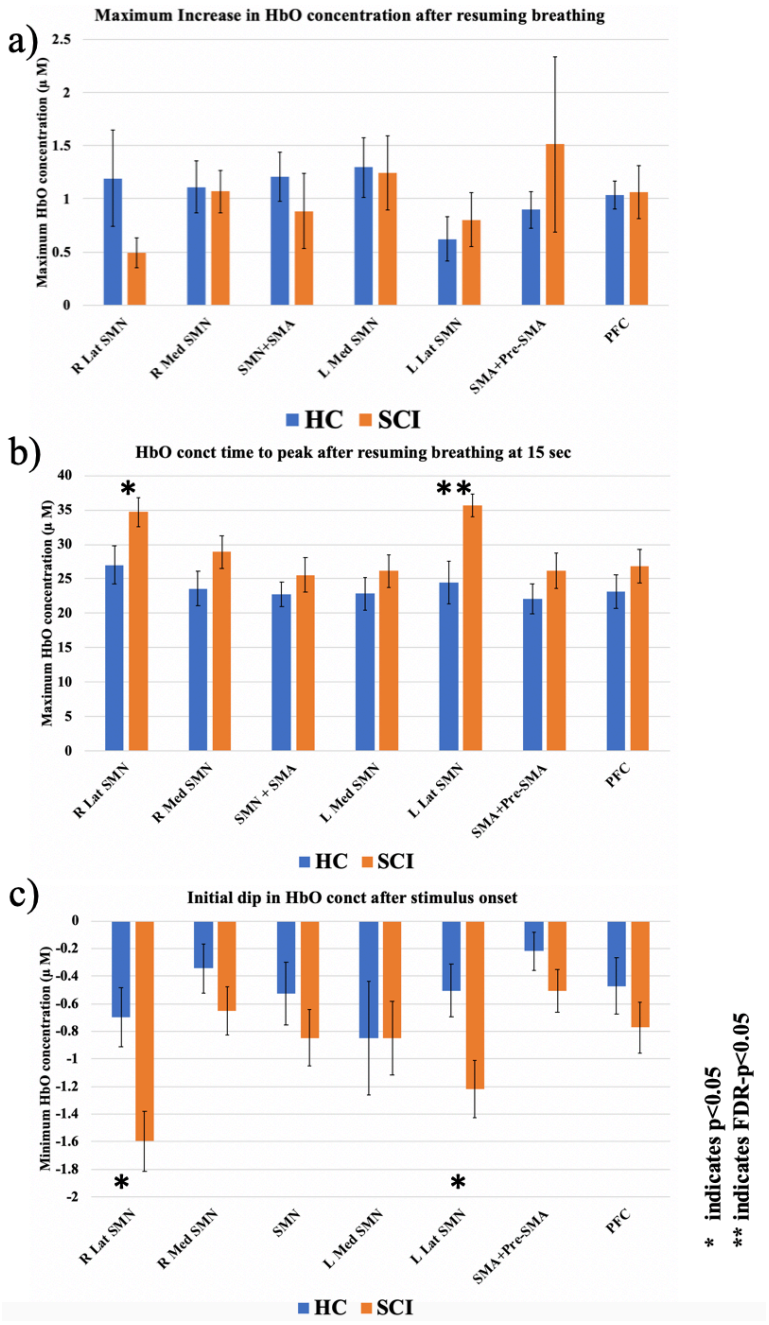

Figure 5.16 Maximum and minimum HbO concentration change during breath hold paradigm in HC and SCI group for the 7 regions of interest: a) Maximum absolute increase or peak response of HbO concentration after breath holding for 15 seconds, b) time to attain peak response in HbO concentration after 15 second breath holding and c) maximum decrease (initial dip) in HbO concentration immediately after breath holding onset. * indicates two-sample t-test outcome of $p<0.05$ and ** indicates two-sample t-test outcome of $p<0.05$ with FDR-correction.

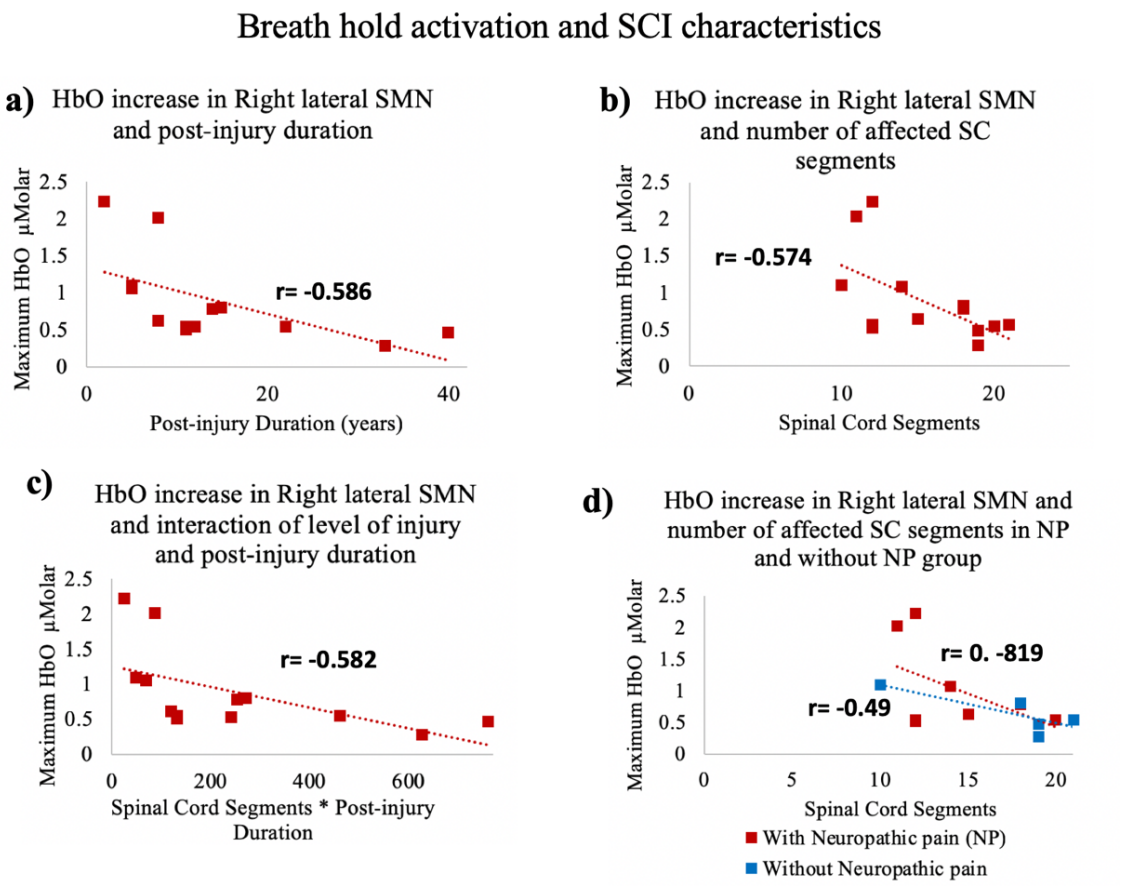

Figure 5.17 Relationship between breath hold activation and characteristics of the injury in 13 people with paraplegic SCI: a) Significant negative relationship between net HbO increase in right lateral SMN and duration since injury (r=-0.586, p=0.03), b) Significant negative relationship between net HbO increase in right lateral SMN and number of affected spinal cord segments or level of injury (r=-0.574, p=0.04), c) Interaction effect between level of injury and post-injury duration in the net HbO increase of right lateral SMN (r=-0.582,p=0.03) and d) Interaction effect between level of injury and presence of neuropathic pain in the net HbO increase of right lateral SMN. The relationship between net HbO increase in right lateral SMN area and number of affected spinal cord segments/level of injury is greater in the group with neuropathic (r= -0.819, p=0.0006) as compared to the group without neuropathic pain (r= -0.49, p=0.08).

5.5.4 Effect of Task-calibration using Breath Hold in Spinal Cord Injury (Aim 3d)

Since no significant differences were found for the maximum HbO measure, only area under the curve measures were used for calibration. Group differences in area under the HbO curve measures for motor tasks after calibration is displayed in Figure 5.18a and Figure 5.18b. Even though no new regions of interest differences were revealed after

calibration, the effect size and probability of independent sample t-test improved for finger tapping-imagery (before calibration effect size r=0.354 and after calibration effect size r=0.415) and finger tapping-ankle tapping (before calibration effect size r=0.349, after calibration effect size r=0.364) after accounting for variance introduced by vascular activity. The group variance of each of the task's area under the curve measures also decreased in the D, E and F sources more than other areas.

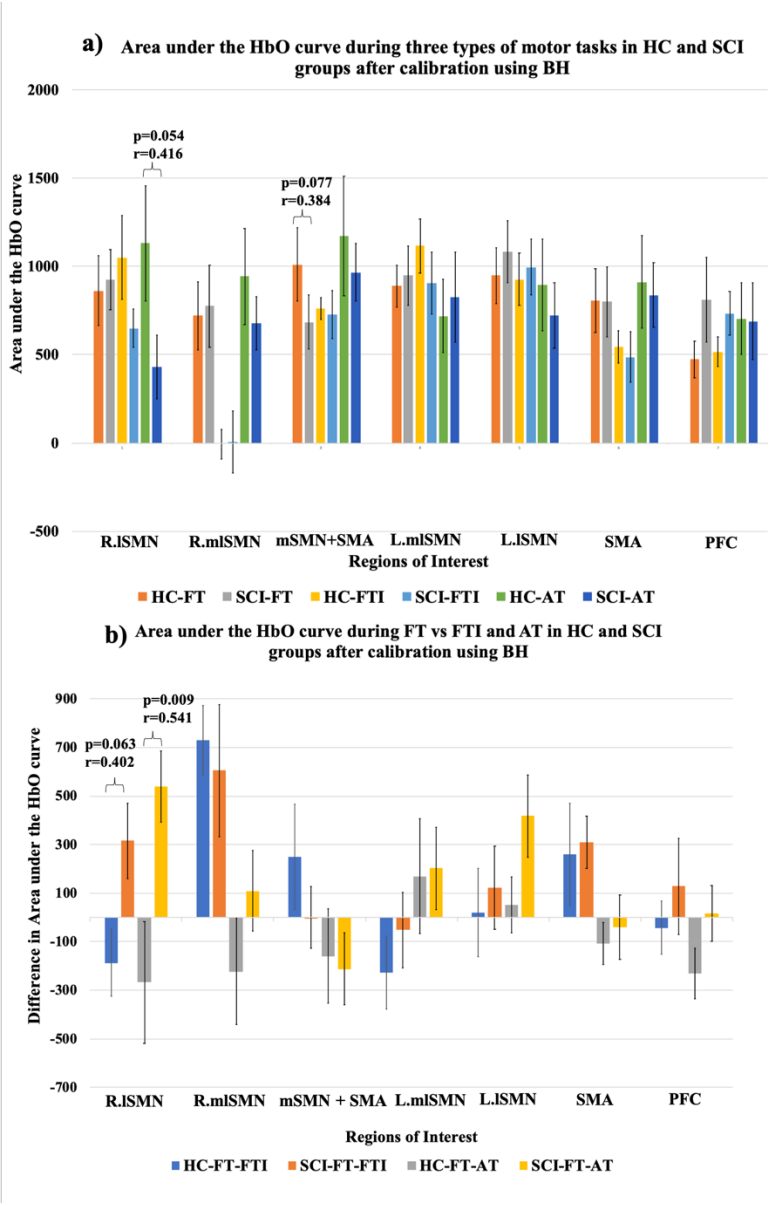

Figure 5.18 Area under the HbO curve measures for HC and SCI groups after accounting for neurovascular variance using BH: Area under the HbO curve for a) FT, FTI and AT and b) FT vs. FTI and FT vs. AT. The regions of interest with low probability outcome from two-sample t-test are specified. The r value indicates the effect size calculated using the t-statistics and degree of freedom. (R.lSMN-Right lateral sensorimotor network, R.mlSMN-Right mediolateral SMN, mSMN+SMA-medial SMN+SMA, L.mlSMN-Left mediolateral SMN, L.lSMN-Left lateral SMN, SMA-Supplementary motor area, PFC-Prefrontal cortex)

5.6 DISCUSSION

5.6.1 Test-Retest Reliability of Cortical Activity using fNIRS

This study demonstrates the stability and reliability of fNIRS metrics in 16 healthy participants acquired at two time points. The reliability findings in this study will pave the groundwork for the choice of functional metrics necessary to study SCI population.

The between-session reliability of resting-state functional connectivity in 16 people scanned at least a week apart ranged from fair to very good reliability. A total of 64 channel pairs out of the 300 pairs showed a fair ICC of 0.4. An excellent reliability of 0.7 and greater were observed in 4 channel pairs that were primarily a part of left SMN and prefrontal cortex regions. These results agree with findings from a previous fNIRS study reporting a fair reliability (0.4 to 0.6) in functional connectivity measures of the whole brain obtained using a similar duration of resting-state scan[194]. The low reliability of RSFC in the medial regions of sensorimotor is notable and leads to the hypothesis that this may be the consequence of cardiac pulsations and respiration on blood vessels. It is also unclear if increasing the scan duration (6.5 mins) of the resting-state scan could increase the reliability of resting-state functional connectivity in the sensorimotor cortex[194]. Graph theoretical metrics such as local-efficiency and global-efficiency are other avenues to investigate as studies report moderate to good reliability in these resting-state measures[195].

Test-Retest reliability of AUC measures from different motor tasks revealed good to excellent reliability within session whereas only poor to moderate reliability in between sessions. Unexceptional between-session reliability scores of AUC measures from motor tasks could arise from 1) incongruence in the optode placements during second scan, 2) insufficient number of task blocks to produce reliable activation and 3) inconsistency in

task performance during the two sessions. Other studies examining reliability of motor task report achieving a reliability of 0.7 using beta estimates of activation to finger tapping performed on two consecutive days[196]. While in this study, only 4 to 5 channel regions exhibit greater than 0.7 reliability in a given task. Again, in addition to the above-mentioned factors, the reliability of different metrics may vary, therefore more work is required to identify the most suited metric to reliably differentiate the different motor tasks. Beta estimation using general linear model, maximum increase in HbO and task-based functional connectome are some of the other metrics that may present with high reliability.

Finally, the breath hold task exhibited the most robust and reliable activity among the three task states recorded using fNIRS. The AUC measures of 15-second breath holding recorded at two time points at least a week apart achieved moderate to very good reliability. Sixteen out of the 25 channels had an ICC of 0.5 or higher and 8 out of the 16 channels had an ICC of 0.75 or higher. Even though no fNIRS studies have examined the reliability of breath hold activation, fMRI studies recommend controlled inspiration depth or deep breathing to decrease variability in breath hold performance[197,198]. However, the high reliability of breath hold activation in spite of an unregulated breath hold paradigm suggests that modifying the breath hold paradigm can further improve reliability of the data. Nevertheless, the ability to reliably measure cerebrovascular reactivity with a 5-minute non-invasive breath hold paradigm demonstrates the promise of fNIRS in clinical research for the evaluation of cerebrovascular reserve capacity after SCI [199].

5.6.2 Altered Cortical Activity in Spinal Cord Injury

This is the first study to our knowledge to implement fNIRS as a neuroinvestigative tool in SCI population with the goal to examine cortical reorganization in the sensorimotor cortex.

A comprehensive examination of cortical hemodynamic response during resting-state, three different types of motor activity (viz. finger tapping, finger tapping imagery with action observation and ankle tapping) and breath holding was performed in 13 people with paraplegia after SCI. In general, the cortical response during all three types of task states exhibited reduced activity in the SCI group when compared to age-matched HC. Essentially, this study delivers an important benchmark on the choice of fNIRS metrics, task paradigm and methodological approach for future studies investigating neuroplasticity after central nervous system injury.

5.6.2.1 Resting-State Functional Connectivity in SCI. During resting-state, the paraplegic SCI group showed reduced but positive resting-state functional connectivity within the sensorimotor cortex particularly between a) bilateral post-central gyrus areas, b) within hemisphere in the pre-central gyrus, c) right SMN (around left M1 area) and right medial SMN +SMA and d) left SMN (around S1 area) and right medial SMN+SMA. These findings corroborate reports from past studies investigating spontaneous cortical activity using fMRI and neurophysiological recordings. For instance, Hou and colleagues described decreased interhemispheric resting-state FC of primary somatosensory cortex in 25 individuals with SCI[17]. An adult mice model by Matsubayashi and colleagues using resting-state FC during pre and post complete thoracic transection also showed decreased connectivity between primary motor cortex and primary sensory cortex in the chronic phase[200]. A recent study using pre-defined seed regions in bilateral precentral gyrus and bilateral postcentral gyrus showed widespread decrease in functional connectivity of these regions to bilateral sensorimotor area[16]. The majority of these studies justify the hypoconnectivity within the motor cortex as an outcome of lack of sensory and motor

inputs to the cortex from injury and the structural changes that are reported as a result. A negative relationship between functional connectivity and the number of affect spinal cord segments where higher levels of injury or greater number of spinal cord segments are associated with smaller functional connectivity between right medial SMA/SMA and left post-central gyrus location; indicating that functional changes may in fact depend on the extent of immobility. Additionally, a single photo emission computer tomography study on people with paraplegia and tetraplegia showed decreased cerebral blood flow in bilateral SMN areas [201]. However, it is not within the capacity of this study to determine if the functional changes in these individuals are accompanied by structural and perfusion changes in the sensorimotor cortex. Some of the past studies also report compensatory increase in connectivity between S1 and secondary motor areas such as thalamus, SMA and basal ganglia which was absent in this study[17,111]. One possible explanation for the lack of increased connectivity could be the heterogeneity in the post-injury durations or completeness of the injury in the participants involved in this study. By the same token, we observed a positive relationship between interhemispheric connectivity of medial post-central gyrus and level of injury, suggesting that higher levels of injury may present with greater interhemispheric connectivity in these locations; and increase in functional connectivity is often considered a compensatory response to accommodate the lost function.

Under the assumption that the channel locations are fairly homologous, we computed the lateralization index of the resting-state mean FC of 11 pairs of channels in the sensorimotor cortex and SMA. SCI group demonstrated an increase in right hemispheric lateralization of lateral post-central gyrus and left hemispheric lateralization

of lateral pre-central gyrus when compared to HC. Strikingly, SCI group also exhibited a significant decrease in right hemispheric lateralization of the mediolateral regions of the post-central gyrus. However, no literature exists on the lateralization of motor or sensory activity after a spinal cord injury. Though ipsilateral cortical activity has been shown to be positively correlated to the spinal cord cross-sectional area in the ipsilateral side of the cord[20]. Signifying that lateralization may arise from the extent of cord transection and the side of nerve damage. However, since both groups showed either left lateralization or right lateralization for a specific region, it is believed that it might instead reflect the fundamental neural organization of motor and sensory control.

Studies collectively suggest that the left hemisphere may be specialized for planning and execution of familiar and routine actions while, the right hemisphere may be specialized for updating ongoing actions and detecting novel stimuli in the environment[202]. Given the aforementioned lateralization, an increased left lateralization of channels in lateral precentral gyrus in the SCI group may indicate a compensatory increase in connectivity to other regions to initiate a movement. While, an increase in right lateralization of channels in lateral post-central gyrus/somatosensory cortex may represent the increased searching for motor and sensory afferents that are no longer available.

5.6.2.2 Altered Sensorimotor Activation during Motor Tasks in SCI. Finger tapping imagery with action observation task failed to reveal a sustained hemodynamic response in either of the groups. One probable explanation for the lack of peak response is that FT imagery, when in combination with action observation may have engaged the visual cortical system more than the motor system making the two sensory systems compete for attention. However, task-based connectome of FT imagery with action observation

revealed a significant decrease in connectivity in interhemispheric channels of the SCI group when compared to HC. Additionally, a significant correlation between AUC measure of FTI in medial SMN+SMA region and PFC with duration since injury and level of injury measures further support the hemodynamic findings to the motor tasks. Neural correlates of imagery, action observation and imitations have been shown to predominantly involve the regions of SMA, prefrontal cortex and inferior frontal gyrus[203,204].

Unlike FTI, the hemodynamic response to finger tapping exhibited a sustained response in both groups for all regions. The AUC measure of HbO concentration to finger tapping revealed reduced AUC in the medial SMN+SMA region of the cortex in SCI group. Regardless of the variation of finger tapping paradigm, bilateral M1 and SMA lie on the foci of brain network involved in execution of movement[185]. Hence a significant correlation between the AUC measures of finger tapping from left mediolateral SMN (proximal to M1) and SMA with injury characteristics once again substantiates the hemodynamic findings. Most interestingly, the same cohort showed a positive net change in HbO during ankle tapping task even though none of the participants were physically able to execute the movement. The hemodynamic response curve of the SCI group to ankle tapping was also distinct with no onset and offset transients as typically seen in HC. The AUC measure of HbO concentration during ankle tapping further revealed a decrease in the left lateral SMN region for SCI group when compared to HC. It is known through various studies that lack of sensory drive induces functional reorganization in the motor and somatosensory cortical regions that have lost peripheral function[9,43,44]. Studies show that presence of such new connections may not only arise as a result of dormant synapses but also due to emergence of lateral cortical and subcortical connections [41]. These connections may have appeared

due to long term deafferentation leading to dendritic sprouting or deafferentation causing disinhibition of suppressed inputs or even due to long term potentiation of weaker synapses[41]. Hence, the increase in HbO concentration we observe in response to ankle tapping in all the 5 sources of SMN area likely reflect the above-mentioned phenomenon.

A study by Henderson and colleagues using fMRI in complete thoracic SCI showed reorganization in the somatosensory cortex with finger representation shifting to medial cortical regions that encode for lower limb function[41]. Such cortical reorganization plays a critical role in reducing the grey matter and white matter atrophy that may result otherwise. Even though no significant compensatory increase in the activity of medial SMN (leg region) region was observed during finger tapping, a significant correlation between AUC of HbO during ankle tapping from the medial SMN (leg region) and SMA with duration of injury and level of injury suggests that cortical activity using fNIRS may in fact reflect underlying spatial distribution of motor activity. In fact, only 4 out of the 13 participants have any level of sensory or motor function preserved, implying that majority of the participants receive no feedback from their lower body and hence are likely to recruit adjacent intact musculature for cortical preservation. The finding that an attempted ankle movement evokes a hemodynamic response even several years post-injury (average of 14.3 years) making the findings encouraging and indicative of a receptive cortical system. This also raises an interesting question however: how much of the hemodynamic response is neuronally driven? We believe calibration of task-evoked hemodynamic response using breath holding response should provide insight into this question.

5.6.2.3 Impaired Cerebrovascular Reactivity in Spinal Cord Injury. Breath-hold is a well-tolerated and reliable technique to induce hypercapnia and study cerebral blood

flow[197]. The hemodynamic response to breath-hold in the SCI group revealed a large initial dip and delayed peak response when compared to HC. The peak HbO response of right lateral SMN area was also significantly lesser in people with long post-injury durations and higher levels of injury. An impaired breath hold response was anticipated in the SCI group due to the low resting blood pressure, orthostatic hypotension and autonomic dysreflexia arising from an imbalance in higher order control of the autonomic system[183]. As cerebral vessels are directly innervated by sympathetic pathways arising from the T1-T4 levels of the spinal cord ganglia, a disruption of the sympathetic system (or domination of the parasympathetic system) is said to affect the reactivity of the vasculature [30]. Due to which injuries above T5 are expected to be at higher risk of developing an impaired cerebrovascular control[184]. Remarkably, a large initial dip suggestive of an impaired cerebrovascular reactivity or sensitivity to arterial CO_2 was observed in the current cohort where 7 of the 13 participants have an injury below the T6 level. This suggests that impairment in cerebrovascular control may also occur in lower-level injuries. Additionally, the lack of significant difference in the peak HbO response between SCI and HC suggest that the over-all maximum cerebral blood flow (known as static cerebral autoregulation) in response to a breath hold induced hypercapnia may be intact. Although, the latency of the cerebral blood flow changes (also known as dynamic cerebral autoregulation) is impaired after SCI. These findings corroborate with to past records of intact static cerebral autoregulation and impaired dynamic cerebral autoregulation in higher-level SCI measured using cerebral blood flow from transcranial doppler technique, mean arterial pressure and blood catecholamine tests [205].

A greater peak HbO response was noted as the level of injury increased in people with neuropathic as compared to those without neuropathic pain. To our knowledge no studies have reported an association between the presence of neuropathic pain and altered cerebrovascular reactivity. But during normal conditions, there should be no cross-communication between the nociceptive afferents and sympathetic control system. Although studies indicate the likelihood of an abnormal pairing between the sensory and autonomic system known as sympathetic-afferent coupling, that may contribute to the development of dysesthesia[37]. The sympathetic pathways have been shown to sprout into the dorsal root ganglion and involve increased expression of adrenergic receptors on the nociceptive afferents[206], causing any form of sympathetic activation or dysfunction to result in central sensitization[207]. Therefore, if cerebrovascular reactivity is associated with pain generation after SCI, studying the cerebrovascular differences over the acute duration of injury could help delineate factors resulting in abnormal pain generation or sensations. Furthermore, cerebrovascular reactivity is identified as an effective indicator of risk of ischemic attack and therefore may also provide insight into the cerebrovascular physiology of the participant[199].

5.6.2.4 Effect of Task-Calibration using Breath Hold. Calibration of task-evoked hemodynamic response using breath hold increased the effect size and probability of difference in activation of sensorimotor regions between HC and SCI groups. Additionally, calibrating for breath hold activity reduced the inter-subject variance of the data in sources D, E and F more than other regions. Our findings, even though introductory are in agreement with results from fMRI studies that recommend accounting for neurovascular variance using breath hold to reduce inter-subject variability[208-210]. A stroke study applying

a similar technique to account for neurovascular differences report suppression of task associated activity following calibration[210]. Another study suggested that the lack of differences in cerebrovascular reactivity is a stronger indication that neuronal activity is contributing to the task-evoked activation measures [211]. In that case, the lack of major differences in the cerebrovascular reactivity of the different regions substantiates differences we observed in the hemodynamic response, functional connectivity and area under the curve measures. SCI disrupts the efferents to the spinal sympathetic centers in the intermediolateral nuclei of T1-L2 spinal cord segments causing a lack of sympathetic regulation below the level of injury and uncontrolled parasympathetic activity below level of injury. This puts the individual at a high risk of cardiovascular dysfunction, especially when the injury is above T5-T6 which is also the site of splanchnic sympathetic outflow[212]. Therefore, it is important to consider that the lack of major differences before and after calibration may be due to the number of people who have lower level injury in the current cohort (<T6). By performing calibration using breath-hold activity, future studies especially including higher level SCI could study brain neuronal activity more accurately.

5.6.3 Conclusion

There are a few limitations to this study. First, the type and intensity of the motor task we chose may not be the most robust in illuminating the spatial differences in imagination vs. execution and hand vs. leg movement. Additionally, the number of task stimuli or the task duration necessary to elicit the most reliable response is uncertain at this juncture. Second, differences in the task performance of subjects were not accounted for during the task analysis. In the future, both number of task blocks and task parameters will be controlled to elicit robust activation. Third, we examined the effects of calibration predominantly in

the sensorimotor cortex; therefore, it is unclear if hemodynamic response from other areas of the brain may also benefit from accounting for vasoreactivity. Hence, we recommend future studies to investigate how manipulation of task, methodology and vascular constraints can improve the robustness and reliability of hemodynamic response measured using fNIRS.

In conclusion, our results suggest that we can achieve spatial and temporal differences in the hemodynamic response of different motor tasks such as hand vs. leg movement and imagination vs. execution of movement using fNIRS in the sensorimotor cortex for both healthy and SCI group. We also demonstrated the potential of breath holding in reducing variability of fNIRS hemodynamic response between channels as well as between subjects arising from vascular origin. Our results validate the potential of multi-channel fNIRS to study neural responses to dynamic tasks involved in physical therapy, including clinical populations such as stroke that may involve vascular pathophysiology.

CHAPTER 6

CONCLUSION AND FUTURE DIRECTIONS

This dissertation is a pioneer study in the implementation of fNIRS for the investigation of cortical reorganization and vascular physiology in a human SCI population. It is also one of the first studies to comprehensively examine the structural and functional alterations of the brain in humans with SCI using multiple neuroimaging modalities. First, MRI scans from 23 healthy participants and 36 individuals with complete SCI within two years of injury were used to demonstrate that both injury level and duration since injury are important factors contributing to recovery. The structural alterations in the first two years after injury also prevailed beyond the sensorimotor system in higher-order systems such as salience and emotion processing. Likewise, fMRI scans from the same cohort showed that changes in the intrinsic connectivity of the thalamocortical system also extend beyond the sensorimotor nuclei and are dynamic during the first two years after injury.

Test-retest reliability of hemodynamic measures from 16 young healthy participants randomly chosen from a pool of 42 participants indicated fair to very good reliability for resting-state, task and cerebrovascular reactivity measures. Lastly, using the hemodynamic data from 13 healthy participants and 13 individuals with chronic paraplegic SCI, it was observed that SCI group, in spite of their inability to perform the movement, retained cortical activity in response to attempted ankle movement-perhaps representing a top-down command to initiate movement. The breath hold response also indicated a compromised hemodynamic response to hypercapnia in paraplegic SCI group including people with lower levels of injury (below T6). The sensitivity and reliability of

hemodynamic measures from fNIRS to static and dynamic stimuli is encouraging and opens new avenues of rehabilitation research in SCI using fNIRS modality. Lastly, this dissertation has established that the retrograde effects of spinal deafferentation on the structural and functional dynamics of the brain are evident not only two years after injury but also decades after the injury.

6.1 Implications of Current Findings

The immediate treatment strategy for SCI during the sub-acute stage usually focuses only on damage control to the site of injury where the goal is to minimize tissue damage, inflammation, hypoxia and spinal shock to prevent and contain imminent nerve degeneration[1]. The supraspinal pathophysiological consequence of SCI is thus far less crucial to the immediate treatment after SCI. However, the structural and anatomical findings during the chronic stage are tremendously valuable to the longitudinal inference of injury outcome. Further investigation of the cause-effect relationship between early treatment and long-term pathophysiology could shed light on the evolution of these changes and improve the prognosis of patients with SCI.

In the light of such potential, evidence from Aim 1 of this dissertation highlights the importance of 1) examining the global effects of injury without confining to sensorimotor deficits, 2) taking into account the effect of level of injury and 3) the importance of early intervention. Marked difference in cortical atrophy of salience and pain processing regions found in people with paraplegia when compared to tetraplegia highlights the significance of level of injury. If greater tissue density is associated with better function, then people with paraplegia ought to experience less severe impairments

in the functions associated with these regions. However, no conclusive evidence exists to suggest differences in the prevalence of maladaptive outcomes or salience detection between paraplegic and tetraplegic groups. It is possible that people with lower level of injury due to greater residual musculature experience more spontaneous recovery and may be more receptive to physical therapy. Alterations within the salience or emotional processing system could be dependent on deficits in mobility and sensation. However, whether or not rehabilitative therapy or other pharmacological treatment targeting motor deficits exhibit secondary effects on emotional/pain and salience processing remains inconclusive.

Results from Aim 2 showed significant changes in the functional dynamics of the thalamus, notably in the higher-order nuclei of paraplegic SCI group. This finding could help better understand the relationship between thalamocortical activity and chronic pain. Regardless of the cause of these changes, one can speculate how altered thalamocortical activity in regions of salience and nociceptive processing could reveal mechanisms specific to the different secondary sensory abnormalities. For instance, visceral pain condition associated with autonomic processing, unlike neuropathic or nociceptive pain, develops much later (~4 years) after the injury and may involve differential thalamocortical connectivity than neuropathic pain[6]. Thus, it is believed that results from this dissertation would encourage future studies to examine the role of different thalamic sub nuclei in the generation of different pain conditions; as well as serve as a benchmark to future studies examining the involvement of thalamus in chronic pain or other maladaptive outcomes of SCI recovery during chronic stages.

The last most significant contribution of this dissertation towards understanding the cortical mechanisms of SCI is the validation of fNIRS to reliably measure brain function in individuals with SCI and HC, during both dynamic and static tasks. This validation paves the way for future research to implement fNIRS to study more dynamic tasks in the SCI population. A positive response to attempted ankle tapping in SCI group indicates a 1) intact cortical activation to planning and 2) the sensitivity of fNIRS to record small variations in hemodynamics in response to movement. The abnormal breath hold response in the paraplegic SCI group, including people with injury below T6 (asymptomatic individuals with lower-level injury), strongly suggests that even mild autonomic impairment could affect neurovascular measures of brain function. This evidence urges future studies to account for vascular differences in SCI population while measuring changes in brain function. More importantly, the hemodynamic response of sensorimotor regions to various tasks such as rest, breath hold, and the different motor tasks can serve as a benchmark for future studies employing fNIRS in other neurological conditions including the ones involving vascular pathology. In brief, fNIRS could be an effective and economical neuroimaging technique to assess the cortical correlates of different rehabilitation therapies that require extensive longitudinal testing in a real-world setting.

6.2 fMRI vs. fNIRS in Spinal Cord Injury

MRI and fMRI have been favored over other imaging techniques due to its high spatial resolution, ability to study deep-seated structures and non-ionizing nature[49]. The novelty permissible in fMRI to investigate the whole brain with or without an exogenous stimulus also makes it an ideal technique for clinical populations whose effects are usually heterogenous. This is illustrated in Chapter 3 of this dissertation, which discusses the

reorganization of the whole brain (both sensorimotor and non-sensorimotor) after SCI using a single resting-state fMRI scan. But even with superior resolution, investigating the subcortical structures using fMRI carries significant challenges due to its small size, inferior signal quality and the lack of comprehensive atlases involving the subcortical areas[213]. Despite these constraints, the ICA based parcellation technique employed in this dissertation using resting-state scans obtained from a 1.5 Tesla MRI scanner generated thalamic sub-nuclei maps that compare qualitatively well with the anatomical boundaries of the thalamus. Nonetheless, caution must be taken when examining and interpreting findings from subcortical areas, especially with smaller structures. Ideally, a higher magnetic strength and a higher spatial resolution could both improve the accuracy of mapping subcortical structures using fMRI. Findings from Chapter 4 using fNIRS demonstrate that it may also be a viable technique to differentiate spatial activity within the regions of a neuroanatomical system, especially beneficial when the goal is to quantify changes in the HbO, HbR and HbT concentration. Though of course, whole-brain mapping cannot be achieved using fNIRS due to its limited depth penetration into the cortex (5-8 mm) and low spatial resolution (~1 cm) making it suitable for mapping only the superficial layers of the cortex.

As discussed in Chapter 4, the BOLD signal or any neuronal recording measured based on the principle of neurovascular coupling may involve heterogeneity introduced by large vessels as well as inter-subject differences in vascular dynamics. As a result, a modified fMRI sequence or hypercapnia may be applied in combination with fMRI to attain more than one physiological measure. For example, arterial spinal labelling can be used in conjunction with task-based fMRI to measure perfusion in addition to task-induced

BOLD activity of SCI patients; or, hypercapnia can be implemented in combination with fMRI to record the task-evoked activity and the cerebrovascular reactivity of the cortical regions of SCI patients. Results from Chapter 4 of this dissertation demonstrated that the same hypercapnic method can be applied using fNIRS and in fact may additionally allow one to explore the spatio-temporal characteristics of hemodynamic response to hypercapnia as a means to understand the vascular physiology more meticulously.

The downside of fMRI is its inability to accommodate and test naturalistic movements such as walking involved in the rehabilitative therapy of SCI or other neuromuscular and neurodegenerative injuries. The blood physiological response to movements may also slightly differ between supine and upright/standing position that may be further exaggerated in SCI patients with below-normal mean arterial pressure. Due to its mechanical design, fNIRS is an economical and portable technique that allows the participant to interact with the environment as in real life. Temporal and spatial distribution of activity in HC and SCI groups during finger and ankle movement in an upright sitting position suggest that fNIRS may also be useful to identify differential activity associated to a dynamic movement such as walking. For instance, a study by Mehrholz and colleagues combined biomechanical measures with cortical measures to assess how robot or body-weight assisted physical training differed from over ground gait training in SCI patients [214]; moreover, it enables the examination of hemodynamic activity at a temporal resolution greater than fMRI and spatial resolution better than electroencephalography[31]. fNIRS also permits the quantification of individual hemoglobin changes viz. HbO, HbR, HbT concentration in micro Molar units in upright sitting position, which is not feasible using fMRI equipment.

In conclusion, the benefits of fMRI are numerous and well-established, but the choice of imaging modality is a trade-off that is settled based on the specific research question. Both modalities allow plenty of novel investigative approaches. For instance, fMRI could be beneficial for exploratory studies examining the less-understood neurological mechanisms of emotional intelligence, salience detection or abnormal pain processing/phantom limb syndrome. Whereas fNIRS could be a suitable approach to monitor cortical motor activity, measure cortical correlates of cognitive impairments such as decreased attention and working memory in SCI patients. Further, combining neuroimaging measures (preferably fNIRS due to reduced cost and setup) with biomechanical and clinical measures could help understand the implications of neuroimaging measures on the neuropathology of SCI.

6.3 Limitations and Future Directions

Several limitations in the methodology and the research process employed in this dissertation must be noted. First, using structural MRI, the study lacked information on the patient's course of rehabilitation and pain status, and hence limited the functional interpretation of the results. As mentioned earlier, the lack of patient information regarding the functional recovery levels, pain status and physical therapy limits the functional and behavioral interpretation of the results. Hence, future studies may wish to explore further into the effect of rehabilitation, neuropathic pain levels and somatosensory abnormalities on the brain functional connectivity of SCI population.

The application of fNIRS to examine the cerebrovascular reactivity and neurovascular activity in people with SCI is novel but also introductory and therefore carry some inherent limitations. Future work examining the response associated with various

task types, methodology and vascular constraints could improve the robustness and reliability of hemodynamic responses measured using fNIRS. There is great potential to improve the methodology in a larger sample and investigate longitudinal changes in brain activity. Concurrent fMRI and fNIRS can also cross-validate the fNIRS findings and thus solidify the foundation of fNIRS implementation in mapping brain activity in clinical populations.

REFERENCES

1. Oyinbo, C.A. Secondary Injury Mechanisms in Traumatic Spinal Cord Injury: A Nugget of This Multiply Cascade. *Acta Neurobiol Exp (Wars)* **71**, 281-299 (2011).

2. National Spinal Cord Injury Statistical Center. in *Facts and figures at a glance.* (University of Alabama at Birmingham, Birmingham, AL, 2018).

3. Nas, K., Yazmalar, L., Sah, V., Aydin, A. & Ones, K. Rehabilitation of Spinal Cord Injuries. *World J Orthop* **6**, 8-16 (2015).

4. Sezer, N., Akkuş, S. & Uğurlu, F.G. Chronic Complications of Spinal Cord Injury. *World Journal of Orthopedics* **6**, 24-33 (2015).

5. Moore, C.I., Stern, C.E., Dunbar, C., Kostyk, S.K., Gehi, A. & Corkin, S. Referred Phantom Sensations and Cortical Reorganization after Spinal Cord Injury in Humans. *Proc Natl Acad Sci U S A* **97**, 14703-14708 (2000).

6. Siddall, P.J., McClelland, J.M., Rutkowski, S.B. & Cousins, M.J. A Longitudinal Study of the Prevalence and Characteristics of Pain in the First 5 Years Following Spinal Cord Injury. *Pain* **103**, 249-257 (2003).

7. Stormer, S., Gerner, H.J., Gruninger, W., Metzmacher, K., Follinger, S., Wienke, C., Aldinger, W., Walker, N., Zimmermann, M. & Paeslack, V. Chronic Pain/Dysaesthesiae in Spinal Cord Injury Patients: Results of a Multicentre Study. *Spinal Cord* **35**, 446-455 (1997).

8. Woolsey, R.M. Chronic Pain Following Spinal Cord Injury. *J Am Paraplegia Soc* **9**, 39-41 (1986).

9. Moxon, K.A., Oliviero, A., Aguilar, J. & Foffani, G. Cortical Reorganization after Spinal Cord Injury: Always for Good? *Neuroscience* **283**, 78-94 (2014).

10. Voss, P., Thomas, M.E., Cisneros-Franco, J.M. & de Villers-Sidani, E. Dynamic Brains and the Changing Rules of Neuroplasticity: Implications for Learning and Recovery. *Front Psychol* **8**, 1657 (2017).

11. Rao, J.S., Liu, Z., Zhao, C., Wei, R.H., Zhao, W., Yang, Z.Y. & Li, X.G. Longitudinal Evaluation of Functional Connectivity Variation in the Monkey Sensorimotor Network Induced by Spinal Cord Injury. *Acta Physiol (Oxf)* **217**, 164-173 (2016).

12. Jain, N., Qi, H.X., Collins, C.E. & Kaas, J.H. Large-Scale Reorganization in the Somatosensory Cortex and Thalamus after Sensory Loss in Macaque Monkeys. *J Neurosci* **28**, 11042-11060 (2008).

13. Dutta, A., Kambi, N., Raghunathan, P., Khushu, S. & Jain, N. Large-Scale Reorganization of the Somatosensory Cortex of Adult Macaque Monkeys Revealed by Fmri. *Brain Struct Funct* **219**, 1305-1320 (2014).

14. Villiger, M., Grabher, P., Hepp-Reymond, M.C., Kiper, D., Curt, A., Bolliger, M., Hotz-Boendermaker, S., Kollias, S., Eng, K. & Freund, P. Relationship between Structural Brainstem and Brain Plasticity and Lower-Limb Training in Spinal Cord Injury: A Longitudinal Pilot Study. *Frontiers in human neuroscience* **9**, 254 (2015).

15. Kambi, N., Halder, P., Rajan, R., Arora, V., Chand, P., Arora, M. & Jain, N. Large-Scale Reorganization of the Somatosensory Cortex Following Spinal Cord Injuries Is Due to Brainstem Plasticity. *Nat Commun* **5**, 3602 (2014).

16. Oni-Orisan, A., Kaushal, M., Li, W., Leschke, J., Ward, B.D., Vedantam, A., Kalinosky, B., Budde, M.D., Schmit, B.D., Li, S.J., Muqeet, V. & Kurpad, S.N. Alterations in Cortical Sensorimotor Connectivity Following Complete Cervical Spinal Cord Injury: A Prospective Resting-State Fmri Study. *PLoS One* **11**, e0150351 (2016).

17. Hou, J.M., Sun, T.S., Xiang, Z.M., Zhang, J.Z., Zhang, Z.C., Zhao, M., Zhong, J.F., Liu, J., Zhang, H., Liu, H.L., Yan, R.B. & Li, H.T. Alterations of Resting-State Regional and Network-Level Neural Function after Acute Spinal Cord Injury. *Neuroscience* **277**, 446-454 (2014).

18. Hou, J., Xiang, Z., Yan, R., Zhao, M., Wu, Y., Zhong, J., Guo, L., Li, H., Wang, J., Wu, J., Sun, T. & Liu, H. Motor Recovery at 6 Months after Admission Is Related to Structural and Functional Reorganization of the Spine and Brain in Patients with Spinal Cord Injury. *Hum Brain Mapp* **37**, 2195-2209 (2016).

19. Freund, P., Weiskopf, N., Ward, N.S., Hutton, C., Gall, A., Ciccarelli, O., Craggs, M., Friston, K. & Thompson, A.J. Disability, Atrophy and Cortical Reorganization Following Spinal Cord Injury. *Brain* **134**, 1610-1622 (2011).

20. Lundell, H., Christensen, M.S., Barthelemy, D., Willerslev-Olsen, M., Biering-Sorensen, F. & Nielsen, J.B. Cerebral Activation Is Correlated to Regional Atrophy of the Spinal Cord and Functional Motor Disability in Spinal Cord Injured Individuals. *Neuroimage* **54**, 1254-1261 (2011).

21. Jurkiewicz, M.T., Crawley, A.P., Verrier, M.C., Fehlings, M.G. & Mikulis, D.J. Somatosensory Cortical Atrophy after Spinal Cord Injury: A Voxel-Based Morphometry Study. *Neurology* **66**, 762-764 (2006).

22. Hains, B.C., Saab, C.Y. & Waxman, S.G. Changes in Electrophysiological Properties and Sodium Channel Nav1.3 Expression in Thalamic Neurons after Spinal Cord Injury. *Brain* **128**, 2359-2371 (2005).

23. Head, H. & Holmes, G. Sensory Disturbances from Cerebral Lesions1. *Brain* **34**, 102-254 (1911).

24. Biswal, B.B., Mennes, M., Zuo, X.N., Gohel, S., Kelly, C., Smith, S.M., Beckmann, C.F., Adelstein, J.S., Buckner, R.L., Colcombe, S., Dogonowski, A.M., Ernst, M., Fair, D., Hampson, M., Hoptman, M.J., Hyde, J.S., Kiviniemi, V.J., Kotter, R., Li, S.J., Lin, C.P., Lowe, M.J., Mackay, C., Madden, D.J., Madsen, K.H., Margulies, D.S., Mayberg, H.S., McMahon, K., Monk, C.S., Mostofsky, S.H., Nagel, B.J., Pekar, J.J., Peltier, S.J., Petersen, S.E., Riedl, V., Rombouts, S.A., Rypma, B., Schlaggar, B.L., Schmidt, S., Seidler, R.D., Siegle, G.J., Sorg, C., Teng, G.J., Veijola, J., Villringer, A., Walter, M., Wang, L., Weng, X.C., Whitfield-Gabrieli, S., Williamson, P., Windischberger, C., Zang, Y.F., Zhang, H.Y., Castellanos, F.X. & Milham, M.P. Toward Discovery Science of Human Brain Function. *Proc Natl Acad Sci U S A* **107**, 4734-4739 (2010).

25. Algarin, C., Karunakaran, K.D., Reyes, S., Morales, C., Lozoff, B., Peirano, P. & Biswal, B. Differences on Brain Connectivity in Adulthood Are Present in Subjects with Iron Deficiency Anemia in Infancy. *Front Aging Neurosci* **9**, 54 (2017).

26. Egbert, A.R., Biswal, B., Karunakaran, K., Gohel, S., Pluta, A., Wolak, T., Szymanska, B., Firlag-Burkacka, E., Sobanska, M., Gawron, N., Bienkowski, P., Sienkiewicz-Jarosz, H., Scinska-Bienkowska, A., Bornstein, R., Rao, S. & Lojek, E. Age and Hiv Effects on Resting State of the Brain in Relationship to Neurocognitive Functioning. *Behav Brain Res* **344**, 20-27 (2018).

27. Egbert, A.R., Biswal, B., Karunakaran, K.D., Pluta, A., Wolak, T., Rao, S., Bornstein, R., Szymanska, B., Horban, A., Firlag-Burkacka, E., Sobanska, M., Gawron, N., Bienkowski, P., Sienkiewicz-Jarosz, H., Scinska-Bienkowska, A. & Lojek, E. Hiv Infection across Aging: Synergistic Effects on Intrinsic Functional Connectivity of the Brain. *Prog Neuropsychopharmacol Biol Psychiatry* **88**, 19-30 (2019).

28. Biswal, B., Yetkin, F.Z., Haughton, V.M. & Hyde, J.S. Functional Connectivity in the Motor Cortex of Resting Human Brain Using Echo-Planar Mri. *Magn Reson Med* **34**, 537-541 (1995).

29. Reid, L.B., Boyd, R.N., Cunnington, R. & Rose, S.E. Interpreting Intervention Induced Neuroplasticity with Fmri: The Case for Multimodal Imaging Strategies. *Neural Plast* **2016**, 2643491 (2016).

30. Phillips, A.A., Ainslie, P.N., Krassioukov, A.V. & Warburton, D.E. Regulation of Cerebral Blood Flow after Spinal Cord Injury. *J Neurotrauma* **30**, 1551-1563 (2013).

31. Wilcox, T. & Biondi, M. Fnirs in the Developmental Sciences. *Wiley Interdiscip Rev Cogn Sci* **6**, 263-283 (2015).

32. Kastrup, A., Kruger, G., Neumann-Haefelin, T. & Moseley, M.E. Assessment of Cerebrovascular Reactivity with Functional Magnetic Resonance Imaging: Comparison of Co(2) and Breath Holding. *Magn Reson Imaging* **19**, 13-20 (2001).

33. Kirshblum, S.C., Burns, S.P., Biering-Sorensen, F., Donovan, W., Graves, D.E., Jha, A., Johansen, M., Jones, L., Krassioukov, A., Mulcahey, M.J., Schmidt-Read, M. & Waring, W. International Standards for Neurological Classification of Spinal Cord Injury (Revised 2011). *J Spinal Cord Med* **34**, 535-546 (2011).

34. Frisbie, J.H. & Aguilera, E.J. Chronic Pain after Spinal Cord Injury: An Expedient Diagnostic Approach. *Paraplegia* **28**, 460-465 (1990).

35. Kirshblum, S. & Waring, W., 3rd. Updates for the International Standards for Neurological Classification of Spinal Cord Injury. *Phys Med Rehabil Clin N Am* **25**, 505-517, vii (2014).

36. Sezer, N., Akkus, S. & Ugurlu, F.G. Chronic Complications of Spinal Cord Injury. *World J Orthop* **6**, 24-33 (2015).

37. Flor, H., Nikolajsen, L. & Staehelin Jensen, T. Phantom Limb Pain: A Case of Maladaptive Cns Plasticity? *Nat Rev Neurosci* **7**, 873-881 (2006).

38. Atkinson, P.P. & Atkinson, J.L. Spinal Shock. *Mayo Clin Proc* **71**, 384-389 (1996).

39. Finnerup, N.B., Johannesen, I.L., Sindrup, S.H., Bach, F.W. & Jensen, T.S. Pain and Dysesthesia in Patients with Spinal Cord Injury: A Postal Survey. *Spinal Cord* **39**, 256-262 (2001).

40. Ding, Y., Kastin, A.J. & Pan, W. Neural Plasticity after Spinal Cord Injury. *Curr Pharm Des* **11**, 1441-1450 (2005).

41. Henderson, L.A., Gustin, S.M., Macey, P.M., Wrigley, P.J. & Siddall, P.J. Functional Reorganization of the Brain in Humans Following Spinal Cord Injury: Evidence for Underlying Changes in Cortical Anatomy. *J Neurosci* **31**, 2630-2637 (2011).

42. Kokotilo, K.J., Eng, J.J. & Curt, A. Reorganization and Preservation of Motor Control of the Brain in Spinal Cord Injury: A Systematic Review. *J Neurotrauma* **26**, 2113-2126 (2009).

43. Mohammed, H. & Hollis, E.R., 2nd. Cortical Reorganization of Sensorimotor Systems and the Role of Intracortical Circuits after Spinal Cord Injury. *Neurotherapeutics* (2018).

44. Nardone, R., Holler, Y., Brigo, F., Seidl, M., Christova, M., Bergmann, J., Golaszewski, S. & Trinka, E. Functional Brain Reorganization after Spinal Cord Injury: Systematic Review of Animal and Human Studies. *Brain Res* **1504**, 58-73 (2013).

45. Frost, S.B., Barbay, S., Friel, K.M., Plautz, E.J. & Nudo, R.J. Reorganization of Remote Cortical Regions after Ischemic Brain Injury: A Potential Substrate for Stroke Recovery. *Journal of neurophysiology* **89**, 3205-3214 (2003).

46. Ghosh, A., Haiss, F., Sydekum, E., Schneider, R., Gullo, M., Wyss, M.T., Mueggler, T., Baltes, C., Rudin, M., Weber, B. & Schwab, M.E. Rewiring of Hindlimb Corticospinal Neurons after Spinal Cord Injury. *Nature neuroscience* **13**, 97-104 (2010).

47. Ghosh, A., Sydekum, E., Haiss, F., Peduzzi, S., Zorner, B., Schneider, R., Baltes, C., Rudin, M., Weber, B. & Schwab, M.E. Functional and Anatomical Reorganization of the Sensory-Motor Cortex after Incomplete Spinal Cord Injury in Adult Rats. *The Journal of neuroscience : the official journal of the Society for Neuroscience* **29**, 12210-12219 (2009).

48. Kassubek, J. The Application of Neuroimaging to Healthy and Diseased Brains: Present and Future. *Front Neurol* **8**, 61 (2017).

49. Matthews, P.M., Honey, G.D. & Bullmore, E.T. Applications of Fmri in Translational Medicine and Clinical Practice. *Nat Rev Neurosci* **7**, 732-744 (2006).

50. Lauterbur, P.C. Image Formation by Induced Local Interactions. Examples Employing Nuclear Magnetic Resonance. 1973. *Clin Orthop Relat Res*, 3-6 (1989).

51. Kulkarni, M.V., Bondurant, F.J., Rose, S.L. & Narayana, P.A. 1.5 Tesla Magnetic Resonance Imaging of Acute Spinal Trauma. *Radiographics* **8**, 1059-1082 (1988).

52. Symms, M., Jager, H.R., Schmierer, K. & Yousry, T.A. A Review of Structural Magnetic Resonance Neuroimaging. *J Neurol Neurosurg Psychiatry* **75**, 1235-1244 (2004).

53. Vemuri, P. & Jack, C.R., Jr. Role of Structural Mri in Alzheimer's Disease. *Alzheimers Res Ther* **2**, 23 (2010).

54. Levine, B., Kovacevic, N., Nica, E.I., Cheung, G., Gao, F., Schwartz, M.L. & Black, S.E. The Toronto Traumatic Brain Injury Study: Injury Severity and Quantified Mri. *Neurology* **70**, 771-778 (2008).

55. Werden, E., Cumming, T., Li, Q., Bird, L., Veldsman, M., Pardoe, H.R., Jackson, G., Donnan, G.A. & Brodtmann, A. Structural Mri Markers of Brain Aging Early after Ischemic Stroke. *Neurology* **89**, 116-124 (2017).

56. Wrigley, P.J., Gustin, S.M., Macey, P.M., Nash, P.G., Gandevia, S.C., Macefield, V.G., Siddall, P.J. & Henderson, L.A. Anatomical Changes in Human Motor Cortex and Motor Pathways Following Complete Thoracic Spinal Cord Injury. *Cereb Cortex* **19**, 224-232 (2009).

57. Zheng, W., Chen, Q., Chen, X., Wan, L., Qin, W., Qi, Z., Chen, N. & Li, K. Brain White Matter Impairment in Patients with Spinal Cord Injury. *Neural Plast* **2017**, 4671607 (2017).

58. Crawley, A.P., Jurkiewicz, M.T., Yim, A., Heyn, S., Verrier, M.C., Fehlings, M.G. & Mikulis, D.J. Absence of Localized Grey Matter Volume Changes in the Motor Cortex Following Spinal Cord Injury. *Brain research* **1028**, 19-25 (2004).

59. Mole, T.B., MacIver, K., Sluming, V., Ridgway, G.R. & Nurmikko, T.J. Specific Brain Morphometric Changes in Spinal Cord Injury with and without Neuropathic Pain. *NeuroImage. Clinical* **5**, 28-35 (2014).

60. Yoon, E.J., Kim, Y.K., Shin, H.I., Lee, Y. & Kim, S.E. Cortical and White Matter Alterations in Patients with Neuropathic Pain after Spinal Cord Injury. *Brain research* **1540**, 64-73 (2013).

61. Bruehlmeier, M., Dietz, V., Leenders, K.L., Roelcke, U., Missimer, J. & Curt, A. How Does the Human Brain Deal with a Spinal Cord Injury? *The European journal of neuroscience* **10**, 3918-3922 (1998).

62. Ashburner, J. & Friston, K.J. Voxel-Based Morphometry--the Methods. *NeuroImage* **11**, 805-821 (2000).

63. Karunakaran, K.D., He, J., Zhao, J., Cui, J.L., Zang, Y.F., Zhang, Z. & Biswal, B.B. Differences in Cortical Gray Matter Atrophy of Paraplegia and Tetraplegia after Complete Spinal Cord Injury. *J Neurotrauma* (2018).

64. Ashburner, J. A Fast Diffeomorphic Image Registration Algorithm. *NeuroImage* **38**, 95-113 (2007).

65. Winkler, A.M., Ridgway, G.R., Webster, M.A., Smith, S.M. & Nichols, T.E. Permutation Inference for the General Linear Model. *NeuroImage* **92**, 381-397 (2014).

66. Rorden, C. & Brett, M. Stereotaxic Display of Brain Lesions. *Behav Neurol* **12**, 191-200 (2000).

67. Barbas, H., Saha, S., Rempel-Clower, N. & Ghashghaei, T. Serial Pathways from Primate Prefrontal Cortex to Autonomic Areas May Influence Emotional Expression. *BMC Neurosci* **4**, 25 (2003).

68. Barrett, L.F., Quigley, K.S., Bliss-Moreau, E. & Aronson, K.R. Interoceptive Sensitivity and Self-Reports of Emotional Experience. *J Pers Soc Psychol* **87**, 684-697 (2004).

69. Pistoia, F., Carolei, A., Sacco, S., Conson, M., Pistarini, C., Cazzulani, B., Stewart, J., Franceschini, M. & Sara, M. Contribution of Interoceptive Information to Emotional Processing: Evidence from Individuals with Spinal Cord Injury. *J Neurotrauma* **32**, 1981-1986 (2015).

70. Obermann, M., Rodriguez-Raecke, R., Naegel, S., Holle, D., Mueller, D., Yoon, M.S., Theysohn, N., Blex, S., Diener, H.C. & Katsarava, Z. Gray Matter Volume Reduction Reflects Chronic Pain in Trigeminal Neuralgia. *NeuroImage* **74**, 352-358 (2013).

71. Rodriguez-Raecke, R., Niemeier, A., Ihle, K., Ruether, W. & May, A. Structural Brain Changes in Chronic Pain Reflect Probably Neither Damage nor Atrophy. *PloS one* **8**, e54475 (2013).

72. Likavcanova, K., Urdzikova, L., Hajek, M. & Sykova, E. Metabolic Changes in the Thalamus after Spinal Cord Injury Followed by Proton Mr Spectroscopy. *Magn Reson Med* **59**, 499-506 (2008).

73. Hirsch, A.R. & Cleveland, L.B. Olfaction and Chronic Spinal Cord Injury. *Journal of Neurologic Rehabilitation* **12**, 101-104 (1998).

74. Nicotra, A., Critchley, H.D., Mathias, C.J. & Dolan, R.J. Emotional and Autonomic Consequences of Spinal Cord Injury Explored Using Functional Brain Imaging. *Brain* **129**, 718-728 (2006).

75. Han, P., Whitcroft, K.L., Fischer, J., Gerber, J., Cuevas, M., Andrews, P. & Hummel, T. Olfactory Brain Gray Matter Volume Reduction in Patients with Chronic Rhinosinusitis. *Int Forum Allergy Rhinol* **7**, 551-556 (2017).

76. Yao, L., Pinto, J.M., Yi, X., Li, L., Peng, P. & Wei, Y. Gray Matter Volume Reduction of Olfactory Cortices in Patients with Idiopathic Olfactory Loss. *Chem Senses* **39**, 755-760 (2014).

77. Freund, P., Weiskopf, N., Ashburner, J., Wolf, K., Sutter, R., Altmann, D.R., Friston, K., Thompson, A. & Curt, A. Mri Investigation of the Sensorimotor Cortex and the Corticospinal Tract after Acute Spinal Cord Injury: A Prospective Longitudinal Study. *The Lancet. Neurology* **12**, 873-881 (2013).

78. Zatorre, R.J., Fields, R.D. & Johansen-Berg, H. Plasticity in Gray and White: Neuroimaging Changes in Brain Structure During Learning. *Nature neuroscience* **15**, 528-536 (2012).

79. Jutzeler, C.R., Huber, E., Callaghan, M.F., Luechinger, R., Curt, A., Kramer, J.L. & Freund, P. Association of Pain and Cns Structural Changes after Spinal Cord Injury. *Sci Rep* **6**, 18534 (2016).

80. Fink GR, M.J., Halligan PW, Frith CD, Driver J, Frackowiak RS, Dolan RJ. The Neural Consequences of Conflict between Intention and the Senses. *Brain : a journal of neurology* **122**, 497-512 (1999).

81. Ionta, S., Villiger, M., Jutzeler, C.R., Freund, P., Curt, A. & Gassert, R. Spinal Cord Injury Affects the Interplay between Visual and Sensorimotor Representations of the Body. *Sci Rep* **6**, 20144 (2016).

82. Cavada, C. & Goldman-Rakic, P.S. Posterior Parietal Cortex in Rhesus Monkey: I. Parcellation of Areas Based on Distinctive Limbic and Sensory Corticocortical Connections. *J Comp Neurol* **287**, 393-421 (1989).

83. Bareyre, F.M., Kerschensteiner, M., Raineteau, O., Mettenleiter, T.C., Weinmann, O. & Schwab, M.E. The Injured Spinal Cord Spontaneously Forms a New Intraspinal Circuit in Adult Rats. *Nat Neurosci* **7**, 269-277 (2004).

84. Jurkiewicz, M.T., Mikulis, D.J., McIlroy, W.E., Fehlings, M.G. & Verrier, M.C. Sensorimotor Cortical Plasticity During Recovery Following Spinal Cord Injury: A Longitudinal Fmri Study. *Neurorehabil Neural Repair* **21**, 527-538 (2007).

85. Jurkiewicz, M.T., Mikulis, D.J., Fehlings, M.G. & Verrier, M.C. Sensorimotor Cortical Activation in Patients with Cervical Spinal Cord Injury with Persisting Paralysis. *Neurorehabil Neural Repair* **24**, 136-140 (2010).

86. Awad, A., Levi, R., Lindgren, L., Hultling, C., Westling, G., Nyberg, L. & Eriksson, J. Preserved Somatosensory Conduction in a Patient with Complete Cervical Spinal Cord Injury. *J Rehabil Med* **47**, 426-431 (2015).

87. Chen, Q., Zheng, W., Chen, X., Li, X., Wang, L., Qin, W., Li, K. & Chen, N. Reorganization of the Somatosensory Pathway after Subacute Incomplete Cervical Cord Injury. *Neuroimage Clin* **21**, 101674 (2019).

88. Chen, X., Wan, L., Qin, W., Zheng, W., Qi, Z., Chen, N. & Li, K. Functional Preservation and Reorganization of Brain During Motor Imagery in Patients with Incomplete Spinal Cord Injury: A Pilot Fmri Study. *Front Hum Neurosci* **10**, 46 (2016).

89. Dietz, V. & Fouad, K. Restoration of Sensorimotor Functions after Spinal Cord Injury. *Brain* **137**, 654-667 (2014).

90. Duggal, N., Rabin, D., Bartha, R., Barry, R.L., Gati, J.S., Kowalczyk, I. & Fink, M. Brain Reorganization in Patients with Spinal Cord Compression Evaluated Using Fmri. *Neurology* **74**, 1048-1054 (2010).

91. Jutzeler, C.R., Freund, P., Huber, E., Curt, A. & Kramer, J.L.K. Neuropathic Pain and Functional Reorganization in the Primary Sensorimotor Cortex after Spinal Cord Injury. *J Pain* **16**, 1256-1267 (2015).

92. Lundell, H., Barthelemy, D., Skimminge, A., Dyrby, T.B., Biering-Sorensen, F. & Nielsen, J.B. Independent Spinal Cord Atrophy Measures Correlate to Motor and Sensory Deficits in Individuals with Spinal Cord Injury. *Spinal Cord* **49**, 70-75 (2011).

93. Stroman, P.W., Khan, H.S., Bosma, R.L., Cotoi, A.I., Leung, R., Cadotte, D.W. & Fehlings, M.G. Changes in Pain Processing in the Spinal Cord and Brainstem after Spinal Cord Injury Characterized by Functional Magnetic Resonance Imaging. *J Neurotrauma* **33**, 1450-1460 (2016).

94. Wrigley, P.J., Siddall, P.J. & Gustin, S.M. New Evidence for Preserved Somatosensory Pathways in Complete Spinal Cord Injury: A Fmri Study. *Hum Brain Mapp* **39**, 588-598 (2018).

95. Lotze, M., Montoya, P., Erb, M., Hulsmann, E., Flor, H., Klose, U., Birbaumer, N. & Grodd, W. Activation of Cortical and Cerebellar Motor Areas During Executed and Imagined Hand Movements: An Fmri Study. *J Cogn Neurosci* **11**, 491-501 (1999).

96. Zaaimi, B., Edgley, S.A., Soteropoulos, D.S. & Baker, S.N. Changes in Descending Motor Pathway Connectivity after Corticospinal Tract Lesion in Macaque Monkey. *Brain* **135**, 2277-2289 (2012).

97. Lenz, F.A., Tasker, R.R., Dostrovsky, J.O., Kwan, H.C., Gorecki, J., Hirayama, T. & Murphy, J.T. Abnormal Single-Unit Activity Recorded in the Somatosensory Thalamus of a Quadriplegic Patient with Central Pain. *Pain* **31**, 225-236 (1987).

98. Lang, S., Duncan, N. & Northoff, G. Resting-State Functional Magnetic Resonance Imaging: Review of Neurosurgical Applications. *Neurosurgery* **74**, 453-464; discussion 464-455 (2014).

99. Lin, W., Kuppusamy, K., Haacke, E.M. & Burton, H. Functional Mri in Human Somatosensory Cortex Activated by Touching Textured Surfaces. *J Magn Reson Imaging* **6**, 565-572 (1996).

100. Shimony, J.S., Zhang, D., Johnston, J.M., Fox, M.D., Roy, A. & Leuthardt, E.C. Resting-State Spontaneous Fluctuations in Brain Activity: A New Paradigm for Presurgical Planning Using Fmri. *Acad Radiol* **16**, 578-583 (2009).

101. Fox, M.D. & Greicius, M. Clinical Applications of Resting State Functional Connectivity. *Front Syst Neurosci* **4**, 19 (2010).

102. Gore, J.C. Principles and Practice of Functional Mri of the Human Brain. *J Clin Invest* **112**, 4-9 (2003).

103. Dechent, P., Merboldt, K.D. & Frahm, J. Is the Human Primary Motor Cortex Involved in Motor Imagery? *Brain Res Cogn Brain Res* **19**, 138-144 (2004).

104. Uddin, L.Q., Kelly, A.M., Biswal, B.B., Castellanos, F.X. & Milham, M.P. Functional Connectivity of Default Mode Network Components: Correlation, Anticorrelation, and Causality. *Hum Brain Mapp* **30**, 625-637 (2009).

105. Shehzad, Z., Kelly, A.M., Reiss, P.T., Gee, D.G., Gotimer, K., Uddin, L.Q., Lee, S.H., Margulies, D.S., Roy, A.K., Biswal, B.B., Petkova, E., Castellanos, F.X. & Milham, M.P. The Resting Brain: Unconstrained yet Reliable. *Cereb Cortex* **19**, 2209-2229 (2009).

106. Lowe, M.J., Dzemidzic, M., Lurito, J.T., Mathews, V.P. & Phillips, M.D. Correlations in Low-Frequency Bold Fluctuations Reflect Cortico-Cortical Connections. *Neuroimage* **12**, 582-587 (2000).

107. Choe, A.S., Belegu, V., Yoshida, S., Joel, S., Sadowsky, C.L., Smith, S.A., van Zijl, P.C., Pekar, J.J. & McDonald, J.W. Extensive Neurological Recovery from a Complete Spinal Cord Injury: A Case Report and Hypothesis on the Role of Cortical Plasticity. *Front Hum Neurosci* **7**, 290 (2013).

108. Rao, J.S., Ma, M., Zhao, C., Zhang, A.F., Yang, Z.Y., Liu, Z. & Li, X.G. Fractional Amplitude of Low-Frequency Fluctuation Changes in Monkeys with Spinal Cord Injury: A Resting-State Fmri Study. *Magn Reson Imaging* **32**, 482-486 (2014).

109. Kaushal, M., Oni-Orisan, A., Chen, G., Li, W., Leschke, J., Ward, B.D., Kalinosky, B., Budde, M.D., Schmit, B.D., Li, S.J., Muqeet, V. & Kurpad, S.N. Evaluation of Whole-Brain Resting-State Functional Connectivity in Spinal Cord Injury: A Large-Scale Network Analysis Using Network-Based Statistic. *J Neurotrauma* **34**, 1278-1282 (2017).

110. Kaushal, M., Oni-Orisan, A., Chen, G., Li, W., Leschke, J., Ward, D., Kalinosky, B., Budde, M., Schmit, B., Li, S.J., Muqeet, V. & Kurpad, S. Large-Scale Network Analysis of Whole-Brain Resting-State Functional Connectivity in Spinal Cord Injury: A Comparative Study. *Brain Connect* **7**, 413-423 (2017).

111. Min, Y.S., Park, J.W., Jin, S.U., Jang, K.E., Nam, H.U., Lee, Y.S., Jung, T.D. & Chang, Y. Alteration of Resting-State Brain Sensorimotor Connectivity Following Spinal Cord Injury: A Resting-State Functional Magnetic Resonance Imaging Study. *J Neurotrauma* **32**, 1422-1427 (2015).

112. Pan, Y., Dou, W.B., Wang, Y.H., Luo, H.W., Ge, Y.X., Yan, S.Y., Xu, Q., Tu, Y.Y., Xiao, Y.Q., Wu, Q., Zheng, Z.Z. & Zhao, H.L. Non-Concomitant Cortical Structural and Functional Alterations in Sensorimotor Areas Following Incomplete Spinal Cord Injury. *Neural Regen Res* **12**, 2059-2066 (2017).

113. Min, Y.S., Chang, Y., Park, J.W., Lee, J.M., Cha, J., Yang, J.J., Kim, C.H., Hwang, J.M., Yoo, J.N. & Jung, T.D. Change of Brain Functional Connectivity in Patients with Spinal Cord Injury: Graph Theory Based Approach. *Ann Rehabil Med* **39**, 374-383 (2015).

114. Chisholm, A.E., Peters, S., Borich, M.R., Boyd, L.A. & Lam, T. Short-Term Cortical Plasticity Associated with Feedback-Error Learning after Locomotor Training in a Patient with Incomplete Spinal Cord Injury. *Phys Ther* **95**, 257-266 (2015).

115. Burke, D., Fullen, B.M., Stokes, D. & Lennon, O. Neuropathic Pain Prevalence Following Spinal Cord Injury: A Systematic Review and Meta-Analysis. *Eur J Pain* **21**, 29-44 (2017).

116. Seminowicz, D.A., Jiang, L., Ji, Y., Xu, S., Gullapalli, R.P. & Masri, R. Thalamocortical Asynchrony in Conditions of Spinal Cord Injury Pain in Rats. *J Neurosci* **32**, 15843-15848 (2012).

117. Jensen, M.P., Sherlin, L.H., Gertz, K.J., Braden, A.L., Kupper, A.E., Gianas, A., Howe, J.D. & Hakimian, S. Brain Eeg Activity Correlates of Chronic Pain in Persons with Spinal Cord Injury: Clinical Implications. *Spinal Cord* **51**, 55-58 (2013).

118. Ching, S., Cimenser, A., Purdon, P.L., Brown, E.N. & Kopell, N.J. Thalamocortical Model for a Propofol-Induced Alpha-Rhythm Associated with Loss of Consciousness. *Proc Natl Acad Sci U S A* **107**, 22665-22670 (2010).

119. Gustin, S.M., Wrigley, P.J., Youssef, A.M., McIndoe, L., Wilcox, S.L., Rae, C.D., Edden, R.A., Siddall, P.J. & Henderson, L.A. Thalamic Activity and Biochemical Changes in Individuals with Neuropathic Pain after Spinal Cord Injury. *Pain* **155**, 1027-1036 (2014).

120. Alonso-Calvino, E., Martinez-Camero, I., Fernandez-Lopez, E., Humanes-Valera, D., Foffani, G. & Aguilar, J. Increased Responses in the Somatosensory Thalamus Immediately after Spinal Cord Injury. *Neurobiol Dis* **87**, 39-49 (2016).

121. Guillery, R.W. Anatomical Evidence Concerning the Role of the Thalamus in Corticocortical Communication: A Brief Review. *J Anat* **187 (Pt 3)**, 583-592 (1995).

122. Tyll, S., Budinger, E. & Noesselt, T. Thalamic Influences on Multisensory Integration. *Commun Integr Biol* **4**, 378-381 (2011).

123. Cappe, C., Rouiller, E.M. & Barone, P. Cortical and Thalamic Pathways for Multisensory and Sensorimotor Interplay. in *The Neural Bases of Multisensory Processes* (eds. Murray, M.M. & Wallace, M.T.) (Boca Raton (FL), 2012).

124. Warren M Grill, R.b. Exploring the Thalamus and Its Role in Cortical Function. Second Edition. By S Murray Sherman and R W Guillery. *The Quarterly Review of Biology* **82**, 176-177 (2007).

125. William Penny, K.F., John Ashburner, Stefan Kiebel, Thomas Nichols. *Statistical Parametric Mapping: The Analysis of Functional Brain Images*, (Elsevier, 2006).

126. Friston, K.J., Williams, S., Howard, R., Frackowiak, R.S. & Turner, R. Movement-Related Effects in Fmri Time-Series. *Magn Reson Med* **35**, 346-355 (1996).

127. Dosenbach, N.U., Nardos, B., Cohen, A.L., Fair, D.A., Power, J.D., Church, J.A., Nelson, S.M., Wig, G.S., Vogel, A.C., Lessov-Schlaggar, C.N., Barnes, K.A., Dubis, J.W., Feczko, E., Coalson, R.S., Pruett, J.R., Jr., Barch, D.M., Petersen, S.E. & Schlaggar, B.L. Prediction of Individual Brain Maturity Using Fmri. *Science* **329**, 1358-1361 (2010).

128. Yuan, R., Di, X., Taylor, P.A., Gohel, S., Tsai, Y.H. & Biswal, B.B. Functional Topography of the Thalamocortical System in Human. *Brain Struct Funct* **221**, 1971-1984 (2016).

129. Smith, S.M., Jenkinson, M., Woolrich, M.W., Beckmann, C.F., Behrens, T.E., Johansen-Berg, H., Bannister, P.R., De Luca, M., Drobnjak, I., Flitney, D.E., Niazy, R.K., Saunders, J., Vickers, J., Zhang, Y., De Stefano, N., Brady, J.M. & Matthews, P.M. Advances in Functional and Structural Mr Image Analysis and Implementation as Fsl. *Neuroimage* **23 Suppl 1**, S208-219 (2004).

130. Zou, Q., Long, X., Zuo, X., Yan, C., Zhu, C., Yang, Y., Liu, D., He, Y. & Zang, Y. Functional Connectivity between the Thalamus and Visual Cortex under Eyes

Closed and Eyes Open Conditions: A Resting-State Fmri Study. *Hum Brain Mapp* **30**, 3066-3078 (2009).

131. Cox, R.W. Afni: Software for Analysis and Visualization of Functional Magnetic Resonance Neuroimages. *Comput Biomed Res* **29**, 162-173 (1996).

132. Winkler, A.M., Ridgway, G.R., Webster, M.A., Smith, S.M. & Nichols, T.E. *Permutation Inference for the General Linear Model*, (2014).

133. Beckmann, C.F., DeLuca, M., Devlin, J.T. & Smith, S.M. Investigations into Resting-State Connectivity Using Independent Component Analysis. *Philos Trans R Soc Lond B Biol Sci* **360**, 1001-1013 (2005).

134. Lotze, M., Erb, M., Flor, H., Huelsmann, E., Godde, B. & Grodd, W. Fmri Evaluation of Somatotopic Representation in Human Primary Motor Cortex. *Neuroimage* **11**, 473-481 (2000).

135. Hawasli, A.H., Rutlin, J., Roland, J.L., Murphy, R.K., Song, S.K., Leuthardt, E.C., Shimony, J.S. & Ray, W.Z. Spinal Cord Injury Disrupts Resting-State Networks in the Human Brain. *J Neurotrauma* (2018).

136. Zhao, Z., Wang, X., Fan, M., Yin, D., Sun, L., Jia, J., Tang, C., Zheng, X., Jiang, Y., Wu, J. & Gong, J. Altered Effective Connectivity of the Primary Motor Cortex in Stroke: A Resting-State Fmri Study with Granger Causality Analysis. *PLoS One* **11**, e0166210 (2016).

137. Whitt, J.L., Masri, R., Pulimood, N.S. & Keller, A. Pathological Activity in Mediodorsal Thalamus of Rats with Spinal Cord Injury Pain. *J Neurosci* **33**, 3915-3926 (2013).

138. Guillery, R.W. & Sherman, S.M. Thalamic Relay Functions and Their Role in Corticocortical Communication: Generalizations from the Visual System. *Neuron* **33**, 163-175 (2002).

139. Sherman, S.M. The Thalamus Is More Than Just a Relay. *Current opinion in neurobiology* **17**, 417-422 (2007).

140. Mitchell, A.S. & Chakraborty, S. What Does the Mediodorsal Thalamus Do? *Frontiers in Systems Neuroscience* **7**, 37 (2013).

141. Mitchell, A.S. The Mediodorsal Thalamus as a Higher Order Thalamic Relay Nucleus Important for Learning and Decision-Making. *Neuroscience & Biobehavioral Reviews* **54**, 76-88 (2015).

142. Krettek, J.E. & Price, J.L. The Cortical Projections of the Mediodorsal Nucleus and Adjacent Thalamic Nuclei in the Rat. *J Comp Neurol* **171**, 157-191 (1977).

143. Goldman-Rakic, P.S. & Porrino, L.J. The Primate Mediodorsal (Md) Nucleus and Its Projection to the Frontal Lobe. *J Comp Neurol* **242**, 535-560 (1985).

144. Parker, A. & Gaffan, D. Interaction of Frontal and Perirhinal Cortices in Visual Object Recognition Memory in Monkeys. *Eur J Neurosci* **10**, 3044-3057 (1998).

145. Klein, J.C., Rushworth, M.F.S., Behrens, T.E.J., Mackay, C.E., de Crespigny, A.J., D'Arceuil, H. & Johansen-Berg, H. Topography of Connections between Human Prefrontal Cortex and Mediodorsal Thalamus Studied with Diffusion Tractography. *NeuroImage* **51**, 555-564 (2010).

146. Craig, A.D. Opinion: How Do You Feel? Interoception: The Sense of the Physiological Condition of the Body. *Nature Reviews Neuroscience* **3**, 655-666 (2002).

147. Seeley, W.W., Menon, V., Schatzberg, A.F., Keller, J., Glover, G.H., Kenna, H., Reiss, A.L. & Greicius, M.D. Dissociable Intrinsic Connectivity Networks for Salience Processing and Executive Control. *J Neurosci* **27**, 2349-2356 (2007).

148. Legrain, V., Iannetti, G.D., Plaghki, L. & Mouraux, A. The Pain Matrix Reloaded: A Salience Detection System for the Body. *Prog Neurobiol* **93**, 111-124 (2011).

149. Nicotra, A., Critchley, H.D., Mathias, C.J. & Dolan, R.J. Emotional and Autonomic Consequences of Spinal Cord Injury Explored Using Functional Brain Imaging. *Brain* **129**, 718-728 (2006).

150. Critchley, H.D., Mathias, C.J. & Dolan, R.J. Neuroanatomical Basis for First- and Second-Order Representations of Bodily States. *Nat Neurosci* **4**, 207-212 (2001).

151. Craig, A.D. A New Version of the Thalamic Disinhibition Hypothesis of Central Pain. *Pain Forum* **7**, 1-14 (1998).

152. Theyel, B.B., Llano, D.A. & Sherman, S.M. The Corticothalamocortical Circuit Drives Higher-Order Cortex in the Mouse. *Nat Neurosci* **13**, 84-88 (2010).

153. Saalmann, Y.B., Pinsk, M.A., Wang, L., Li, X. & Kastner, S. Pulvinar Regulates Information Transmission between Cortical Areas Based on Attention Demands(). *Science (New York, N.Y.)* **337**, 753-756 (2012).

154. Shipp, S. The Functional Logic of Cortico-Pulvinar Connections. *Philos Trans R Soc Lond B Biol Sci* **358**, 1605-1624 (2003).

155. Taube, J.S. Head Direction Cells Recorded in the Anterior Thalamic Nuclei of Freely Moving Rats. *J Neurosci* **15**, 70-86 (1995).

156. Snow, J.C., Allen, H.A., Rafal, R.D. & Humphreys, G.W. Impaired Attentional Selection Following Lesions to Human Pulvinar: Evidence for Homology between Human and Monkey. *Proceedings of the National Academy of Sciences* **106**, 4054 (2009).

157. Weller, R.E., Steele, G.E. & Kaas, J.H. Pulvinar and Other Subcortical Connections of Dorsolateral Visual Cortex in Monkeys. *J Comp Neurol* **450**, 215-240 (2002).

158. Fang, P.C., Stepniewska, I. & Kaas, J.H. The Thalamic Connections of Motor, Premotor, and Prefrontal Areas of Cortex in a Prosimian Primate (Otolemur Garnetti). *Neuroscience* **143**, 987-1020 (2006).

159. Mesulam, M.M. Large-Scale Neurocognitive Networks and Distributed Processing for Attention, Language, and Memory. *Ann Neurol* **28**, 597-613 (1990).

160. Guillery, R.W. & Sherman, S.M. The Thalamus as a Monitor of Motor Outputs. *Philosophical Transactions of the Royal Society B: Biological Sciences* **357**, 1809-1821 (2002).

161. Dietz, V. & Harkema, S.J. Locomotor Activity in Spinal Cord-Injured Persons. *J Appl Physiol (1985)* **96**, 1954-1960 (2004).

162. Karunakaran, K.K. New Jersey Institute of Technology (2016).

163. Kiran Karunakaran, G.A., Richard Foulds. Natural User-Controlled Ambulation of Lower Extremity Exoskeletons for Individuals with Spinal Cord Injury. in *Wearable Robotics: Challenges and Trends. Biosystems & Biorobotics* (ed. González-Vargas J., I.J., Contreras-Vidal J., van der Kooij H., Pons J.) (Springer, Cham, Switzerland, 2017).

164. El-Sayes, J., Harasym, D., Turco, C.V., Locke, M.B. & Nelson, A.J. Exercise-Induced Neuroplasticity: A Mechanistic Model and Prospects for Promoting Plasticity. *Neuroscientist* **25**, 65-85 (2019).

165. Hoffman, L.R. & Field-Fote, E.C. Cortical Reorganization Following Bimanual Training and Somatosensory Stimulation in Cervical Spinal Cord Injury: A Case Report. *Phys Ther* **87**, 208-223 (2007).

166. Mihara, M. & Miyai, I. Review of Functional near-Infrared Spectroscopy in Neurorehabilitation. *Neurophotonics* **3**, 031414 (2016).

167. Sangani, S., Lamontagne, A. & Fung, J. Cortical Mechanisms Underlying Sensorimotor Enhancement Promoted by Walking with Haptic Inputs in a Virtual Environment. *Prog Brain Res* **218**, 313-330 (2015).

168. Villringer, A. & Chance, B. Non-Invasive Optical Spectroscopy and Imaging of Human Brain Function. *Trends Neurosci* **20**, 435-442 (1997).

169. Ferrari, M. & Quaresima, V. A Brief Review on the History of Human Functional near-Infrared Spectroscopy (Fnirs) Development and Fields of Application. *Neuroimage* **63**, 921-935 (2012).

170. Huppert, T.J., Hoge, R.D., Diamond, S.G., Franceschini, M.A. & Boas, D.A. A Temporal Comparison of Bold, Asl, and Nirs Hemodynamic Responses to Motor Stimuli in Adult Humans. *Neuroimage* **29**, 368-382 (2006).

171. Hoshi, Y. Functional near-Infrared Optical Imaging: Utility and Limitations in Human Brain Mapping. *Psychophysiology* **40**, 511-520 (2003).

172. Irani, F., Platek, S.M., Bunce, S., Ruocco, A.C. & Chute, D. Functional near Infrared Spectroscopy (Fnirs): An Emerging Neuroimaging Technology with Important Applications for the Study of Brain Disorders. *Clin Neuropsychol* **21**, 9-37 (2007).

173. Attwell, D. & Iadecola, C. The Neural Basis of Functional Brain Imaging Signals. *Trends Neurosci* **25**, 621-625 (2002).

174. Ferrari, M., Mottola, L. & Quaresima, V. Principles, Techniques, and Limitations of near Infrared Spectroscopy. *Can J Appl Physiol* **29**, 463-487 (2004).

175. Cutini, S. & Brigadoi, S. Unleashing the Future Potential of Functional near-Infrared Spectroscopy in Brain Sciences. *J Neurosci Methods* **232**, 152-156 (2014).

176. Hoshi, Y. Functional near-Infrared Spectroscopy: Potential and Limitations in Neuroimaging Studies. *Int Rev Neurobiol* **66**, 237-266 (2005).

177. Brigadoi, S. & Cooper, R.J. How Short Is Short? Optimum Source-Detector Distance for Short-Separation Channels in Functional near-Infrared Spectroscopy. *Neurophotonics* **2**, 025005 (2015).

178. Marcel Simis, K.S., João Sato, Felipe Fregni, Linamara Battistella. T107. Using Functional near Infrared Spectroscopy (Fnirs) to Assess Brain Activity of Spinal Cord Injury Patient, During Robot-Assisted Gait. *Clinical Neurophysiology* **129**, Pages e43-e44 (2018).

179. Lloyd-Fox, S., Papademetriou, M., Darboe, M.K., Everdell, N.L., Wegmuller, R., Prentice, A.M., Moore, S.E. & Elwell, C.E. Functional near Infrared Spectroscopy (Fnirs) to Assess Cognitive Function in Infants in Rural Africa. *Sci Rep* **4**, 4740 (2014).

180. Keehn, B., Wagner, J.B., Tager-Flusberg, H. & Nelson, C.A. Functional Connectivity in the First Year of Life in Infants at-Risk for Autism: A Preliminary near-Infrared Spectroscopy Study. *Front Hum Neurosci* **7**, 444 (2013).

181. Batula, A.M., Mark, J.A., Kim, Y.E. & Ayaz, H. Comparison of Brain Activation During Motor Imagery and Motor Movement Using Fnirs. *Comput Intell Neurosci* **2017**, 5491296 (2017).

182. Piper, S.K., Krueger, A., Koch, S.P., Mehnert, J., Habermehl, C., Steinbrink, J., Obrig, H. & Schmitz, C.H. A Wearable Multi-Channel Fnirs System for Brain Imaging in Freely Moving Subjects. *Neuroimage* **85 Pt 1**, 64-71 (2014).

183. Furlan, J.C. & Fehlings, M.G. Cardiovascular Complications after Acute Spinal Cord Injury: Pathophysiology, Diagnosis, and Management. *Neurosurg Focus* **25**, E13 (2008).

184. Kim, D.I. & Tan, C.O. Alterations in Autonomic Cerebrovascular Control after Spinal Cord Injury. *Auton Neurosci* **209**, 43-50 (2018).

185. Witt, S.T., Laird, A.R. & Meyerand, M.E. Functional Neuroimaging Correlates of Finger-Tapping Task Variations: An Ale Meta-Analysis. *Neuroimage* **42**, 343-356 (2008).

186. Molavi, B. & Dumont, G.A. Wavelet-Based Motion Artifact Removal for Functional near-Infrared Spectroscopy. *Physiol Meas* **33**, 259-270 (2012).

187. Yamada, T., Umeyama, S. & Matsuda, K. Multidistance Probe Arrangement to Eliminate Artifacts in Functional near-Infrared Spectroscopy. *J Biomed Opt* **14**, 064034 (2009).

188. Kim, H.Y. Statistical Notes for Clinical Researchers: Evaluation of Measurement Error 1: Using Intraclass Correlation Coefficients. *Restor Dent Endod* **38**, 98-102 (2013).

189. Zuo, X.N., Di Martino, A., Kelly, C., Shehzad, Z.E., Gee, D.G., Klein, D.F., Castellanos, F.X., Biswal, B.B. & Milham, M.P. The Oscillating Brain: Complex and Reliable. *Neuroimage* **49**, 1432-1445 (2010).

190. Joseph L. Fleiss, B.L., Myunghee Cho Paik. *Statistical Methods for Rates and Proportions*, (Wiley, California, 2003).

191. Seghier, M.L. Laterality Index in Functional Mri: Methodological Issues. *Magn Reson Imaging* **26**, 594-601 (2008).

192. Di, X., Kannurpatti, S.S., Rypma, B. & Biswal, B.B. Calibrating Bold Fmri Activations with Neurovascular and Anatomical Constraints. *Cereb Cortex* **23**, 255-263 (2013).

193. Landis, J.R. & Koch, G.G. The Measurement of Observer Agreement for Categorical Data. *Biometrics* **33**, 159-174 (1977).

194. Geng, S., Liu, X., Biswal, B.B. & Niu, H. Effect of Resting-State Fnirs Scanning Duration on Functional Brain Connectivity and Graph Theory Metrics of Brain Network. *Front Neurosci* **11**, 392 (2017).

195. Niu, H., Li, Z., Liao, X., Wang, J., Zhao, T., Shu, N., Zhao, X. & He, Y. Test-Retest Reliability of Graph Metrics in Functional Brain Networks: A Resting-State Fnirs Study. *PLoS One* **8**, e72425 (2013).

196. Dravida, S., Noah, J.A., Zhang, X. & Hirsch, J. Comparison of Oxyhemoglobin and Deoxyhemoglobin Signal Reliability with and without Global Mean Removal for Digit Manipulation Motor Tasks. *Neurophotonics* **5**, 011006 (2018).

197. Bright, M.G. & Murphy, K. Reliable Quantification of Bold Fmri Cerebrovascular Reactivity Despite Poor Breath-Hold Performance. *Neuroimage* **83**, 559-568 (2013).

198. Thomason, M.E. & Glover, G.H. Controlled Inspiration Depth Reduces Variance in Breath-Holding-Induced Bold Signal. *Neuroimage* **39**, 206-214 (2008).

199. Pillai, J.J. & Mikulis, D.J. Cerebrovascular Reactivity Mapping: An Evolving Standard for Clinical Functional Imaging. *AJNR Am J Neuroradiol* **36**, 7-13 (2015).

200. Matsubayashi, K., Nagoshi, N., Komaki, Y., Kojima, K., Shinozaki, M., Tsuji, O., Iwanami, A., Ishihara, R., Takata, N., Matsumoto, M., Mimura, M., Okano, H. & Nakamura, M. Assessing Cortical Plasticity after Spinal Cord Injury by Using Resting-State Functional Magnetic Resonance Imaging in Awake Adult Mice. *Sci Rep* **8**, 14406 (2018).

201. Cermik, T.F., Tuna, H., Kaya, M., Tuna, F., Gultekin, A., Yigitbasi, O.N. & Alavi, A. Assessment of Regional Blood Flow in Cerebral Motor and Sensory Areas in Patients with Spinal Cord Injury. *Brain Res* **1109**, 54-59 (2006).

202. Mutha, P.K., Haaland, K.Y. & Sainburg, R.L. The Effects of Brain Lateralization on Motor Control and Adaptation. *J Mot Behav* **44**, 455-469 (2012).

203. Higuchi, S., Holle, H., Roberts, N., Eickhoff, S.B. & Vogt, S. Imitation and Observational Learning of Hand Actions: Prefrontal Involvement and Connectivity. *Neuroimage* **59**, 1668-1683 (2012).

204. Macuga, K.L. & Frey, S.H. Neural Representations Involved in Observed, Imagined, and Imitated Actions Are Dissociable and Hierarchically Organized. *Neuroimage* **59**, 2798-2807 (2012).

205. van der Scheer, J.W., Kamijo, Y.I., Leicht, C.A., Millar, P.J., Shibasaki, M., Goosey-Tolfrey, V.L. & Tajima, F. A Comparison of Static and Dynamic Cerebral Autoregulation During Mild Whole-Body Cold Stress in Individuals with and without Cervical Spinal Cord Injury: A Pilot Study. *Spinal Cord* **56**, 469-477 (2018).

206. Chen, Y., Michaelis, M., Janig, W. & Devor, M. Adrenoreceptor Subtype Mediating Sympathetic-Sensory Coupling in Injured Sensory Neurons. *J Neurophysiol* **76**, 3721-3730 (1996).

207. Baron, R. & Schattschneider, J. Chapter 25 the Autonomic Nervous System and Pain. *Handb Clin Neurol* **81**, 363-382 (2006).

208. Murphy, K., Harris, A.D. & Wise, R.G. Robustly Measuring Vascular Reactivity Differences with Breath-Hold: Normalising Stimulus-Evoked and Resting State Bold Fmri Data. *Neuroimage* **54**, 369-379 (2011).

209. Thomason, M.E., Foland, L.C. & Glover, G.H. Calibration of Bold Fmri Using Breath Holding Reduces Group Variance During a Cognitive Task. *Hum Brain Mapp* **28**, 59-68 (2007).

210. Nair, V.A., Raut, R.V. & Prabhakaran, V. Investigating the Blood Oxygenation Level-Dependent Functional Mri Response to a Verbal Fluency Task in Early Stroke before and after Hemodynamic Scaling. *Front Neurol* **8**, 283 (2017).

211. Geranmayeh, F., Wise, R.J., Leech, R. & Murphy, K. Measuring Vascular Reactivity with Breath-Holds after Stroke: A Method to Aid Interpretation of Group-Level Bold Signal Changes in Longitudinal Fmri Studies. *Hum Brain Mapp* **36**, 1755-1771 (2015).

212. Grigorean, V.T., Sandu, A.M., Popescu, M., Iacobini, M.A., Stoian, R., Neascu, C., Strambu, V. & Popa, F. Cardiac Dysfunctions Following Spinal Cord Injury. *J Med Life* **2**, 133-145 (2009).

213. Keuken, M.C., van Maanen, L., Boswijk, M., Forstmann, B.U. & Steyvers, M. Large Scale Structure-Function Mappings of the Human Subcortex. *Sci Rep* **8**, 15854 (2018).

214. Mehrholz, J., Harvey, L.A., Thomas, S. & Elsner, B. Is Body-Weight-Supported Treadmill Training or Robotic-Assisted Gait Training Superior to Overground Gait Training and Other Forms of Physiotherapy in People with Spinal Cord Injury? A Systematic Review. *Spinal Cord* **55**, 722-729 (2017).